Final Report
November 2017

Cost and Ecological Feasibility of using UHPC in Highway Bridges

SOLARIS Consortium, Tier 1 University Transportation Center
Center for Advanced Transportation Education and Research
Department of Civil and Environmental Engineering
University of Nevada, Reno
Reno, NV 89557

Christopher D. Joe
Mohamed Moustafa, PhD, PE
Keri L. Ryan, PhD
Department of Civil and Environmental Engineering
University of Nevada, Reno
Reno, NV 89557

***DISCLAIMER*:**

The contents of this report reflect the views of the authors, who are responsible for the facts and accuracy of the information presented herein. This document is disseminated under the sponsorship of the U.S. Department of Transportation's University Transportation Centers Program, in the interest of information exchange. The U.S. Government assumes no liability for the contents or use thereof.

NDOT TECHNICAL REPORT DOCUMENTATION PAGE

1. Report No. ###-##-803	2. Government Accession No.	3. Recipient's Catalog No.
4. Title and Subtitle Cost and Ecological Feasibility of using UHPC in Highway Bridges		5. Report Date November 2017 6. Performing Organization Code University of Nevada, Reno
7. Author(s) Christopher D. Joe, Mohamed A. Moustafa, Keri L. Ryan		8. Performing Organization Report No.
9. Performing Organization Name and Address University of Nevada, Reno 1664 N. Virginia St. Reno, NV 89557		10. Work Unit No. 11. Contract or Grant No. P224-14-803
12. Sponsoring Agency Name and Address Nevada Department of Transportation 1263 South Stewart Street Carson City, NV 89712		13. Type of Report and Period Covered Final Report 06/01/2016-08/31/2017 14. Sponsoring Agency Code
15. Supplementary Notes		

16. Abstract

There is a growing interest in expanding the use of Ultra-high performance concrete (UHPC) from bridge deck joints for accelerated bridge construction to complex architectural and advanced structural applications. The high costs currently associated with UHPC might limit its widespread use. However, the more compact cross-sections, higher strength, and durability of UHPC should result in safer structures and a much longer service life with minimal maintenance. This study aims at exploring the extended use of UHPC to entirely replace conventional concrete in a multi-column bent of a typical highway bridge. This is to provide a pilot design and investigate the structural and seismic performance of UHPC piers for potential future use in highway bridges. The objective of the investigation is to see whether using UHPC in bridge columns and bent caps is economically and environmentally feasible if UHPC cross-sections are optimized to have a comparable structural and seismic response to conventional concrete bridges.

Four different UHPC mix designs of varying mechanical properties were considered to design a two-column bridge bent using current analytical tools (OpenSees) while following standard AASHTO design guidelines. Sectional analysis was used for initial, cross-sectional design optimization. Nonlinear lateral pushover and time history analyses were used to perform seismic capacity checks and compare the seismic performance of UHPC piers to a conventional concrete design. The results show that the comparable-strength designed UHPC piers can achieve lower peak (maximum) displacements, ductility demands, maximum drift ratios, and residual displacements along with higher maximum base shear capacities when compared to a conventional concrete pier. For economic and environmental analysis, a bill of quantities was created to calculate the amount of materials consumed and saved. For fewer UHPC design cases where there was a savings in cement consumption, a direct, positive impact is made possible on carbon dioxide emissions caused by the harsh clinker production processes in the cement industry. The study also found significant water savings, due to UHPC's low water-to-cement ratio, with savings averaging approximately 50% of the conventional concrete design case. Lastly, using the optimized UHPC sections, a cost analysis was performed and found that UHPC designs are not necessarily cheaper, but will only add a slight percent increase in overall costs that is worth considering for a safer structure, longer service life, and minimal maintenance.

17. Key Words	18. Distribution Statement No restrictions. This document is available through the: National Technical Information Service Springfield, VA 22161		
19. Security Classif. (of this report) Unclassified	20. Security Classif. (of this page) Unclassified	21. No. of Pages 142	22. Price

Form DOT F 1700.7 (8-72) Reproduction of completed page authorized

ABSTRACT

There is a growing interest in expanding the use of Ultra-high performance concrete (UHPC) from bridge deck joints for accelerated bridge construction to complex architectural and advanced structural applications. The high costs currently associated with UHPC might limit its widespread use. However, the more compact cross-sections, higher strength, and durability of UHPC should result in safer structures and a much longer service life with minimal maintenance. This study aims at exploring the extended use of UHPC to entirely replace conventional concrete in a multi-column bent of a typical highway bridge. This is to provide a pilot design and investigate the structural and seismic performance of UHPC piers for potential future use in highway bridges. The objective of the investigation is to see whether using UHPC in bridge columns and bent caps is economically and environmentally feasible if UHPC cross-sections are optimized to have a comparable structural and seismic response to conventional concrete bridges.

Four different UHPC mix designs of varying mechanical properties were considered to design a two-column bridge bent using current analytical tools (OpenSees) while following standard AASHTO design guidelines. Sectional analysis was used for initial, cross-sectional design optimization. Nonlinear lateral pushover and time history analyses were used to perform seismic capacity checks and compare the seismic performance of UHPC piers to a conventional concrete design. The results show that the comparable-strength designed UHPC piers can achieve lower peak (maximum) displacements, ductility demands, maximum drift ratios, and residual displacements along with higher maximum base shear capacities when compared to a conventional concrete pier. For economic and environmental analysis, a bill of quantities was created to calculate the amount of materials consumed and saved. For fewer UHPC design cases where there was a savings in cement consumption, a direct, positive impact is made possible on carbon dioxide emissions caused by the harsh clinker production processes in the cement industry. The study also found significant water savings, due to UHPC's low water-to-cement ratio, with savings averaging approximately 50% of the conventional concrete design case. Lastly, using the optimized UHPC sections, a cost analysis was performed and found that UHPC designs are not necessarily cheaper, but will only add a slight percent increase in overall costs that is worth considering for a safer structure, longer service life, and minimal maintenance.

Table of Contents

List of Tables

List of Figures

1 Introduction

Over the past century, building materials and construction methods have evolved immensely opening doors to new design potentials. The availability of new research and testing methods have allowed for many new practical structural and architectural applications of concrete. Ultra-high performance concrete (UHPC) is an advanced concrete making quick strides in the industry due to its high strength, exceptional durability, and ductile behavior. Unfortunately, applications of UHPC have been limited and is lacking in large scale structural application or an in-depth ecological assessment.

1.1 MOTIVATION

As of today, UHPC is still an expensive product in North America due to the limited number of UHPC manufacturers and minute amount of actual industry application. As more research is performed on UHPC at a larger scale, more engineering and architectural firms will gain interest and confidence in utilizing UHPC for their projects. Theoretically, with more interests and applications of UHPC, more UHPC manufacturers and vendors will become available. This will eventually lead to reducing UHPC material and production costs for different manufacturers to remain competitive in the industry. The motivation of this study is to demonstrate that UHPC can generate smaller structural cross sections (e.g. bridge columns and bent caps), and in turn, reduce the footprint of the bridge. Smaller columns can make more room for additional lanes or shoulder space for traffic below the bridge and ease the constructability of the bridge itself. Due to the nature of cementitious materials in general, and UHPC in particular, as smaller cross sections are achieved, less cement, water, and steel can be consumed, which makes UHPC a potentially environmental-friendly material. Drought stricken states such as California, Nevada, and Texas will benefit immensely from the reduced water consumption. The carbon footprint of UHPC structural members can be reduced if overall less cement is consumed. From another structural perspective, structures with less materials consumed and lighter mass could have a favorable seismic performance in earthquake prone zones such as California. Thus, expanding the use of UHPC to bridge structural members can enhance its structural behavior and durability, minimize maintenance throughout the lifespan of the bridge, and minimize negative ecological effects.

1.2 PROBLEM STATEMENT AND OBJECTIVES

Bridge piers consist of large volumes of concrete and reinforcing steel. Naturally, where concrete is used, cement, water, and steel is consumed. The cement production process consumes vast amounts of energy and fuel and creates large quantities of carbon dioxide gases. UHPC is an advanced material with exceptional mechanical properties and very low water-to-cement ratios. Although UHPC used more cement per cubic yard than conventional concrete, it requires smaller cross-sections and overall less quantities, which might require overall less cement as well. A big drawback of expanding the use of UHPC at larger scales is the high UHPC per-cubic-yard material cost, which can be 15 or 20 times higher than conventional concrete. Thus, the problem statement of this study is assessing whether using UHPC in bridge piers is economically and environmentally feasible if UHPC cross-sections are optimized to have a comparable structural and seismic response to conventional concrete bridges.

The overall goal of this report is to study the feasibility and effects of UHPC as an alternative material to conventional concrete for a substructure of a typical California highway bridge. The specific objectives are: (1) conduct a literature review of available UHPC mixes and analyze such mixes to select four different mixes to use for this study; (2) optimize a prototype bridge pier design using the selected different UHPC mixes and using different reinforcement ratios; (3) check and compare the structural and seismic performance of the different UHPC bridge piers against a conventional concrete pier; (4) compile bills of quantities for the UHPC and conventional concrete piers with focus on environmentally sensitive components such as cement, water, and reinforcement; (5) carry out a monetary cost analysis and environmental assessment of the different UHPC piers as compared to the conventional concrete case.

1.3 METHODOLOGY

To achieve the study objectives listed above, an extensive computational framework is used. Four UHPC mix designs are selected from the literature and utilized to design a full prototype bridge pier, which is commonly referred to as a bridge bent. The prototype bridge used in this study is a typical three-span California highway bridge with a prestressed reinforced concrete box-girder superstructure and two bents. Each bent consists of two columns and an integral bent cap beam

that is monolithically attached to the box-girder superstructure. The conventional concrete and UHPC piers are designed in accordance to the California Department of Transportation (Caltrans) latest Seismic Design Criteria (SDC 1.7, 2013) and AASHTO LRFD Bridge Design Specifications (2012).

Four different UHPC mixes with varying mechanical strength are considered along with four different column reinforcement ratios to optimize the UHPC cross-sections. Existing computational tools are utilized to do sectional analysis to estimate the flexural moment capacity and optimize the design of UHPC cross-sections. The improved mechanical properties of UHPC are expected to result in smaller column and bent cap beam cross-sections. To verify that the compact UHPC sections do not compromise the bridge structural or seismic performance, detailed nonlinear pushover and time history analyses are conducted for the conventional concrete and different UHPC bridge piers using the finite element platform OpenSees (Open System for Earthquake Engineering Simulation). Readily available concrete constitutive models in OpenSees, are altered to approximately represent the UHPC behavior.

After the UHPC pier cross-sections are optimized and satisfactory seismic performance is verified, bills of quantities are compiled for the full conventional and UHPC bridge piers. The estimated quantities are used along with the different mix designs and ingredients break down to carry out a cost analysis and environmental (ecological) impact assessment. The cost study uses different estimates for unit UHPC material costs to compare an estimated overall construction cost for the prototype bridge with conventional concrete and UHPC piers. For the environmental impact assessment, this study estimates and compares carbon dioxide (CO_2) emissions and energy consumption associated with consumed cement and reinforcement in the different conventional and UHPC bridge piers. Another important environmental metric that is considered here is the potential savings in water consumption when using UHPC as a result of its low water-to-cement ratio. The seismic analysis along with the cost and ecological analyses considered in this study can then demonstrate whether UHPC has potential structural and/or ecological benefits as compared to conventional concrete.

1.4 ORGANIZATION OF REPORT

This report is divided into eight chapters and two appendices. The first chapter is an introduction of the study objectives and methodology. Chapter 2 presents a literature review of UHPC research studies, available mix designs, and real life applications. Chapter 3 presents a preliminary analysis of the different UHPC mixes mechanical properties. The sectional analysis and design optimization of bridge piers using selected UHPC mixes is discussed in Chapter 4, while Chapter 5 focuses on the seismic pushover and time history analysis. The cost analysis and environmental assessment of the different UHPC piers as compared to conventional concrete piers are presented in Chapters 6 and 7, respectively. Finally, a summary of the conclusions drawn from this study and recommendations for future work is presented in Chapter 8.

2 Literature Review

This chapter briefly introduces different types of advanced concrete including ultra-high performance concrete (UHPC). Then, a more detailed discussion focuses on UHPC including material and mechanical properties, mix designs, architectural applications, structural applications, life cycle assessment, cost assessment, and global warming potential.

2.1 INNOVATIVE MATERIALS

There are many types of advanced concrete used today to conform to specific conditions such as physical or environmental impact conditions. Some examples include: self-consolidating concrete, pervious concrete, lightweight concrete fiber-reinforced concrete, rubberized asphalt concrete, green concrete, UHPC, and High Volume Fly Ash (HVFA) concrete. Each of these contribute to both an increased life cycle and/or improved global warming potential making it the ideal alternative to normal strength concrete.

Self-Consolidating Concrete: Self-consolidating concrete (SCC) is a low viscosity, self-compacting concrete used when mechanical consolidation is not desired or available. SCC is also used in architectural settings when a high quality surface finish is required for complex shapes not normally attainable with normal strength concrete. SCC pumps quickly and saves time in both transportation and labor costs (NRMCA 2004).

Pervious Concrete: Pervious concrete is a porous, large aggregate concrete used when drainage of water is desired. This allows runoff to be decreased significantly and filters the runoff before it enters back into the ground water. By reducing runoff significantly, the need for retention basins and large storm sewers are no longer required (NRMCA 2004).

Lightweight Concrete: Lightweight concrete is used to decrease the dead load of a structure, allowing for more efficiently sized members. Lightweight concrete has a unit weight between 90 lb/ft^3 and 115 lb/ft^3 (compared to 150 lb/ft^3 for typical conventional concrete) and provides excellent insulation with improved fire protection. The lightness is achieved through lightweight aggregate and increased air voids in the cement paste and should generally have a compressive strength of 2500 psi before it is used for a structural application (NRMCA 2003).

Fiber-Reinforced Concrete: Fiber-reinforced concrete (FRC) is concrete created with thin fibers as a substitute for reinforcing steel. Fiber materials can vary from steel, glass, natural or synthetic

materials such as acrylic, aramid, nylon, and polyester. FRC applications include slabs and flooring, tunnel lining, blast resistant structures, and thin shells (Pike 2009).

Rubberized Asphalt Concrete: Rubberized asphalt concrete (RAC) is a paving material for roads created by compacting recycled tires and asphalt. The materials are then bound together with asphalt-rubber and terminal blends. Asphalt-rubber is "…a blend of paving grade asphalt cement, ground recycled tire (that is, vulcanized) rubber and other additives, as needed, for use as binder in pavement construction. The rubber shall be blended and interacted in the hot asphalt cement sufficiently to cause swelling of the rubber particles prior to use" (ASTM D6114, 2009). Terminal blend is another binder made of scrap tire rubber finely ground into an irregular shape (Gauff 2012).

Green Concrete: Green concrete, or Novacem Concrete, is a magnesium oxide substitute for cement. When combined with water, the magnesium reacts to the surrounding carbon dioxide gases creating carbonates that strengthen the cement. Carbon dioxide gases are absorbed during mixing, which makes this a very environmental-friendly alternative. The final product is very comparable to normal strength concrete with little to no differences in mechanical properties (Bradley 2010). As more attention is being placed on carbon dioxide emissions and environmental-friendly options, many companies are beginning to develop their own green cement and mixing processes. These companies include, Celera Corporation, Lafarge, CarbonCure, and Solidia Technologies.

Ultra-High Performance Concrete: The next sections discuss in full details the definition and characteristics of UHPC, which is the main focus of this study.

High Volume Fly Ash Concrete (HVFA): This is a family of concrete materials where a large portion of the cement is replaced with fly ash to minimize the negative environmental impacts associated with cement. Thus, this type is a promising "green concrete" that has been extensively considered in previous and ongoing studies. Due to the high potential for environmental benefits that this type of concrete has, Appendix A of this study provides more details regarding typical HVFA concrete mixes and different mix designs for interested readers to acquire more information.

2.2 ULTRA-HIGH PERFORMANCE CONCRETE

2.2.1 Definition

UHPC is a new and commercially available concrete unique for its high strength, ductile behavior, and long-term stability (FHWA, 2013). UHPC is a combination of portland cement, silica fume, ground quartz, fine sand, superplasticizers (high range water reducers), steel fibers, and water (Portland Cement Association, n.d.). Use of UHPC in some applications might reduce the need for reinforcing steel and allows for uniquely cast shapes. While UHPC is still a fairly new material, major advances have been made in the past five decades. Table 2-1 shows a history of advances of the concrete matrix (binding substance) and fibers by Naaman et al. (2002). These advances ultimately lead to the development of UHPC with its modern definition.

Because of the minute amount of water used in the mix design (UHPC features very low water-to-cement ratios), not all cement particles are hydrated completely. These un-hydrated cement particles will act as the aggregate in the mix design, making the method of mixing particularly crucial (ChunPing et al., 2015). Figure 2.1 shows a scanning electron microscopic image of cast UHPC at 28 days. The white particles labeled “A” are the un-hydrated cement particles acting as aggregate.

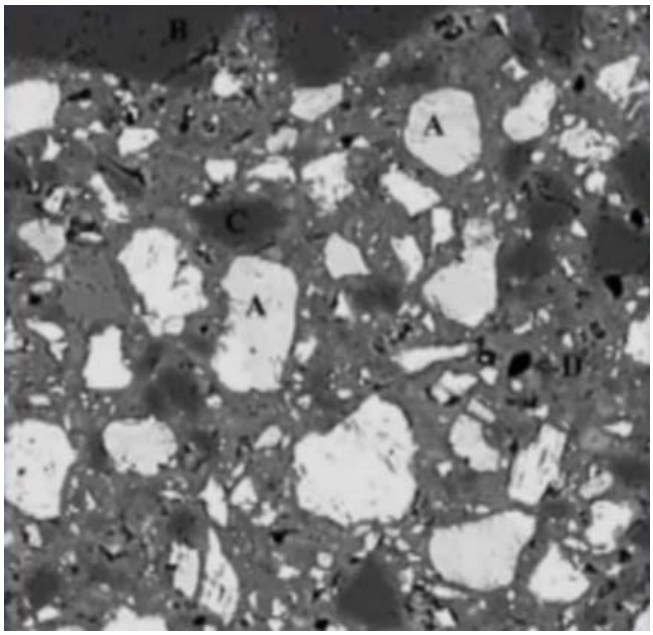

Figure 2.1 Scanning electron microscopic image of cast UHPC at 28 days (Wiss, Janney, and Elstner Associates, 2011).

Table 2-1 Chronological Advances in Concrete and Fibers (Naaman et al., 2012)

Decade	Cementitious Matrix and Concrete	Fiber
1970's	• Better understanding of hydration reactions and gel structure • Better understanding of shrinkage, creek, and porosity • High strength concrete reaches 7250 psi in practice • Development of water reduces • Advances in concrete treatment and curing conditions	• Smooth steel fibers • Glass fibers • Some synthetic fibers
1980's	• Increased development of chemical additives such as high range water reducers • Increased utilization of fly ash, silica fume, and other mineral additives • Increased flowability • Reduced water to cement ratio	• Deformed steel fibers: normal and high strength
1980's	• Redefined concrete strength terminology ▪ High Strength Concrete – 9000 psi ▪ Special High Strength – 12000 psi ▪ Exotic High Strength – 17000 psi • High Performance Concrete defined: high strength concrete with improved durability properties	• Low-modulus synthetic fibers • Micro fibers • High performance polymer fibers
1990's	• Increased development of chemical additives such as superplasticizers and viscosity agents • Increased use of supplementary cementitious materials as cement replacement • UHPC: application of concept of high packing density, addition of fine particles, low porosity, lower water to cementitious material ratio • Self-consolidating concrete • Self-compacting concrete • First UHPC bridge constructed (Sherbrooke Pedestrian Bridge – Quebec, Canada)	• Twisted steel fibers introduced • PVA fibers with chemical bond to concrete • Improved availability of synthetic fibers
2000's	• Increased developments of proprietary and non-proprietary UHPC • UHPC: Improved understanding of high packing density and applications of nanotechnology concepts • UHPC made commercially available by DUCTAL® • First application of UHPC waffle deck panels on a bridge (Little Cedar Creek Bridge, Wapello County, Iowa) • First architectural application of UHPC shells for a train station canopy (Shawnessy Light Rail Transit Station – Calgary, Canada) • First field deployment of UHPC in the United States highway transportation infrastructure (FHWA, 2013)	• Ultra high strength steel fibers (smooth or deformed with diameters as low as 0.005 in with strengths up to 490 ksi) • Carbon nano-tubes/fibers
2010's	• Increased understanding of the cementitious matrix at the nano-scale • First ACI UHPC Committee 239 meeting.	• Carbon nano-fibers and grapheme.

2.2.2 Mix Design

In order to identify the most efficient and eco-friendly UHPC mix design, this literature review compiles over 70 different mix designs from various sources across the world. Table 2-2 shows some components of each mix design (see Appendix B for a complete table). From the shown mix designs, typical components of UHPC include fine sand, ground quartz, cement, and steel fibers.

According to the Federal Highway Administration (FHWA), the largest granular material used in their test program for their UHPC mix designs is the fine sand which measures between 150-600 micrometers (μm) in diameter. The next two largest particles are the Portland cement and ground quartz, which measure at approximately 15 μm and 10 μm, respectively. The smallest particle is the silica fume, which is small enough to fill any voids between the cement and crushed quartz (FHWA, 2006).

The steel fibers play a major role in UHPC's ductile behavior in structural applications. The size of the steel fibers is typically proportional to the size of the finer particles. For the mix and particle sizes stated above, the steel fibers are typically 0.2 millimeters (mm) in diameter and 12.7 mm in length (FHWA, 2006). The typical steel fibers used in the FHWA's test program had a minimum tensile strength of 377 kips/in^2 (ksi), an average yield stress of 458 ksi, a modulus of elasticity of 29700 ksi, and an average ultimate strength of 474 ksi (FHWA, 2006). The chemical composition of the steel fibers is shown in Table 2-3.

Mixing times for UHPC can range from 7 to 18 minutes and can be further reduced by improving the particle size distribution, replacing cement and quartz flower with silica fume, choosing the right high-range water reducer for the specific cement used, and increasing mixer speeds. To further decrease mixing times, the mixing procedures can be split into two parts, high-speed mixing for 40 seconds and low-speed mixing for 70 seconds immediately after.

Table 2-2 UHPC Mix Designs from Various Sources

Mix No.	lb/yd^3					W/C	Source
	Portland Cement	White Cement (CEM I 52.5 R)	Class C Fly Ash	Silica Fume	Steel Fibers		
1	1200	-	-	390	263	0.15	Graybeal, 2006
2	924	-	-	70	263	0.27	Khayat et al., 2014
3	1000	-	-	-	263	0.29	
4	1118	-	619	71	263	0.15	
5	819	-	937	-	263	0.17	
6	-	1475	-	74	82	0.23	Yu et al., 2014
7	-	1032	-	74	82	0.33	
8	-	1180	-	74	82	0.29	
9	1601	-	-	401	46	0.20	Yang, 2009
10	1107	-	-	201	44	0.17	Hassan, 2012
11	1107	-	-	201	44	0.15	Yang, 2010
12	1704	-	-	98	41	0.15	Toledo Filho, 2012
13	1618	-	-	405	57	0.16	Corinaldesi, 2012
14	1770	-	-	464	149	0.14	Habel 2006
15	-	1229	-	209	261	0.27	Randl et al., 2014
16	-	676	553	209	261	0.27	
17	-	676	-	209	261	0.50	
18	-	676	-	209	261	0.50	
19	1878	-	-	285	394	0.19	Hajar et al., 2004
20	2191	-	-	548	22	0.12	Talebinejad et al., 2004
21	2528	-	-	632	25	0.12	
22	2950	-	-	737	29	0.12	
23	3203	-	-	801	32	0.12	
24	3548	-	-	887	35	0.12	
25	2191	-	-	548	22	0.13	
26	2528	-	-	632	25	0.13	
27	2950	-	-	737	29	0.13	
28	3548	-	-	887	35	0.13	

Table 2-2 UHPC Mix Designs from Various Sources (Continued)

Mix No.	lb/yd^3					W/C	Source
	Portland Cement	White Cement (CEM I 52.5 R)	Class C Fly Ash	Silica Fume	Steel Fibers		
29	2191	-	-	548	22	0.17	Talebinejad et al., 2004
30	2528	-	-	632	25	0.17	
31	2950	-	-	737	29	0.17	
32	3548	-	-	887	35	0.17	
33	3203	-	-	641	32	0.12	
34	3203	-	-	941	32	0.12	
35	3203	-	-	1121	32	0.12	
36	3203	-	-	641	32	0.12	
37	3203	-	-	801	32	0.12	
38	3203	-	-	961	32	0.12	
39	3203	-	-	1121	32	0.12	
40	3203	-	-	641	32	0.13	
41	3203	-	-	801	32	0.13	
42	3203	-	-	961	32	0.13	
43	3203	-	-	1121	32	0.13	
44	3203	-	-	641	32	0.17	
45	3203	-	-	801	32	0.17	
46	3203	-	-	961	32	0.17	
47	3203	-	-	1121	32	0.17	
48	3203	-	-	801	32	0.10	
49	3203	-	-	801	32	0.11	
50	3203	-	-	801	32	0.20	
51	3203	-	-	801	32	0.12	
52	3203	-	-	801	32	0.13	
53	3203	-	-	801	32	0.17	
54	3203	-	-	801	32	0.20	
55	3203	-	-	801	32	0.12	
56	3203	-	-	801	32	0.12	
57	3203	-	-	801	32	0.12	
58	1210	-	-	394	263	0.16	Graybeal et al., 2008
59	1198	-	-	391	261	0.19	
60	-	1402	-	228	324	0.20	Ritter et al., 2015
61	-	1601	-	253	51	0.19	Shakhmenko et al., 2012
62	-	1601	-	34	34	0.21	Justs et al., 2012
63	-	1601	-	169	34	0.21	
64	1053	-	-	-	-	0.26	Ha et al., 2012

Table 2-2 UHPC Mix Designs from Various Sources (Continued)

Mix No.	lb/yd^3					W/C	Source
	Portland Cement	White Cement (CEM I 52.5 R)	Class C Fly Ash	Silica Fume	Steel Fibers		
65	811	-	120	-	-	0.28	Ha et al., 2012
66	585	-	232	-	-	0.31	
67	696	-	118	99	-	0.31	
68	1257	-	-	408	271	0.19	Ductal ®
69	1878	-	-	285	394	0.19	BSI ®
70	1770	-	-	464	792	0.18	$CEMTEC_{multiscale}$ ®
71	1476	-	-	240	-	0.21	Heinz et al., 2012
72	375	-	-	243	-	0.81	
73	964	-	821	243	-	0.18	
74	1517	-	-	303	265	0.20	Francisco et al., 2012
75	1328	-	-	332	33	0.22	Prem et al., 2012
76	1328	-	-	332	27	0.22	
77	1328	-	-	332	33	0.22	
78	1328	-	-	332	27	0.22	
79	1328	-	-	332	-	0.22	
80	1*	-	-	0.25*	1%	0.17	Prabha et al., 2014
81	1*	-	-	0.25*	2%	0.17	
82	1*	-	-	0.25*	3%	0.20	
83	1*	-	-	0.25*	1%	0.17	
84	1*	-	-	0.25*	2%	0.17	
85	1*	-	-	0.25*	2%	0.17	
86	1*	-	-	0.25*	3%	0.20	
87	1*	-	-	0.25*	0.27*	0.19	Wille et al., 2013

*Mix design by volume
W/C = water-to-cement ratio

Table 2-3 Chemical Composition of Steel Fibers Used in UHPC (FHWA 2006)

Element	Composition (%)
Carbon	0.69-0.76
Silicon	0.15-0.30
Manganese	0.40-0.60
Phosphorus	$\leq$ 0.025
Sulfur	$\leq$ 0.025
Chromium	$\leq$ 0.08
Aluminum	$\leq$0.003

Because UHPC mixing requires an increased amount of energy input, conventional mixing methods may not always work. Due to the elimination of coarse aggregate and decreased water

content, the mixture should not overheat during the mixing process. This can be avoided if a high-energy mixer such as a high shear mixer is used (FHWA, 2013). A high shear mixer will evenly release water and admixtures onto the cement particles without heating the mixture through kinetic energy produced by the mixing process. Another method used to avoid overheating the mixture is to add water in the form of ice. While much less efficient and more time consuming, mortars, horizontal shaft mixers, and pan mixers have also been used to mix UHPC (NPCA, 2013).

2.2.3 Curing Methods

Curing methods for UHPC vary for different circumstances and rely on two components, temperature and moisture (FHWA, 2013). Curing UHPC in its early stages in room temperature water leads to stronger formations of silicate hydrates. To continue this process, a high temperature cure either through steam or another heat source is applied to accelerate the silicate hydrate formation (Neville, 1995). Various methods of curing include steam curing at 140 ^{o}F or 194^{o}F for 48 hours, 24 hours post-casting, and steam curing at 194 ^{o}F 15 days post-casting, and curing at standard, controlled temperatures in a laboratory until satisfactory results are achieved. According to Heinz et al., 2012, curing UPHC at 194 ^{o}F: "accelerates the hydration of clinker phases and the reaction of silica fume and quartz flour completely binding portlandite while increasing the amount of C-S-H (calcium silicate hydrate) and their chain length". By curing UHPC with heat or steam, there is a noticeable decrease in chloride ion penetrability, increased abrasion resistance, and a near elimination of dry shrinkage effects (FHWA, 2013).

A study by Heinz et al. (2012) revealed that storage periods also contribute to the general strength of UHPC in addition to temperature and time of curing methods. Specimens immediately cured after setting for eight hours at 194 ^{o}F, achieved compressive strengths greater than 29,000 psi when tested 30 hours post-cure. Other specimens that were 24 hours old were heat treated for eight hours in an autoclave at 300 ^{o}F, cooled down to room temperature within 11 hours, and stored at 68 ^{o}F and 65% relative humidity until tested. These specimens achieved compressive strengths up to 38000 psi (Heinz et al., 2012).

2.2.4 Mechanical Properties

UHPC is known for its high compressive and flexural strength. Because of the fine composition in the mix design, the concrete is nearly impermeable and quite compact. The particularly low

porosity increases the uniformity of the mix design which allows the concrete to attain its extreme properties and a more uniform stress distribution (NPCA, 2014). UHPC can achieve high compressive strengths regardless of the addition of steel fibers as shown in Mix No. 71-73 from Table 2-2. The addition of steel fibers simply provides additional flexural and tensile strength (ChunPing et al., 2015).

While there are published methods of calculating estimated values of various mechanical properties, they can vary based on different curing methods, admixtures, types of silica fume, and steel fibers used. Reported in a study conducted by FHWA on the behavior of typical UHPC, Graybeal (2014) found a direct relationship between UHPC's tensile strength, compressive strength, and modulus elasticity. These relationships are presented and discussed in more details in the next chapter of this report. However, a quick comparison between Graybeal's equations (2014) and the American Concrete Institute's (ACI) equations (ACI 318, 2011) on normal strength concrete (NSC) are shown in Table 2-4.

Table 2-4 UHPC vs. NSC Equations (FHWA, 2014)

Mechanical Property	UHPC (psi)	NSC (psi)
Tensile Strength, f_{ct} For untreated UHPC	$f_{ct} = 6.7\sqrt{f'_c}$	$f_{ct} = 6.7\sqrt{f'_c}$ (ACI 318-11 R8.6.1)
Tensile Strength, f_{ct} Depending on method of steam curing	$f_{ct} = 7.8\sqrt{f'_c}$ or $f_{ct} = 8.3\sqrt{f'_c}$	-
Modulus of Elasticity, E For f'$_c$ values between 4000-28000 psi	$E = 46{,}200\sqrt{f'_c}$	$E = {w_c}^{1.5}33\sqrt{f'_c}$ where w_c is the unit weight of NSC between 90-155 lb/ft^3 (ACI 318-11 8.5.1)

A summary of the reported mechanical proprieties (mainly 28-day compressive strength and modulus of elasticity) for the compiled UHPC mix designs from Table 2-2 is shown in Table 2-5. Note that because this mix design literature review compiles various mixes and its respective mechanical properties from different published sources, some values were not reported or made available. However, more details can be still found in Appendix B. For some of the mixes, the 28-day tensile strength was reported as well. Table 2-6 compares the compressive and tensile strengths for those mixes that had its mechanical strength measured in compression and tension. Because of the use of steel fibers, higher tensile-to-compression strength ratio is obtained from UHPC as compared to conventional or NSC. Table 2-6 shows that this ratio can reach as high as 13%.

Table 2-5 Mechanical Properties of UHPC Mix Designs from Various Sources

Mix No.	28-Day f'c w/o Heat Cure (psi)	28-Day f'c w/ Heat Cure (psi)	Modulus of Elasticity (psi)	Source
1	17200	-	6.07E+06	Graybeal, 2006
1		28900	7.46E+06	
2	18130	-	7.27E+06	Khayat et al., 2014
3	17985	-	7.18E+06	
4	17985	-	7.48E+06	
5	15519	-	6.64E+06	
6	22626	-	-	Yu et al., 2014
7	20595	-	-	
8	21611	-	-	
9	27557	-	-	Yang, 2009
10	21756	-	-	Hassan, 2012
11	17405	-	-	Yang, 2010
12	23206	-	-	Toledo Filho, 2012
13	22481	-	-	Corinaldesi, 2012
14	23207	-	-	Habel 2006
15	24091	-	-	Randl et al., 2014
16	18086	-	-	
17	20218	-	-	
18	23714	-	-	
19	25382	-	9.28E+06	Hajar et al., 2004
20	-	37855	-	Talebinejad et al., 2004
21	-	39740	-	
22	-	44527	-	
23	-	47137	-	
24	-	34954	-	
25	-	33359	-	
26	-	36985	-	
27	-	42786	-	
28	-	30748	-	
29	-	23641	-	
30	-	27122	-	
31	-	33359	-	
32	-	22626	-	
33	-	41771	-	
34	-	44672	-	
35	-	42206	-	
36	-	39160	-	

Table 2-5 Mechanical Properties of UHPC Mix Designs from Various Sources (Continued)

Mix No.	28-Day f'c w/o Heat Cure (psi)	28-Day f'c w/ Heat Cure (psi)	Modulus of Elasticity (psi)	Source
37	-	44817	-	Talebinejad et al., 2004
38	-	42351	-	
39	-	40611	-	
40	-	36695	-	
41	-	41916	-	
42	-	38000	-	
43	-	34374	-	
44	-	26832	-	
45	-	33069	-	
46	-	30313	-	
47	-	28282	-	
48	-	32489	-	
49	-	39160	-	
50	-	25092	-	
51	-	35969	-	
52	-	35244	-	
53	-	29443	-	
54	-	23206	-	
55	-	36114	-	
56	-	33794	-	
57	22046	-	-	
58	-	29733	-	Graybeal et al., 2008
58	-	27557	-	
59	-	29000	-	
59	-	21756	-	
60	-	25240	7.33E+06	Ritter et al., 2015
61	-	23525	-	Shakhmenko et al., 2012
62	-	20755	-	Justs et al., 2012
63	-	21973	-	
64	-	16244	-	Ha et al., 2012
65	-	15954	-	
66	-	15664	-	
67	-	16389	-	
68	-	28718	-	Ductal ®
69	-	28863	-	BSI ®
70	-	24366	-	$CEMTEC_{multiscale}$ ®
71	-	33765	-	Heinz et al., 2012
72	-	23670	-	

Table 2-5 Mechanical Properties of UHPC Mix Designs from Various Sources (Continued)

Mix No.	28-Day f'c w/o Heat Cure (psi)	28-Day f'c w/ Heat Cure (psi)	Modulus of Elasticity (psi)	Source
73	-	28877	-	
74	-	27267	-	Francisco et al., 2012
75	-	26147	5.80E+06	Prem et al., 2012
76	-	24698	5.66E+06	
77	-	25919	6.38E+06	
78	-	23786	5.80E+06	
79	-	19145	4.64E+06	
80	-	17796	5.66E+06	Prabha et al., 2014
81	-	21147	6.09E+06	
82	-	23467	6.38E+06	
83	-	19856	5.95E+06	
84	-	24845	6.50E+06	
85	-	22640	5.51E+06	
86	-	22669	6.09E+06	
87	-	36260	8.85E+06	Wille et al., 2013

Table 2-6 Compressive vs. Tensile Strength of UHPC

Mix No.	28-Day Compressive Strength		28-Day Tensile Strength		f_t/f'_c	Source
	f'_c w/o Heat Cure (psi)	f'_c w/ Heat Cure (psi)	f_t w/o Heat Cure (psi)	f_t w/ Heat Cure (psi)		
2	18130	-	2031		11.20	Khayat et al., 2014
3	17985	-	1595		8.87	
4	17985	-	1740		9.67	
5	15519	-	1450		9.34	
19	25382	-	1160		4.57	Hajar et al., 2004
60	-	25240	-	1160	4.60	Ritter et al., 2015
68	-	28718	-	1160	4.04	Ductal ®
69	-	28863	-	1276	4.42	BSI ®
75	-	26147	-	3452	13.20	Prem et al., 2012
76	-	24698	-	3278	13.27	
77	-	25919	-	2930	11.30	
78	-	23786	-	2611	10.98	
79	-	19145	-	1639	8.56	
87	-	36260	-	2611	7.20	Wille et al., 2013

A notable feature of UHPC tensile behavior is strain hardening. Figure 2.2 illustrates the tensile behavior of strain-hardening UHPC and conventional fiber reinforced concrete (FRC). The UHPC experiences three stages in the stress-strain curve. Stage I exhibits linear-elastic behavior until its

first series of cracks at σ_{cc} (point A). Stage II is the strain-hardening stage where numerous cracks develop throughout the entire specimen. On the other hand, FRC loses all its strength after its first signs of cracking. Stage III is where the post-cracking stress σ_{pc} (point B) is reached where crack localization and softening occurs for both UHPC and FRC (Naaman, 2002).

Another superior mechanical property of UHPC is exceptional freeze-thaw durability that results from UHPC low porosity. When water freezes, it experiences an approximate 9% increase in volume. When water penetrates the voids of normal strength concrete and freezes, the sudden increase in volume of water, once frozen, can rupture the voids causing the concrete to crack (Portland Cement Association, n.d.).

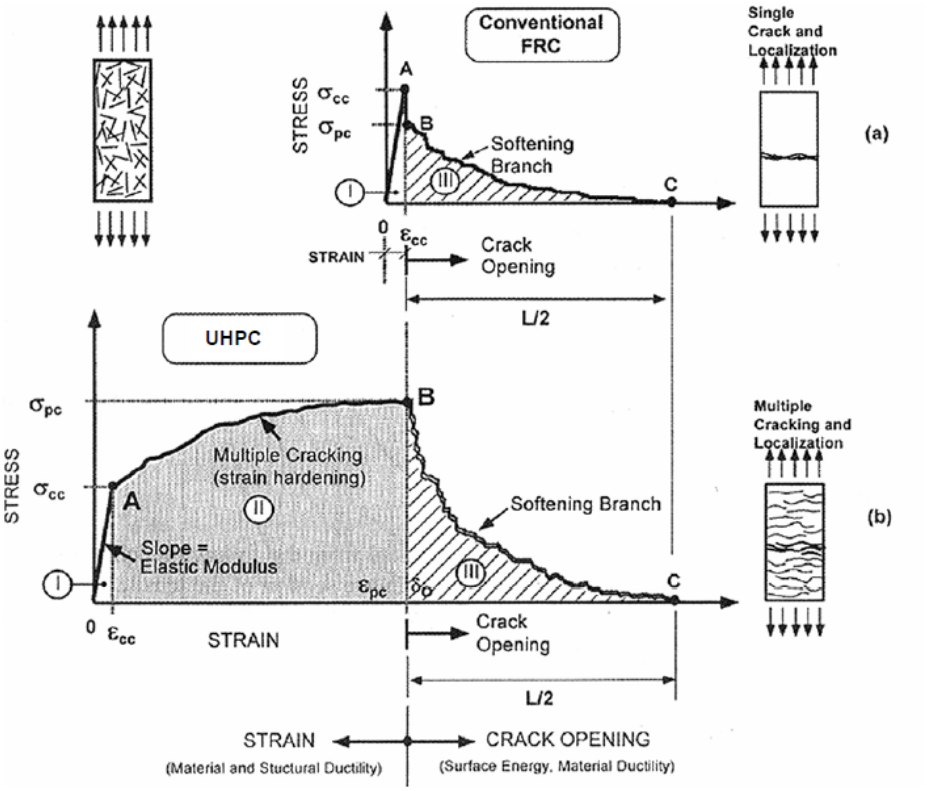

Figure 2.2 Tensile behavior of FRC and UHPC (Naaman, 2002).

2.2.5 Applications

In this section, several examples and real life projects that utilized UHPC for different architectural and structural applications (in both buildings and bridges) are briefly presented.

2.2.5.1 Architectural Applications

Shawnessy Light Rail Transit Station (Calgary, Canada): The Shawnessy Light Rail Transit Station utilizes the first architectural application of UHPC. Completed in 2004, this was the first station to utilize thin-shelled UHPC canopies on single column supports. The Shawnessy Light Rail Transit Station has 24 thin-shelled canopies measuring 16.7 ft x 19.7 ft x 0.79 in and was cast through an injection process into steel forms. UHPC was used for this architectural application for its high compressive and tensile strength, ease of fabrication, and high quality surface finish (Perry et al., 2004).

Fondation Louis Vuitton (Paris, France): Designed by Frank Gehry, the Fondation Louis Vuitton stands tall at 150 ft and covers approximately 130,000 sq. ft. In collaboration with the precast concrete manufacturer, Bonna Sabla, the team used Lafarge's Ductal UHPC mix design to fabricate and erect 16,000 exterior UHPC wall panels each measuring approximately 5 ft long, 1.3 ft high, and 1 in thick. Since each panel has its own curvature and unique geometry, they were cast using a combination of vacuum processes and flexible molds that can take form of any 3-D curvature. This process, RFR/teSS, was devised by Lafarge and Cogitech Design as a result of two years of research and later patented by Lafarge in 2008. The panels are then heat cured for 20 hours and scanned to produce a 3-D model for a quality check to ensure it is within a one millimeter tolerance. Because of the immense number of panels, to avoid confusion during fabrication, each panel is assigned a number and a radio frequency ID chip for tracking purposes (Ductal® Solutions, 2011).

The Atrium (Victoria, Canada): With thermal insulation, shading from the sun, and impact resistance in mind, the Atrium utilizes approximately 690 UHPC panels to form a complex façade surrounding a seven story structure. Because of the tight radial curves in the façade design, a flat panel system was originally planned. Unfortunately, this would require unwanted cuts around the curves creating undesirable seams that were unpleasant to the eye. As a solution, Ductal was contracted for the spandrel panel section of the curtain wall system to create all 690 panels from three different molds. Because of UHPC's absence of rebar, tighter radial curves were achieved without gaps or unpleasant seams all while keeping the panels thin and lightweight. The 204,000 sq. ft structure earned a LEED Gold rating through the Canada Green Building Council for its use of UHPC (Ductal® Solutions, 2011).

The Rotman School of Management Expansion (Toronto, Canada): Designed by the architects, Kuwabara Payne McKenna Blumberg, the Rotman School of Management required a panel design with a specific color and texture quality. To add to that, the university required a long span façade panel that was thin, lightweight, and strong with little to no wear from weather. Conventional materials such as stone panels had severe limitations in size and weight and aluminum panels just simply did not fit the desired finish. UHPC was eventually selected as the panel material because it provided a thin, monolithic-plate, slab-type design that provided the desired color and surface finish. More than 350 precast Ductal® panels were used with sizes ranging from 1.6 ft – 3.3 ft wide to 11.5ft – 17ft high with a thickness of 1.2 in. The structural received a LEED Silver rating for its use of UHPC (Ductal®, n.d.).

Cap Cinéma (Rodez, France): The entrance of the multiplex cinema, Cap Cinéma, utilizes an overhanging UHPC canopy measuring 47 ft x 57 ft x 1.6 in that can shelter up to 300 people from various elements. Composed of 12 thin, precast UHPC panels, the uniqueness of this architectural canopy comes from its ability to accept LED lighting within the structure. cast by Bonna Sabla, block-outs were placed into the molds so that LED lighting systems can later be installed in the canopy. With the use of UHPC, the color and texture of the canopy present a seamless, and attractive appearance (Ductal®, n.d.).

Museum of European and Mediterranean Civilizations (Marseille, France): Designed by the architect, Rudy Ricciotti, the Museum of European and Mediterranean Civilizations features some of the most intriguing applications of UHPC. The museum is linked to the City of Marseille through two slender concrete pathways measuring 138 ft in length and 2.2 ft in height. The museum is also encased with a UHPC mesh that allows light to permeate through the structure as well as the aromas of the surrounding Mediterranean Sea. 384 panels were cast for two façades and the roof of the museum. A long 981 ft walkway suspended between the inside of the museum to the outside was made possible with the use of UHPC (Ductal®, n.d.).

2.2.5.2 Structural Applications in Bridges

Sherbrooke Pedestrian Bridge (Quebec, Canada): Constructed in 1997, the Sherbrooke Pedestrian Bridge was the first pedestrian/bikeway bridge to incorporate UHPC in Canada. The Sherbrooke Pedestrian Bridge illustrates a very innovative composite use between steel and UHPC. The bridge spans a little under 200 ft and is constructed with six 1.2 in deep precast

segments. An underside space truss design was also utilized with the truss members formed with stainless steel tubes filled with tri-axially confirmed, post-tensioned UHPC (Perry et al., n.d.).

Little Cedar Creek Bridge (Wapello County, Iowa): Completed in May 2007, the Little Cedar Creek Bridge is the first bridge to utilize UHPC waffle deck panels, girders, and field-cast joints in North America. The 63 ft long x 32 ft wide bridge utilizes five Iowa bulb-tee precast, prestressed concrete girders in conjunction with fourteen 8 in deep waffle slabs that are 15 ft long x 8 ft wide. The waffle slabs are connected through short extended rebar with field-cast UHPC closures. Due to the use of UHPC in the Iowa bulb-tee girders and panels, each girder has a reduced section size with no non-prestressed reinforcements leading to a less invasive structure with lower applied loads. Since each panel was installed individually, repairs are especially convenient. Lanes can be replaced one at a time without disturbing the flow of traffic; an ideal concept for future highway design (Moore, 2012).

Mission Bridge (British Columbia, Canada): Completed in 1973, the old Mission Bridge was in need of seismic retrofit to account for today's seismic standards. Original plans of compaction piles (which was deemed too expensive) and conventional concrete jackets (which would be too invasive) were scraped and Ductal® jacketing was eventually chosen for the piers. UHPC provides high seismic deformation capacities making it the ideal material for this retrofit. The retrofit design called for tapered, rectangular columns measuring 7 ft x 8.5 ft with a height of approximately 10.5 ft. Dowels one inch in diameter were installed into the existing concrete with rebar spaced at 9 in in both directions. A strong formwork was then installed around the column and a 9 in thick UHPC jacket was cast using a standard hopper. To avoid cold joints, Lafarge used their ready-mix concrete plant in Abbotsford, British Columbia with two ready-mix trucks making two trips each. The casting was completed in one day with approximately $1.5 Million Canadian Dollars saved (Ductal®, n.d.).

Mackenzie River Twin Bridges (Ontario, Canada): Part of the TransCanada Highway realignment, the project consisted of two, two-lane, three-span bridges spanning 591 ft over the Mackenzie River. The bridges utilize steel plate girders of varying depths with 130 lightly prestressed, precast concrete deck panels that run the entire length of the bridge. Each panel is approximately 10 ft. x 48 ft. x 9 in. and is connected by Ductal® field-cast between the transverse joints, shear pockets, and haunches of each panel. This project is currently the largest field-cast

Ductal® project in North America and was completed by an 18-man crew over 10 days (Ductal®, n.d.).

Chukuni River Bridge (Ontario, Canada): The Chukuni River Bridge spans 274 ft and is currently the longest single span bridge in Canada. The elimination of pier construction in the water allows for a less invasive erection of the bridge ultimately leaving a smaller environmental footprint. Constructed with four 12-ft deep steel beams and 54 precast concrete deck panels, UHPC field-cast connections were used to connect each panel to one another with shear pockets to connect the deck to the steel girders. UHPC field-cast connections were used because it is significantly stronger than the precast concrete deck panel itself and has a very short bond development length. This allows for smaller field connections which in return reduces the manufacturing costs of the precast concrete panels (Ductal®, n.d.).

Gärtnerplatz Bridge (Kassel, Germany): The Gärtnerplatz Bridge is a 437 ft hybrid bridge constructed for pedestrians and cyclists and was one of the first structures in Germany to utilize UHPC. The bridge is made up of a steel and UHPC composite space frame design and consists of UHPC precast, prestressed upper chords, tubular steel for the lower chords, and UHPC precast prestressed bridge deck panels that span across the entire length of the bridge. The deck panels are unusually glued to the upper chords without any mechanical connections (Stengel et al., 2009).

2.2.5.3 Structural Applications in Buildings

Haneda Airport (Tokyo, Japan): With an increasing amount of flights arriving and departing from the Haneda Airport, a new runway was proposed to meet these demands. However, due to the limitations of space, the runway had to be constructed into the neighboring sea stretching over an area of 620,000 yd^2 and divided into two structures. The first structure consists of 230 ft steel pillars with special coatings submerged underwater. The second structure is a concrete slab with an area of 230,000 yd^2 attached to steel girders. Because of UHPC's extreme resistance to salt corrosion, it was selected as the material of choice for the concrete slabs. The final product contained 6,139 pre-tensioned, lightweight UHPC slabs joined together to form the entire structure (Ductal®, n.d.).

Renovation of a Pool (Amiens, France): Contracted by the City of Amiens, 15 reinforced concrete columns surrounding an indoor swimming pool were in desperate need of repairs due to corrosion caused by the pool's chlorine. UHPC was selected to rebuild the columns because the

diffusion of chlorine ions is 100 times slower in UHPC compared to conventional concrete (Ductal®, n.d.).

2.3 LIFE CYCLE ASSESSMENT

To help understand and quantify its environmental impacts, this section briefly discusses UHPC contribution to the life cycle assessment of three actual bridges from a previous study. A life cycle assessment is defined as an analysis of a structure's environmental impact from construction to demolition. This includes many stages before, in-between, and after the structure's life including raw material extraction, manufacturing, normal use, repairs, and maintenance (Environment Protection Agency, EPA n.d.). Thorsten Stengel and Peter Schieβl (2009) performed a life cycle assessment on the materials used on three bridges where UHPC was an essential component of the structure. The three bridges they analyzed are the Sherbrooke Pedestrian Bridge (Quebec, Canada), the Gärtnerplatz Bridge (Kassel, Germany), and the Mars Hill Bridge (Wapello County, Iowa). Stengel and Schieβl (2009) measured the ecological effects of global warming (GWP100), the depletion of the stratospheric ozone (ODP), the photo-oxidant formation (POCP), acidification (AP), and eutrophication (NP). While UHPC is considered a sustainable product for its durability, its cement content, unusual amount of superplasticizer, and use of micro steel fibers slightly offset the advantages of UHPC (Stengel et al., 2009).

The three aforementioned bridges life cycle (or environmental impact) assessment is shown in Figures 2.3, 2.4, and 2.5. The first (left hand side) part of each of Figure 2.3, 2.4, and 2.5 shows the results of the environmental impact assessment of the production of the materials used for the construction of the Sherbrooke Pedestrian Bridge, Gärtnerplatz Bridge, and Mars Hill Bridge, respectively. For example, the materials used for the Sherbrooke Pedestrian Bridge produced an environmental impact, using the metrics previously defined, of the following: GWP100: 4.45×104 kg CO_2 -eq, ODP: 1.85×10-3 kg CFC_{11} -eq, POCP: 21.6 kg C_2H_4 -eq, AP: 161.5 kg SO_2 -eq, and NP: 18.7 kg PO_4^3 -eq. The second part (right hand side) of Figures 2.5, 2.6, and 2.7 shows the percent contribution of each of the consumed materials to the environmental impact for the Sherbrooke Pedestrian Bridge, Gärtnerplatz Bridge, and Mars Hill Bridge, respectively.

Stengel and Schieβl (2009) concluded that even with reduced cross-sectional areas due to UHPC's high load bearing capacity (which implies less materials used), many other components are energy-intensive and are increased to guarantee its unique mechanical properties. Results show that UHPC

in the Sherbrooke Pedestrian Bridge contribute about 60 – 85% of the environmental impact and 44 – 74% for the Mars Hill Bridge. Accordingly, Stengel and Schieβl (2009) recommended to keep the use of cement, superplasticizers, and steel fibers to a minimum to reduce its environmental impact. This study conducted here and presented in this report uses the GWP environmental metric to compare the environmental impact of UHPC bridge piers against conventional NSC piers.

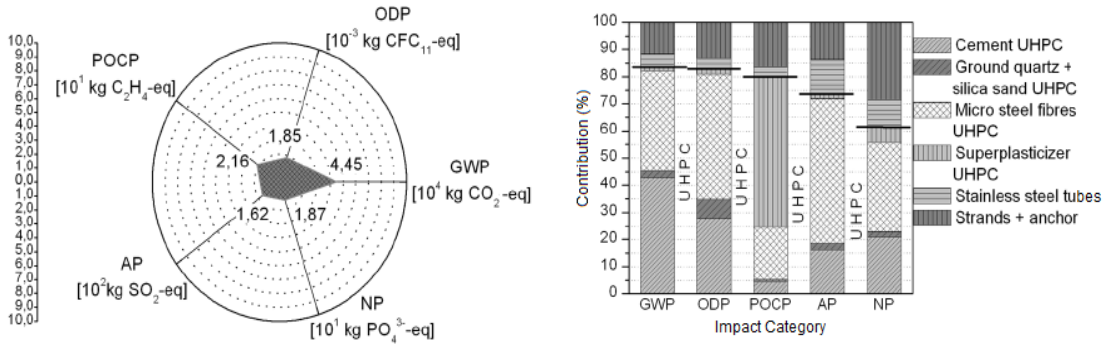

Figure 2.3 Environmental impact assessment of the production (left) and the percent contribution of each material (right) used in the Sherbrooke Pedestrian Bridge (Stengel et al., 2009).

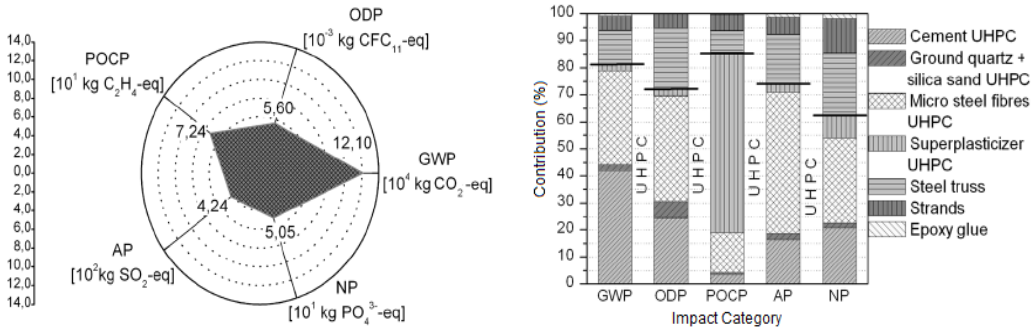

Figure 2.4 Environmental impact assessment of the production (left) and the percent contribution of each material (right) used in the Gärtnerplatz Bridge (Stengel et al., 2009).

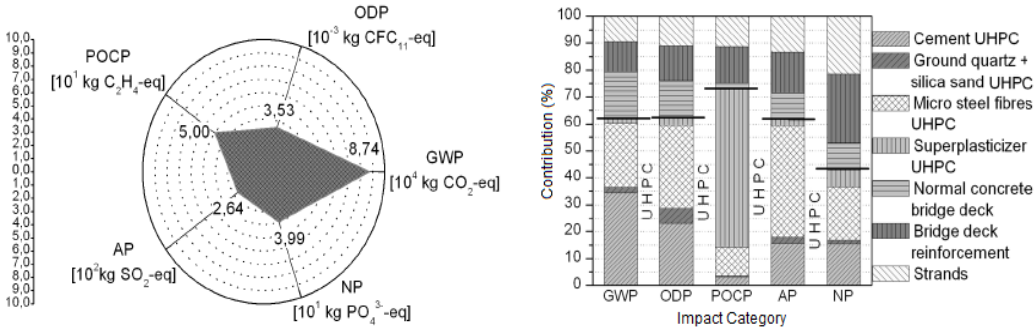

Figure 2.5 Environmental impact assessment of the production (left) and the percent contribution of each material (right) used in the Mars Hill Bridge (Stengel et al., 2009).

2.4 COST ASSESSMENT

As monetary cost analysis is an important part of this study, this section presents a brief summary of structural materials (including UHPC) cost comparisons over time. A comprehensive summary is provided by Voort et al. (2008) as follows: "UHPC is much more expensive than normal concrete. Much of the cost of UHPC comes from its steel fiber reinforcement, so the cost of the material is largely contingent on the cost of this component. In 1996, Bonneau et al. (1996) estimated the price of UHPC with fibers in Europe as \$1070/yd^3. Aïtcin (2000) reported a lower 1996 price of UHPC in Europe at \$760/yd^3. Aïtcin reported the price had decreased to \$570/yd^3 by the year 2000, which agrees fairly closely with Blais and Couture (1999) who reported a price of \$250/ton or \$520/yd^3 in 1999. As usage of UHPC becomes more common, the cost per cubic yard is expected to decrease significantly. Aïtcin (2000) predicts the cost of UHPC will soon reduce to \$460/yd^3 to \$500/yd^3 in Europe. The cost of UHPC in North America as of the year 2007 was comparatively high at approximately \$2000/yd^3 but is also expected to reduce with increased application in North America."If we compare \$570/yd^3 UHPC to a typical cost of 5000 psi NSC, UHPC is about 5.8 times more expensive based on volumetric values. While initial cost analyses may show UHPC to be an unnecessarily expensive alternative, overall reduced construction times, increased available floor space and clearances, longer service life, and minimal maintenance contribute to the cost savings significantly (Voort et al., 2008). Voort et al. (2008) also showed a cost per unit weight comparison between normal concrete, UHPC, and structural steel (Table 2-7), where the value used for UHPC is just an estimated value based on what has been achieved in Europe. The cost of UHPC is still high across North America due to the fact that there are not many UHPC manufacturers. Therefore, for the cost analysis conducted in this study (Chapter 6), different values are used for the UHPC cost per unit that range from current US market price (~\$2000/yd^3) to a hopeful reduced price when UHPC gets more common as in Europe (~\$550/yd^3). It is worth noting that for other materials such as HVFA concrete, fly ash replacement is more cost effective as it is approximately half the cost of cement (Voltz et al. 2012). Therefore, one way to reduce monetary and ecological costs of UHPC is natural replacements such as fly ash.

Table 2-7 Cost comparison between NSC, UHPC, and steel (Voort et al., 2008)

Material	Cost	Ratio to UHPC
Normal Strength Concrete	\$49/ton	1:5.6
UHPC	\$270/ton	1:1
Structural Steel	\$810/ton	3:1

3 Mix Design Analysis

UHPC mix designs and in turn, mechanical properties can vary significantly based on many different factors such as admixtures, steel fibers ratio, and curing methods. In order to identify the most structurally efficient and eco-friendly mix design, it is important to understand the effects of factors such as cement content, water-to-cement (W/C) ratio, silica fume, superplasticizers, etc. on UHPC mechanical properties (compressive strength, tensile strength, and modulus of elasticity). This chapter provides a preliminary analysis, based on data from available literature, of the effects of UHPC mix ingredients and relationships/trends between the resulting different mechanical properties.

3.1 EFFECTS OF CEMENT CONTENT

One of the disadvantages of UHPC is the large amount of cement required. While UHPC can achieve compressive strengths over 30 ksi, these strengths are not always a required design property. Based on data from the complied list of UHPC mixes (Table 2-2), the variation of the UHPC 28-day compressive strength with respect to its cement content is illustrated in Figure 3.1. Note that cases with and without heat curing are identified in the figure.

Higher cement contents can achieve higher compressive strengths especially with a heat cure. But high cement contents may not be practical for larger structures due to problems created by the heat of hydration of concrete. Temperatures as high as 100^{o}F have been observed in mixes with a high cement content during its setting period (PCA, 1997). While most minor concrete structures dissipate heat into the air or ground, larger structures have trouble releasing the heat and undergo non-uniform cooling. This can lead to thermal contraction, ultimately leading to cracking. In a separate study, Graybeal et al. (2003) recorded temperature as it varied with time for the same mix design (Mix #1 from Table 2-2 and 2-5) as shown in Figure 3.2. The figure illustrates the temperature in a 6 in diameter by 12 in tall cylinder with and without accelerator throughout a 70 hour period. Specimens with accelerator experienced a spike in temperature 30 hours sooner than specimens without accelerator and also produced higher peak temperatures. Moreover, Figure 3.3 illustrates the temperature versus time results of a cylinder from casting through steam curing throughout a 100-hour period. In this case of steam curing, much higher temperatures were observed, which also lasted for longer periods.

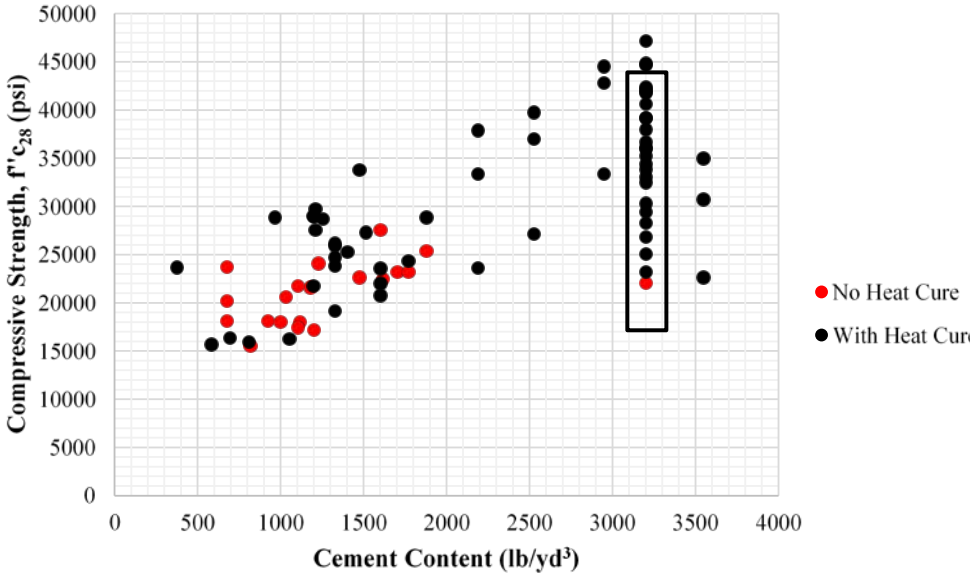

Figure 3.1 UHPC f'c at 28 days versus cement content.

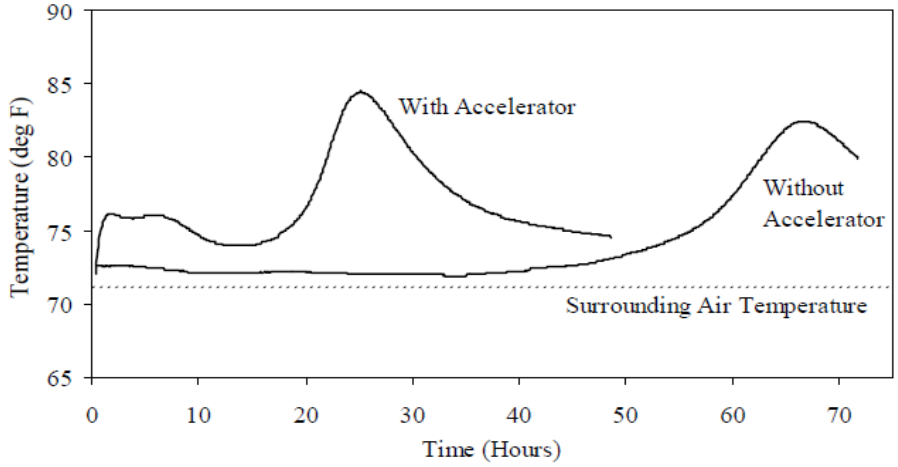

Figure 3.2 Temperature versus time with and without accelerator (Graybeal et al., 2003).

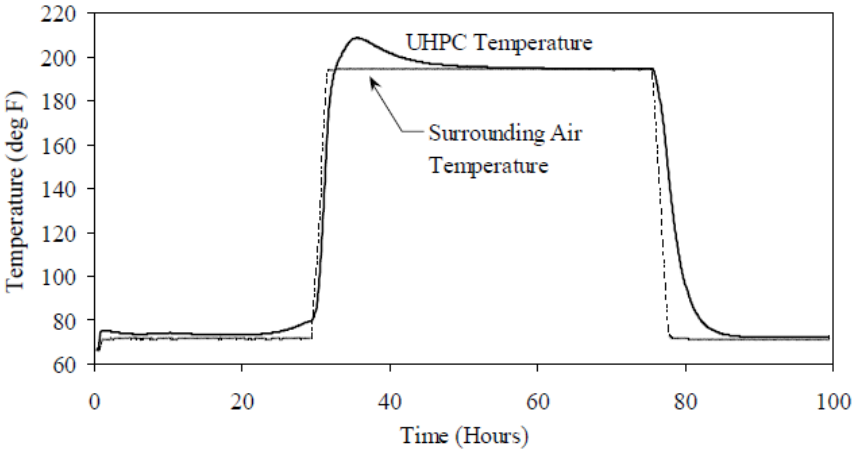

Figure 3.3 Temperature vs. time from casting through steam curing (Graybeal et al., 2003).

By identifying a mix design with a practical compressive strength and optimal cement content, the chances of a high exothermic reaction can be lowered, along with the amount of CO_2 produced. Using approximated metrics from the Portland Cement Association (1 lb of CO_2 is emitted for every 1.08 lb of portland cement produced), Figure 3.4 was produced to show the various CO_2 emissions for each mix design compared to its compression strength. Compressive strengths between 25-30 ksi can still be achieved while producing the equivalent CO_2 to mix designs below 20 ksi.

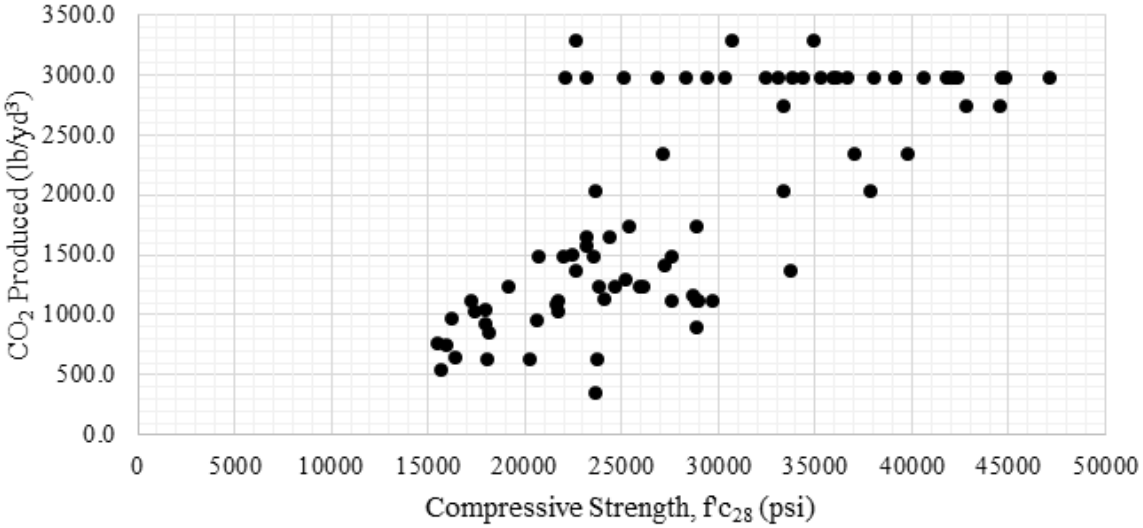

Figure 3.4 CO_2 produced versus UHPC compressive strength.

3.2 EFFECTS OF SILICA FUME

Silica fume, or microsilica, is a byproduct of silicon metal or ferrosilicon alloys. Because of the fine composition of noncrystalline silica, large surface area, and high silicon dioxide (SiO_2) content, silica fume is a very effective pozzolanic additive for UHPC (ACI 116R-00; SFA, n.d.).

UHPC mix design numbers #23 and #33-#56 from Table 2-2 (also marked on Figure 3.1 with a box) all have the same 3203 lb/yd^3 of cement but each vary in compressive strength and silica fume content. Talebinejad et al. (2004) performed laboratory tests on those mixes (#23 and #33-#56 which are summarized again in more details in Table 3-1 below) and considered the following: sieve analysis, cement and silica fume grounding, and curing methods. The quartzite used in the mix designs were ground to a maximum size of 0.0393 in and mixed with micro steel fibers with a diameter and length of 0.00393 in and 0.47 in, respectively. Talebinejad et al. (2004) utilized

type 5 cement because of its absence of tricalcium aluminate (C_3A). The lack of C_3A allows for the superplasticizers to be more effective and therefore requiring a smaller water-to-cement (W/C) ratio. The mix was compressed in a 3-cell 2x2x2 in mold and pressed with a 2-ton load to remove any entrained air. Four different curing processes were then used on each mix design.

In order to compare the effects of silica fume on W/C ratio, the study by Talebinejad et al. (2004) focused on Type-4 curing only (seven days in 68 ^oF water, two days in 194 ^oF water, two days in 392 ^oF dry air, and the remaining 17 days in 68 ^oF water). Figure 3.5 shows that silica fume is most effective when its weight is 800 lb/yd^3, i.e. 25% of the given 3203 lb/yd^3 cement content. The addition of this amount of silica fume produces the highest compressive strengths with lowest W/C ratio at 11.5%.

Table 3-1 Mix Designs Utilized by Talebinejad et al. (2004)

Mix No.	lb/yd^3				W/C	Cure Type	psi
	Cement	Silica Fume	Steel Fibers	Water			$f'c_{28}$
23	3203	801	32	368	0.115	4	47137
33	3203	641	32	368	0.115	4	41771
34	3203	961	32	368	0.115	4	44672
35	3203	1121	32	368	0.115	4	42206
36	3203	641	32	384	0.120	4	39160
37	3203	801	32	384	0.120	4	44817
38	3203	961	32	384	0.120	4	42351
39	3203	1121	32	384	0.120	4	40611
40	3203	641	32	416	0.130	4	36695
41	3203	801	32	416	0.130	4	41916
42	3203	961	32	416	0.130	4	38000
43	3203	1121	32	416	0.130	4	34374
44	3203	641	32	544	0.170	4	26832
45	3203	801	32	544	0.170	4	33069
46	3203	961	32	544	0.170	4	30313
47	3203	1121	32	544	0.170	4	28282
48	3203	801	32	320	0.100	4	32489
49	3203	801	32	352	0.110	4	39160
50	3203	801	32	641	0.200	4	25092
51	3203	801	32	368	0.115	4	35969
52	3203	801	32	416	0.130	4	35244
53	3203	801	32	544	0.170	4	29443
54	3203	801	32	641	0.200	4	23206

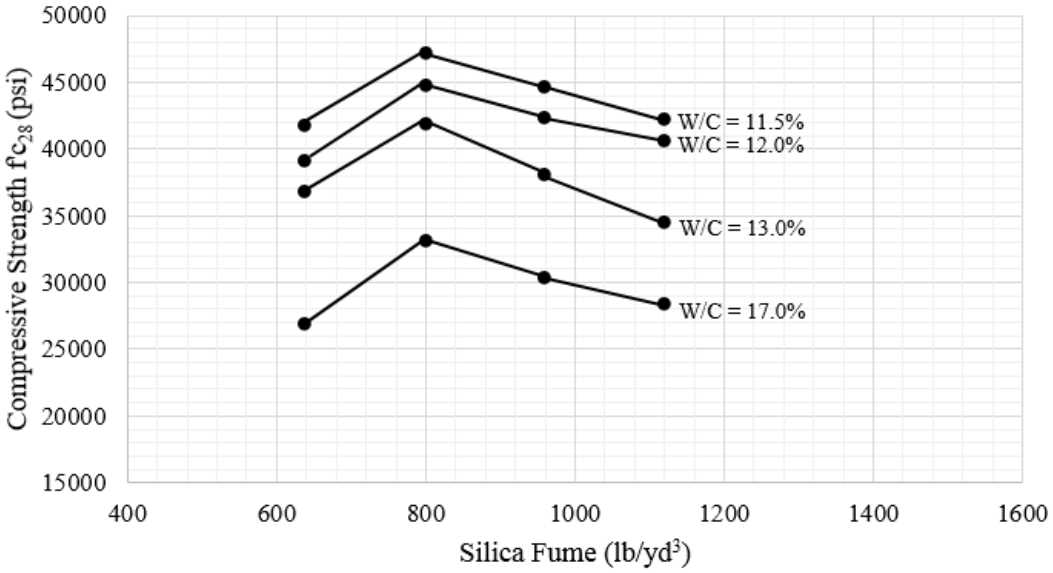

Figure 3.5 f'c at 28 days versus silica fume content (Talebinejad et al., 2004).

3.3 EFFECTS OF W/C RATIO

The W/C ratio dictates the workability of UHPC and decreases the amount of voids within the mix. With an increased packing density, porosity of UHPC is lowered significantly and the un-hydrated cement particles can then act as aggregate. If reinforcing steel bars are used in conjunction with UHPC for larger structures, corrosion in the rebar can be neglected assuming no cracks develop. More than 80 W/C–f'_{c28} data points are available from the compiled UHPC mix designs list, which are compared in Figure 3.6. It is noted that mix designs with W/C ratios higher than 0.44 were omitted from this analysis as such high W/C is less typical for UHPC. The figure suggests that a lower W/C ratio produces a higher compressive strength for mix designs with the same volume of cement. This agrees with the well-known effect of W/C from conventional and NSC. Because the data trend in Figure 3.6 takes the form of an inverse function (y=1/x), we suggest to plot the f'_c versus the inverse of the W/C ratio, i.e. 1/(W/C) to better capture the trend mathematically through best fitting.

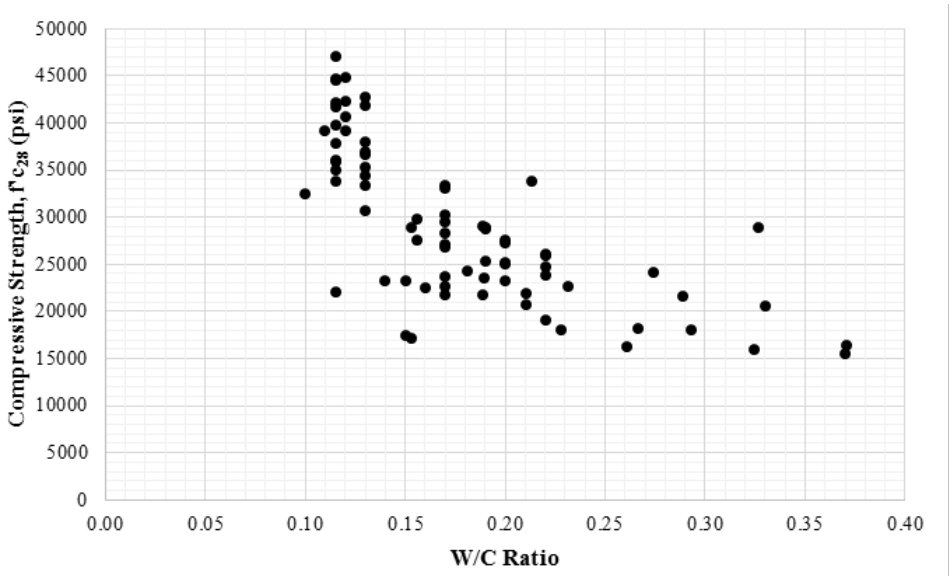

Figure 3.6 f'c_{28} vs. W/C ratio for different UHPC mixes.

The f'$_c$ at 28 days from the complied UHPC mix designs are plotted again but versus 1/(W/C) and a linear, exponential, and second-degree polynomial functions are best fitted to the data as shown in Figures 3.7, 3.8, and 3.9, respectively. The resulting equations from the best fitting are shown in each figure along with the coefficient of determination (R^2), which is a measure of how well the regression line represents the data, and summarized in Table 3-2. These equations provide a quick and reasonably accurate way of estimating the expected UHPC compressive strength based on a given W/C ratio or vice versa, which can be beneficial for UHPC mix design and optimization. Since the R^2 values are nearly the same, there is no preference on which equation to use. However, the linear equation might be recommended for simplicity to provide an estimate of f'$_c$.

Table 3-2 Summary of f'$_{c28}$ versus [1/(W/C)] best fit equations

Equation	Best Fit Type	Coefficient of Determination, R^2
$f'_c = 3720.2\left(\frac{1}{W/C}\right) + 7064.6$	Linear	0.7209
$f'_c = 13375e^{0.1254\left(\frac{1}{W/C}\right)}$	Exponential	0.7215
$f'_c = -45.196\left(\frac{1}{W/C}\right)^2 + 4302.9\left(\frac{1}{W/C}\right) + 5331.9$	2nd degree polynomial	0.7212

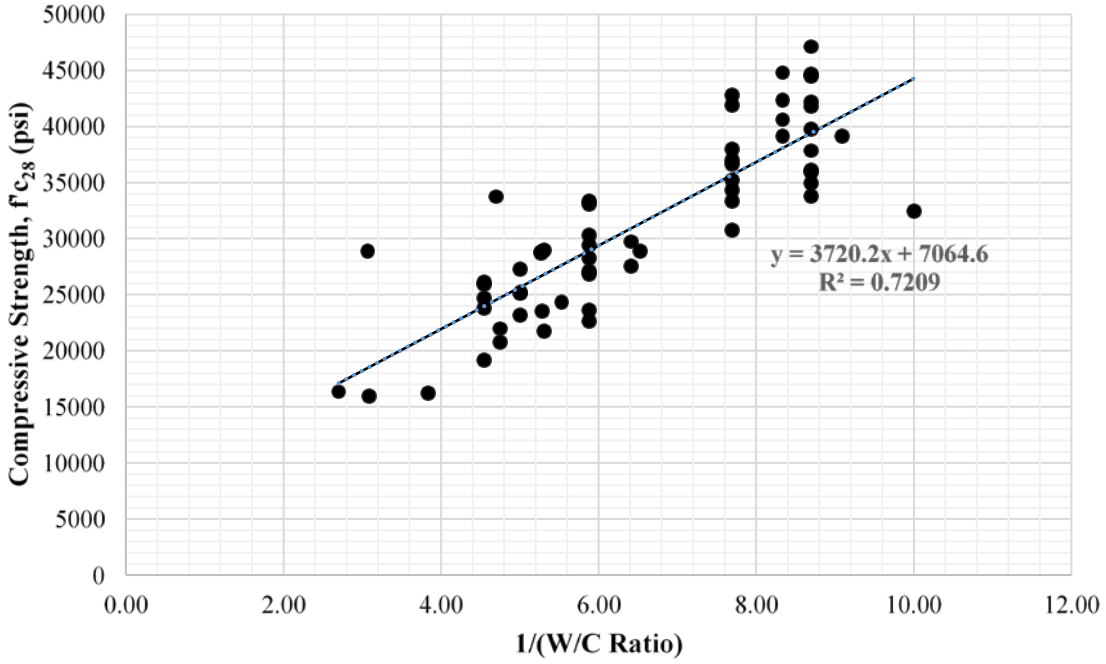

Figure 3.7 f'$_{c28}$ vs. [1/(W/C)] with a linear best fit.

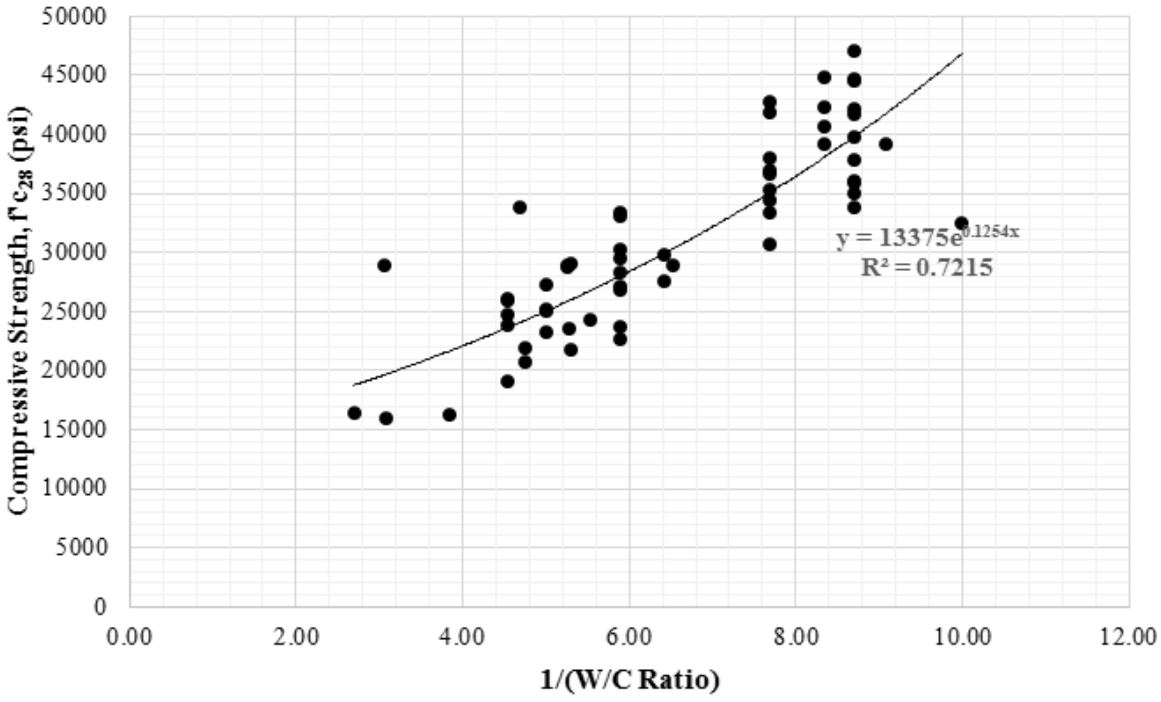

Figure 3.8 f'$_{c28}$ vs. [1/(W/C)] with an exponential best fit.

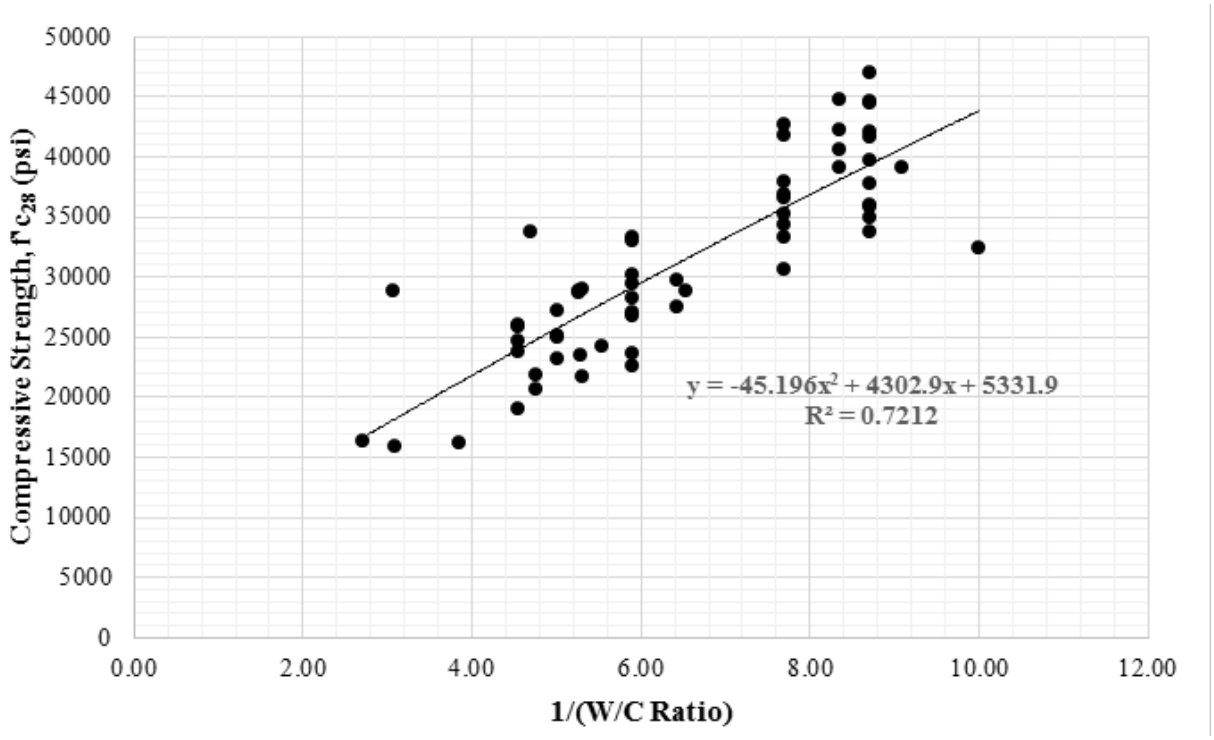

Figure 3.9 f'_{c28} vs. [1/(W/C)] with a 2nd degree polynomial best fit.

3.4 EFFECTS OF STEEL FIBERS

Tensile strength allows for the design of UHPC shells and structural members that can support pre-cracking and post-cracking loads without succumbing to brittle failures. Due to the small diameter and spacing of the steel fibers, the area of the steel is better distributed providing higher bonding capacity. To enhance the design of members in tension, steel fibers can be specially oriented in specific directions to better accept tensile forces (Khayat et al., 2014). Graybeal et al. (2013) found that UHPC can continue to carry a significant amount of tensile loads post-cracking due to the uniformly distributed steel fibers. This unique property will allow an increase in ductility and energy dissipation capacity throughout structural members. While properties such as tensile strength of the steel fibers or various curing methods can alter the tensile strength of the UHPC itself, Camacho et al. (2012) states that fiber geometry, such as fibers with hooked ends, may improve tensile performance and require additional studies. Recorded tensile strengths can also vary between each mix design depending on the testing method. Some methods include: mortar briquette tension test, direct cylinder tension tests, and split cylinder tension test. Figure 3.10 shows the failure mode from split cylinder tensile tests for mixes 2-5 from Table 2-2 performed

by Khayat and Meng (2014). The varying cracks come from different bond strengths between the steel fibers and concrete matrix.

Mix #2 **Mix #3** **Mix #4** **Mix #5**

Figure 3.10 Failure modes of UHPC test cylinders from split cylinder tests (Khayat et al., 2014).

3.5 EFFECTS OF HEAT CURING (WATER)

Talebinejad et al. (2004) conducted experiments using the same mix design but with four different curing methods. Each specimen was cured in room temperature water for the first seven days before any additional treatment. Table 3-3 summarizes the curing water temperature at each stage for each curing method. Only days 9-11 for the Type-4 cure are pursued in 392^{o}F dry air. It should be noted that methods 2-4 may not be practical for cast-in-place UHPC, but can be used for precast UHPC in controlled environments. While controlled curing can significantly increase the UHPC compressive strength, Table 3-4 summarizes the highest strength values obtained for each of the four curing methods. Type-4 curing produces the highest compressive strength at 47,137 psi, Type-3 at 36,114 psi, Type-2 at 33,794, and Type-1 at 22,046 psi. Thus, the overall highest compressive strengths were achieved using the Type-4 method.

Table 3-3 Curing Methods Utilized by Talebinejad et al. (2004)

<table>
<tr><th>Days</th><th>Type-1</th><th>Type-2</th><th>Type-3</th><th>Type-4</th></tr>
<tr><td>0-7</td><td rowspan="4">68^{o}F</td><td>68^{o}F</td><td>68^{o}F</td><td>68^{o}F</td></tr>
<tr><td>7-9</td><td>194^{o}F</td><td rowspan="2">194^{o}F</td><td>194^{o}F</td></tr>
<tr><td>9-11</td><td rowspan="2">68^{o}F</td><td>392^{o}F*</td></tr>
<tr><td>11-28</td><td>68^{o}F</td><td>68^{o}F</td></tr>
</table>

*Cured in dry air

Table 3-4 Variation of UHPC Highest Compressive Strength Obtained for Different Curing Methods Utilized by Talebinejad et al. (2004)

Mix No.	lb/yd^3				W/C	Cure Type	psi
	Cement	Silica Fume	Steel Fibers	Water			f'c_{28}
23	3203	801	32	368	0.115	4	47137
55	3203	801	32	368	0.115	3	36114
56	3203	801	32	368	0.115	2	33794
57	3203	801	32	368	0.115	1	22046

3.6 EFFECTS OF HEAT CURING (STEAM)

Rather than using varying temperatures of water, Graybeal et al. (2003) performed a study on mix #1 (Table 2-2, and summarized again in Table 3-5 for convenience) using different steaming methods. The specimens were processed through four different curing methods. The first method (steam) is a steam cure at 194^{o}F / 95% relative humidity for 48 hours, 24 hours after removing the specimen from the mold. The second method (ambient air) is to allow the specimen to remain at laboratory temperatures until it is ready for testing. The third method (tempered steam) is a lower temperature steam cure applied at 140^{o}F / 95% relative humidity for 48 hours, 24 hours after removing the specimen from the mold. The fourth and final method (delayed steam) is a delayed steaming method where the specimens are allowed to sit in laboratory temperatures for 15 days until it is finally cured at 194^{o}F / 95% relative humidity for 48 hours. Graybeal et al. (2003) performed various tests on many specimens including compressive testing of cylinders, mortar briquette tension tests, direct cylinder tension tests, and split cylinder tension tests to compare the effect of the four aforementioned steam curing methods. Table 3-6 summarizes the results for the compression tests for each curing method.

Table 3-5 Mix Design Utilized by Graybeal et al. (2003)

Mix No.	lb/yd^3						W/C
	Cement	Fine Sand	Silica Fume	Ground Quartz	Steel Fibers	Water	
1	1200	1720	390	355	263	184	0.153

Table 3-6 Average Compressive Strengths for Varying Curing Methods by Graybeal et al. (2003)

Curing Method	# of Samples	$f'c_{28}$ (ksi)	Standard Deviation (ksi)
Steam	96	28.0	2.1
Ambient Air	44	18.0	1.8
Tempered Steam	18	25.2	1.3
Delayed Steam	18	24.9	1.5

Graybeal et al. (2003) performed mortar briquette tension tests for samples cured by steam, ambient air, tempered steam, and delayed steam for various time intervals, according to AASHTO T132 with slight modifications. Figure 3.11 illustrates the tensile cracking results from the mortar briquette tension tests and the number of days after casting until testing for the different curing methods. As expected, steam curing has positive effects on tensile properties while specimens cured in ambient air for 28 days produced the lowest tensile strengths at an average of 0.9 ksi. Graybeal et al. (2003) also recorded the load-displacement relationship within the mortar briquette tension tests. They observed that the concrete sections continuously carried tensile loads after initial cracking. The load capacity finally reached zero when the steel fibers gradually pulled out and the entire section split. Figure 3.12 shows the load-displacement response for a steam cured mortar briquette and a circle marking where the UHPC begins to crack. They observed that the steam cured specimens demonstrated the best post-cracking behavior and had approximately twice the toughness of ambient air cured specimens. The tempered steam and delayed steam cured specimens had 1.5 times the toughness of ambient air cured specimens.

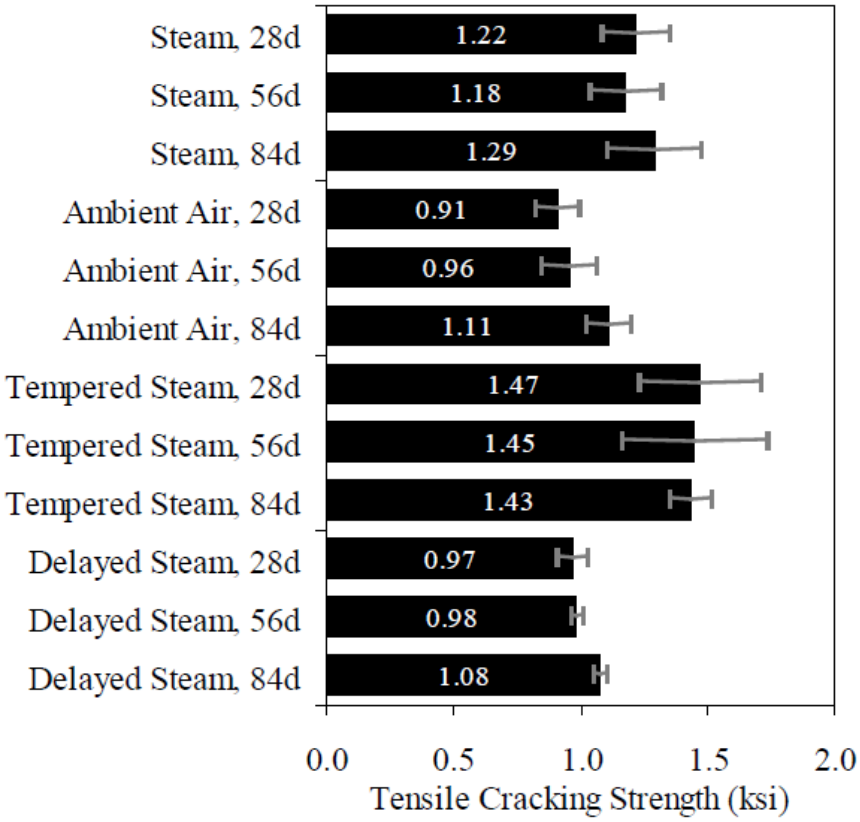

Figure 3.11 Tensile cracking results for mortar briquette tension tests (Graybeal et al., 2003).

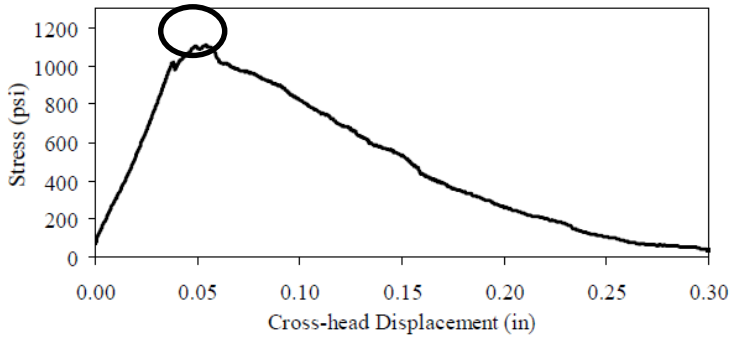

Figure 3.12 Load-displacement response for steam cured mortar specimens (Graybeal et al., 2003).

Spilt cylinder tests were also performed to estimate the tensile strength of UHPC indirectly through standard compression tests. Graybeal et al. (2003) used ASTM C496 testing standards with slight modifications. Figure 3.13 illustrates the tensile cracking results from the split cylinder tension tests and the number of days after casting before the tests were performed. Again, steam cured specimens produced the highest tensile cracking strengths at an average of 1.7 ksi. Tempered steam

specimens produced lower tensile cracking strengths at 1.6 ksi. Specimens cured in ambient air displayed continuously improving tensile strengths for each day that passed. The recorded load-displacement relationship within the split cylinder tension tests (Figure 3.14) showed significant post-cracking tensile strengths. It should be noted that there is a significant change in stiffness and lateral deformation after the initial cracking due to strain hardening effects.

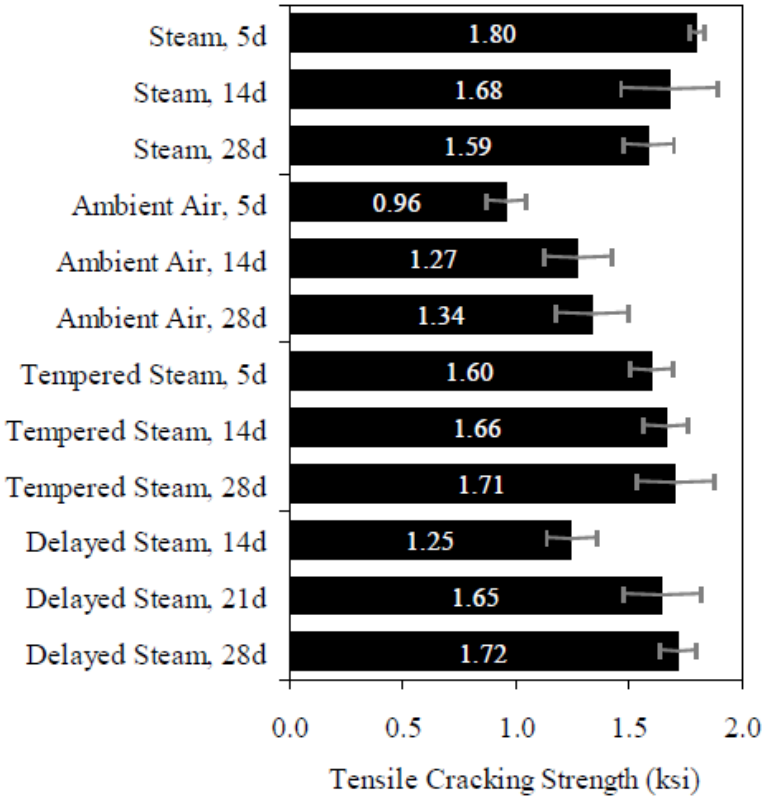

Figure 3.13 Tensile Cracking Results for Split Cylinder Tests (Graybeal et al., 2003).

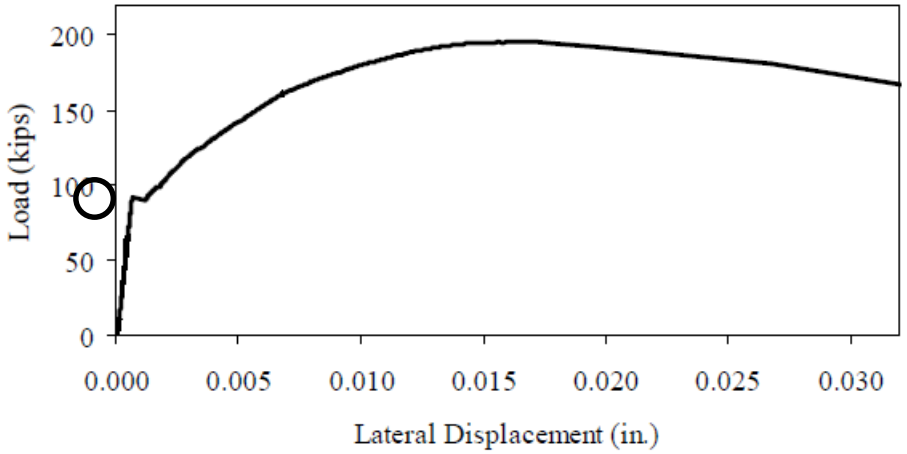

Figure 3.14 Load Displacement Response for Steam Cured, Split Cylinder Test Specimens (Graybeal et al., 2003).

The last type of tests conducted by Graybeal et al. (2003) to study how UHPC mechanical properties vary with curing types is direct cylinder tension tests, where the ends of the cylinder are adhered to the heads of the testing device. The cylinder direction tension test is based on the RILEM uniaxial tension test for steel fiber reinforced concrete and USBR 4914. Due to limited time constraints, tests were performed, at minimum, 50 days after casting. Table 3-7 summarizes the cylinder direction tension test results. Steam and delayed steam curing methods observed the highest average cracking strengths at 1.60 ksi and 1.62 ksi, respectively while specimens cured in ambient air had the lowest cracking strength at 0.82 ksi.

Table 3-7 Cylinder Direction Tension Testing Results Under Various Curing Methods (Graybeal et al., 2003)

Curing Method	# of Samples	Cracking Strength (ksi)	Standard Deviation (ksi)
Steam	3	1.60	0.13
Ambient Air	1	0.82	-
Tempered Steam	3	1.14	0.13
Delayed Steam	2	1.62	0.07

3.7 MODULUS OF ELASTICITY

All the previous sections in this chapter focused on summarizing the effects of UHPC mix ingredients or curing methods on its mechanical properties. In this section, and the subsequent one, the relation between the different mechanical properties are investigated. In one study performed by Graybeal (2006), an equation was proposed to estimate the modulus of elasticity (E_c) of UHPC using its compressive strength (f'_c) as follows:

$$E_c = 46{,}200\sqrt{f'_{c_{28}}} \tag{3-1}$$

Graybeal found that the above equation is not appropriate for UHPC mix designs with compressive strengths between 14 to 26 ksi, but also found that the modulus of elasticity is not dependent to the curing temperature of the specimen. More recently, Graybeal (2013) developed an updated equation to estimate the modulus of elasticity for all compressive strengths as follows:

$$E_c = 49{,}000\sqrt{f'_{c_{28}}} \tag{3-2}$$

In another study, Ma et al. (2004) was able to estimate the modulus of elasticity for mix designs not containing coarse aggregate.

$$E_c = 525{,}000\sqrt[3]{\frac{f'_{c_{28}}}{10}} \tag{3-3}$$

Equations 3-1, 3-2, and 3-3 (theoretical values) were compared to the modulus of elasticity actual values determined from actual tests for some of the mixes reported in Table 2-5 (rounded to the nearest 0.01E+06 psi) as summarized in Table 3-8. Ma et al. (2004) equation generated the lowest average percent error at 14% while Equation 3-2 generated the highest percent error at 19%. Moreover, Figure 3.15 shows the graph of the theoretical modulus of elasticity values calculated using compressive strength from the three equations as compared to the corresponding actual modulus of elasticity from experimental tests.

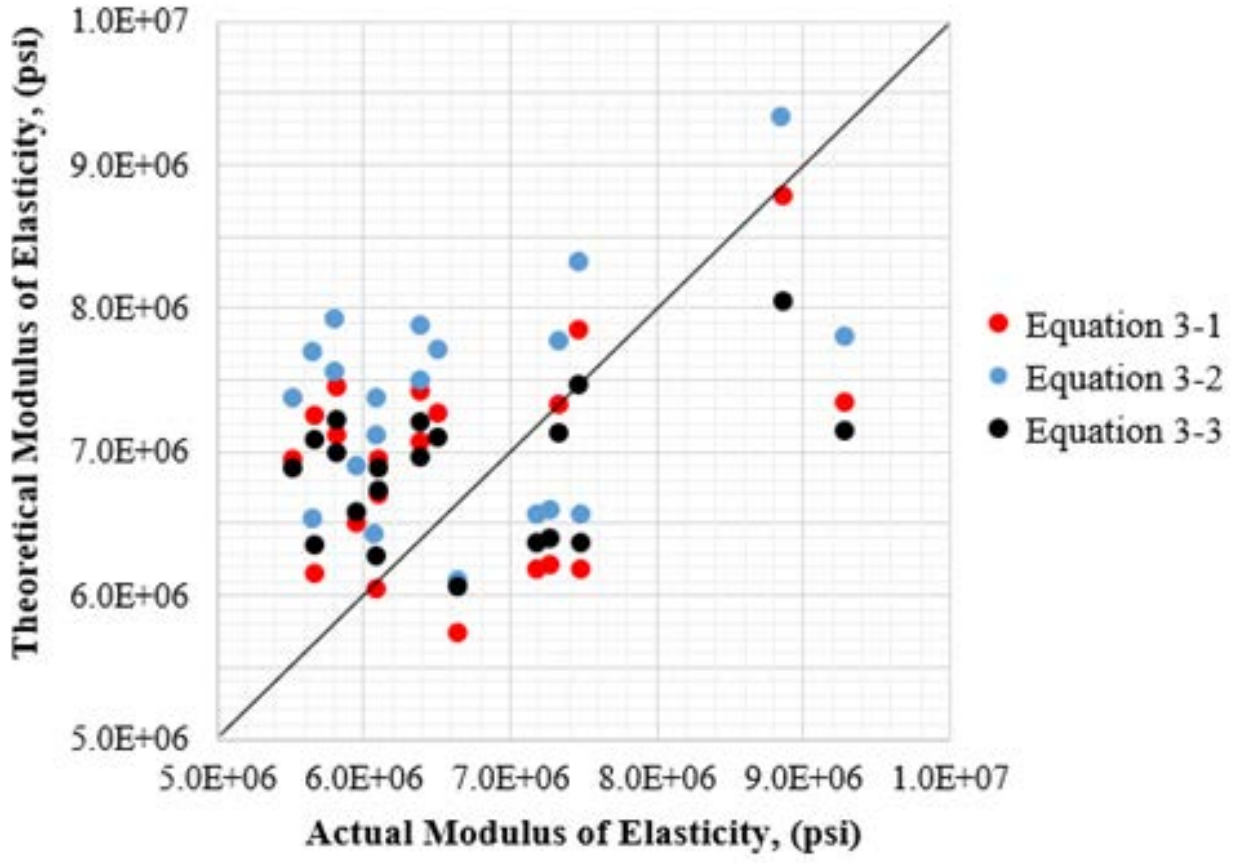

Figure 3.15 Theoretical E (from Equations 3-1, 3-2, and 3-3) vs. actual E from experimental tests.

Table 3-8 Comparison of Actual E_c vs. Theoretical E_c

Mix No.	f'c	E (psi)	Eq. 3.5 (psi)	Error (Eq. 3-1)	Eq. 3.6 (psi)	Error (Eq. 3-2)	Eq. 3.7 (psi)	Error (Eq. 3-3)
1	17200	6.07E+06	6.06E+06	0%	6.43E+06	6%	6.29E+06	4%
1	28900	7.46E+06	7.85E+06	5%	8.33E+06	12%	7.48E+06	0%
2	18130	7.27E+06	6.22E+06	14%	6.60E+06	9%	6.40E+06	12%
3	17985	7.18E+06	6.20E+06	14%	6.57E+06	8%	6.38E+06	11%
4	17985	7.48E+06	6.20E+06	17%	6.57E+06	12%	6.38E+06	15%
5	15519	6.64E+06	5.76E+06	13%	6.10E+06	8%	6.08E+06	8%
19	25382	9.28E+06	7.36E+06	21%	7.81E+06	16%	7.16E+06	23%
60	25240	7.33E+06	7.34E+06	0%	7.78E+06	6%	7.15E+06	2%
76	24698	5.66E+06	7.26E+06	28%	7.70E+06	36%	7.10E+06	25%
77	25919	6.38E+06	7.44E+06	17%	7.89E+06	24%	7.21E+06	13%
78	23786	5.80E+06	7.13E+06	23%	7.56E+06	30%	7.01E+06	21%
79	19145	4.64E+06	6.39E+06	38%	6.78E+06	46%	6.52E+06	40%
80	17796	5.66E+06	6.16E+06	9%	6.54E+06	16%	6.36E+06	12%
81	21147	6.09E+06	6.72E+06	10%	7.13E+06	17%	6.74E+06	11%
82	23467	6.38E+06	7.08E+06	11%	7.51E+06	18%	6.98E+06	9%
83	19856	5.95E+06	6.51E+06	9%	6.90E+06	16%	6.60E+06	11%
84	24845	6.50E+06	7.28E+06	12%	7.72E+06	19%	7.11E+06	9%
85	22640	5.51E+06	6.95E+06	26%	7.37E+06	34%	6.89E+06	25%
86	22669	6.09E+06	6.96E+06	14%	7.38E+06	21%	6.90E+06	13%
87	36260	8.85E+06	8.80E+06	1%	9.33E+06	5%	8.07E+06	9%
			Avg % Error	**15%**	**Avg % Error**	**19%**	**Avg % Error**	**14%**
			S.Dev	**10%**	**S.Dev**	**12%**	**S.Dev**	**9%**

To better check the validity of the shown prediction equations for E, Figure 3.16 and Figure 3.17 respectively shows the graph of the square root of f'_c and the cubic root of f'_c divided by 10, for mixes shown in Table 3-8, versus actual modulus of elasticity values. The square root of f'_c is chosen to relate to Equations 3-1 and 3-2, while the cubic root divided by 10 is to relate to Equation 3-3. The best fit linear equation and R^2 values are shown on the figures. The slight linear trend suggests that the modulus of elasticity can be dependent to compressive strength with both Figure 3.16 and 3.17 showing nearly the same fit. The best fit equations (3-4 and 3-5) are as follows:

$$E = 28318\sqrt{f'_{c_{28}}} + 2.3E06 \tag{3-4}$$

$$E = 478296\sqrt[3]{\frac{f'_{c_{28}}}{10}} + 323467 \tag{3-5}$$

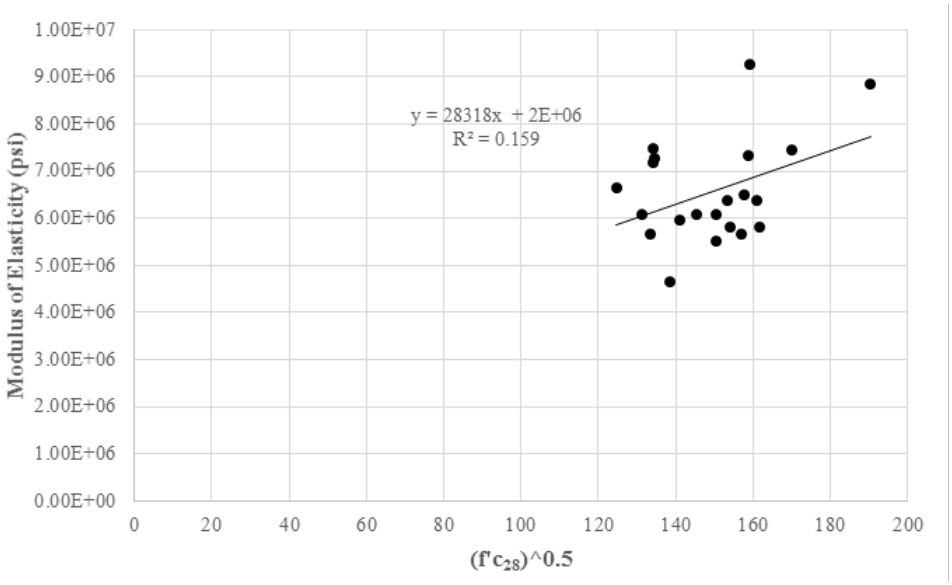

Figure 3.16 Modulus of Elasticity vs. (f'c_{28})^0.5

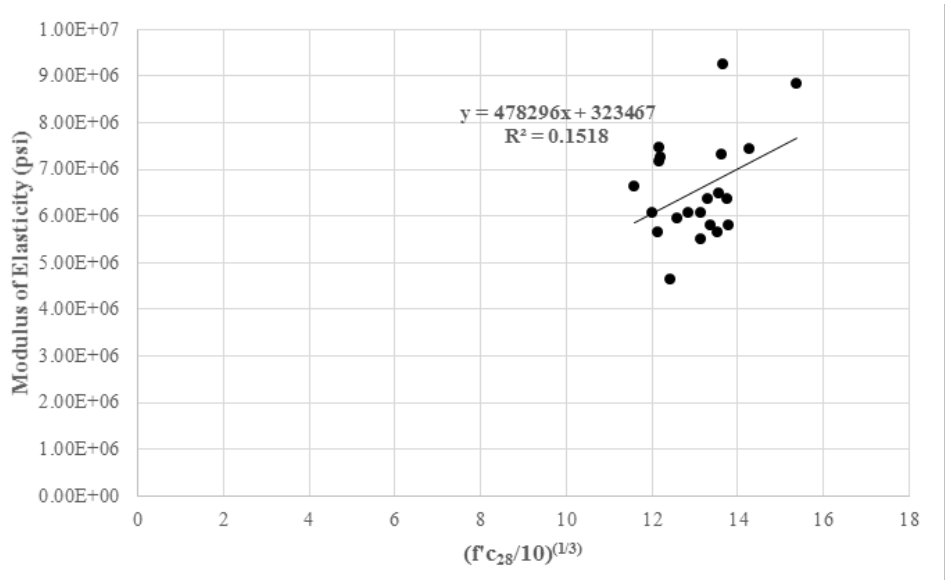

Figure 3.17 Modulus of Elasticity vs. (f'c_{28}/10)$^{(1/3)}$

3.8 TENSILE STRENGTH

As previously demonstrated, there are many direct and indirect methods of calculating various tensile strengths of UHPC through mortar briquette tension tests, direct cylinder tension tests, and split cylinder tension tests. Graybeal (2013) reports three equations (3-6 through 3-8) to calculate direct tensile strengths from UHPC cylinders using compressive strength. Moreover, Khayat et al. (2014) reports Equation 3-9 for splitting tensile strengths for UHPC cylinders using applied loads (P) and diameter (D) and length (L) of the test specimen (Adapted from ASTM C496). This method is generally not favored to measure the direct tensile strength of UHPC. Table 3.9 compares Graybeal's equations (3-6 and 3-8) to the reported values of mix numbers 2-5 and 68-69 from Table 2-5.

$f_{ct} = 7.8\sqrt{f'_c}$ direct tension depending on steam curing method (3-6)

$f_{ct} = 8.3\sqrt{f'_c}$ direct tension depending on tempered steam curing method (3-7)

$f_{ct} = 6.7\sqrt{f'_c}$ direct tension for untreated specimens (ambient air) (3-8)

$f_t = \frac{2P}{\pi DL}$ for splitting tension (3-9)

Table 3-9 Comparison of Actual f'$_{ct}$ vs. theoretical f'$_{ct}$ from Graybeal (2013)

Mix No.	f'$_c$ w/o Heat Cure (psi)	f'$_c$ w/ Heat Cure (psi)	f'$_{ct}$ w/o Heat Cure (psi)	f'$_{ct}$ w/ Heat Cure (psi)	Eq. 3-8 (psi)	Error Eq. 3-8	Eq. 3-6 (psi)	Error Eq. 3-6
2	18130	-	2031	-	902	56%	-	-
3	17985	-	1595	-	899	44%	-	-
4	17985	-	1740	-	899	48%	-	-
5	15519	-	1450	-	835	42%	-	-
68	-	28718	-	1160	-	-	1322	14%
69	-	28863	-	1276	-	-	1325	4%
75	-	26147	-	3452	-	-	1261	63%
76	-	24698	-	3278	-	-	1226	63%
77	-	25919	-	2930	-	-	1256	57%
78	-	23786	-	2611	-	-	1203	54%
79	-	19145	-	1639	-	-	1079	34%
					Avg. error	**41%**	**Avg. error**	**48%**
					S. Dev	**24%**	**S. Dev**	**6%**

It appears that both equations generate fairly high percent errors. This considerable underestimation of tensile strength may be caused by the fact that mix numbers 2-5 were left in

room temperature lime water until one hour before its tests. These effects are similar to Graybeal's results from his mortar briquette tension test and split cylinder test specimens left in ambient air, which increased in strength over time (Graybeal, 2003). Mix numbers 68-79 could have also been underestimated due to different heat curing methods or mix designs. Graybeal's Equation 3-6 through 3-8 are not accurate estimations of tensile strength in a universal setting, but may only serve for his mix designs and curing method only. Mortar briquette and direct cylinder tension tests should be performed to best estimate the tensile strength of the specimen.

4 Design of UHPC Piers using Computational Methods

This chapter focuses on the design of the substructure (bridge pier) of a prototype bridge using four different UHPC mixes with different mechanical properties. The selected prototype is the Caltrans Academy Bridge, for which the full cross-sections design and bridge detailing are available using conventional NSC. Thus, the new design achieved here using UHPC can be compared to the NSC baseline case. The chapter presents the design details of the original prototype NSC bridge pier, the modeling assumptions considered, and the sectional analysis used to design/optimize the UHPC piers.

4.1 PROTOTYPE BRIDGE

The prototype bridge considered in this study, designated as the Caltrans Academy Bridge, is a typical three-span California highway bridge with a prestressed reinforced concrete box-girder superstructure. The prototype bridge pier is redesigned using UHPC such that a bridge pier consists of two UHPC columns and a UHPC bent cap with a capacity controlled foundation. All design is made in accordance to the Caltrans Seismic Design Criteria (SDC 1.7, 2013) and AASHTO LRFD Bridge Design Specifications (2012). Table 4-1 displays a summary of the prototype bridge design specifications. The design of the superstructure is not considered in this study, and only the bridge piers are redesigned using UHPC, i.e. the new changes are on the column diameter and bent cap dimensions, and their reinforcing steel.

The UHPC columns are designed using four of the published UHPC mix designs, (summarized in Table 4-3) each selected with increasing strength from the comprehensive compiled list in Chapter 2. Actual values (based on experimental testing) of compressive strength, tensile strength, ultimate strain, strains at peak stress, and modulus of elasticity are used for the computational modeling as discussed in the following sections. By selecting a wide spectrum of mix designs with varying strengths, the most ecological and cost-friendly mix design can be discovered to create the most efficient multi-column bridge pier. Columns include longitudinal and transverse steel reinforcement with an expected yield strength (f_{ye}) and expected tensile strength (f_{ue}) of 66 ksi and 92 ksi, respectively. The gross area (A_g) of the columns is reduced to determine if the amount of cement consumed can ultimately be reduced and impact the amount of CO_2 produced. The design procedure is based on the Caltrans LRFD Bridge Design Example B (2004) from the Caltrans

Bridge Design Academy. This Caltrans design document (2004) readily provides the baseline case that consider conventional NSC (f'c = 4.0 ksi) for the bridge. A summary of the original NSC design is shown in Table 4.2 along with preliminary costs and environmental impact.

Table 4-1 Caltrans Academy Bridge (prototype) specifications

Superstructure Type	Prestressed reinforced concrete box girder
Substructure Type	Two bents; each bent has two columns
Span Lengths	126 ft. – 168 ft. – 118 ft.
Foundation	Piles
Seismic Design Category	D
Seismic Design Strategy	Type 1
Soil Profile	Type C
Peak Rock Acceleration	0.5g
Design Spectral Acceleration (S_{D1})	0.97g

Table 4-2 Original Column Design for Bent 2

Column Diameter	6.0 ft.
Column Height	44.0 ft.
Compressive Strength (f'_c)	4.0 ksi
Modulus of Elasticity of Concrete (E_c)	4,372 ksi
Longitudinal Reinforcement	26, #14 bars
Transverse Reinforcement	#8 hoop at 5 in. OC

Table 4-3 Summary of the Mechanical Properties of the UHPC Considered in this Study

Property	Original	UHPC 1	UHPC 2	UHPC 3	UHPC 4
Mix No.	-	#1	#81	#1	#87
f'_c (psi)	4,000	17,260	21,147	28,900	36,360
f_t (psi)	-	1,300	1,500*	1,700	2,611
E (ksi)	4,372	6,070	6,092	7,460	8,847
Strain at Peak Stress	0.002	0.0035	0.004442	0.0046	0.0047
Ultimate Strain	0.005	0.009	0.0146	0.01	0.015*

* Minimum value estimated for analysis.

4.2 COMPUTATIONAL MODELING

OpenSees (2000), or Open System for Earthquake Engineering Simulation, is an open source software framework that permits users to create serial and parallel finite element computer

applications used to simulate the response of structural and geotechnical systems subjected to various events such as earthquakes. Simulation applications for earthquake engineering through finite element methods can be produced using OpenSees, which ultimately focuses on capabilities used for performance-based design. Unlike many typical programs used in engineering, OpenSees remains an open source software framework to promote the research community to excel and allow for user experimentation and sharing. (OpenSeesWiki, n.d.)

In this study, the OpenSees platform is used to perform first column and beam cross-sectional analysis, then a nonlinear lateral pushover analysis on two-column bents, and ultimately, nonlinear time history analysis using several ground motions on two-column bents. All the analysis sets are conducted for five cases: normal strength concrete (NSC) and four UHPC mix designs each with increasing compressive strengths and added tensile properties. Due to the lack of previous research in UHPC modeling within OpenSees, the current existing concrete material models are investigated to check which model can better approximate the UHPC mechanical properties (especially tensile behavior). This investigation include analyses from OpenSees using Concrete02 and Concrete04 as well as the classical cross-sectional analysis platform XTRACT (Chadwell and Imbsen, 2004). Four UHPC mix designs are analyzed and compared to NSC in order to optimize the column and bent cap design. The following defines examples for the reinforcing steel and concrete uniaxial material models available in OpenSees.

ReinforcingSteel: "This command is used to construct a ReinforcingSteel uniaxial material object. This object is intended to be used in a reinforced concrete fiber section as the steel reinforcing material." (OpenSees Command Manual, 2003). The typical Code Line: *"uniaxialMaterial ReinforcingSteel $matTag $fy $fu $Es $Esh $esh $eult"*

where,

$fy	Yield stress in tension
$fu	Ultimate stress in tension
$Es	Initial elastic tangent
$Esh	Tangent at initial strain hardening
$esh	Strain corresponding to initial strain hardening
$eult	Strain at peak stress

Concrete01: "This command is used to construct a uniaxial Kent-Scott-Park concrete material object with degraded linear unloading/reloading stiffness according to the work of Karsan-Jirsa

and no tensile strength." (OpenSees Command Manual, 2003). Typical Code Line: *"uniaxialMaterial Concrete01 $matTag $fpc $epsc0 $fpcu $epsU"*

where,

$fpc	Concrete compressive strength at 28 days (inputted as a negative value)
$epsc0	Concrete strain at maximum strength
$fpcu	Concrete crushing strength
$epsU	Concrete strain at crushing strength

Concrete02: "This command is used to construct a uniaxial material with linear tensile softening." (OpenSees Command Manual, 2003). Typical Code line: *"uniaxialMaterial Concrete02 $matTag $fpc $epsc0 $fpcu $epsU $lambda $ft $Ets"*

where,

$lambda	Ratio between unloading slope at $epscu and initial slope
$ft	Tensile Strength
$Ets	Ratio between unloading slope at $epscu and initial slope tension softening stiffness (absolute value) (slope of the linear tension softening branch)

Concrete04: "This command is used to construct a uniaxial Popovics concrete material object with degraded linear unloading/reloading stiffness according to the work of Karsan-Jirsa and tensile strength with exponential decay." (OpenSees Command Manual, 2003). Typical Code line: *"uniaxialMaterial Concrete04 $matTag $fc $ec $ecu $Ec <$fct $et>"*

where,

$fc	Floating point values defining compressive strength at 28 days (compression is negative)
$ec	Floating point values defining concrete strain at maximum strength
$ecu	Floating point values defining concrete strain at crushing strength
$Ec	Floating point values defining initial stiffness
$fct	Floating point value defining the maximum tensile strength of concrete
$et	Floating point value defining ultimate tensile strain of concrete

A schematic representation of two of the uniaxial concrete constitutive models discussed above (Concrete01 and Concrete02) is shown in Figures 4.1 and 4.2, respectively. The figures define the input parameters used to define the material. An illustration of how Concrete02 is slightly modified to better capture the UHPC compressive and tensile behaviors is shown in Figure 4.2b.

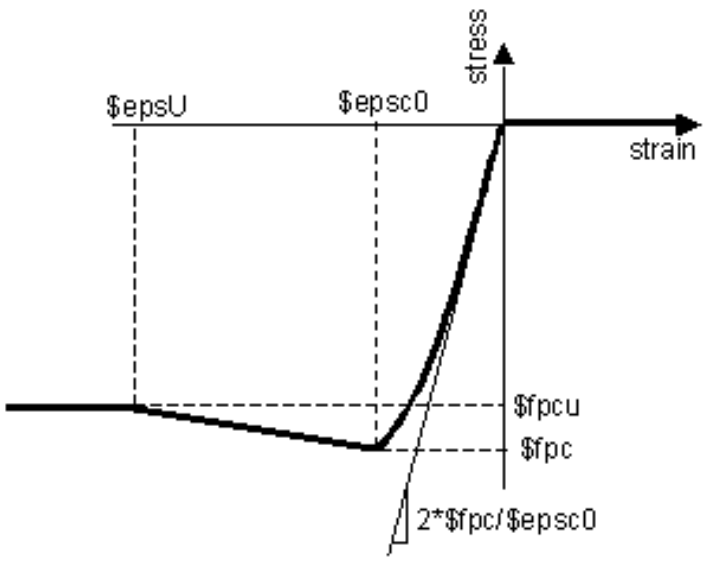

Figure 4.1 Typical Stress-Strain Relationship for Concrete01 (OpenSees Command Manual, 2013).

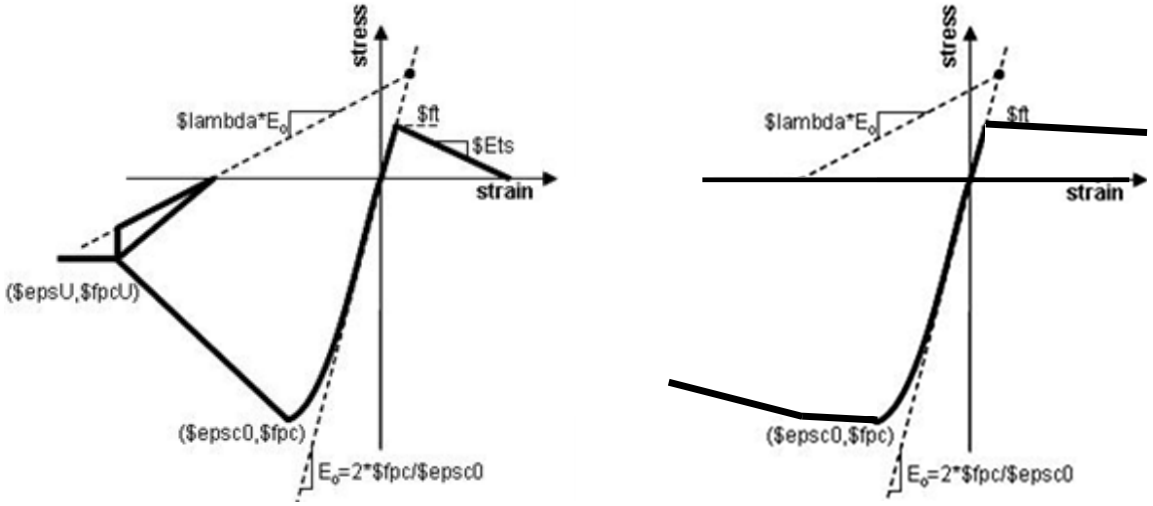

(a) Original Parameters (b) Expected for UHPC-tailored

Figure 4.2 Typical Stress-Strain Relationship for Concrete02 (OpenSees Command Manual, 2013).

In order to see the effects of using Concrete01, Concrete02, Concrete04, and XTRACT, each material model is used to optimize a column section while considering four different longitudinal reinforcement ratios (A_{st}) of ~1.5%, 2.0-2.5%, 3.0-3.5%, and 5.0-6.0%. Note that currently, Caltrans SDC (2013) and AASHTO (2012) limit the maximum longitudinal reinforcement ratio to 4%. However, this study is investigating the alternative of higher longitudinal reinforcement ratios that fully utilize the UHPC high strength. Concrete01 does not feature any tensile properties and trials that involved this material model are not shown here. Likewise, for XTRACT, the

implemented concrete model is the Mander confined concrete model (Mander et al. 1988). It has compressive strength limitations that does not allow a user to input compressive strengths over 12,000 psi. The only input over 12,000 psi that can be added is by overriding the confined compressive strength in the confined properties. Furthermore, additional tensile properties such as strain parameters are not available, removing XTRACT as an alternative analysis.

4.3 UHPC CROSS-SECTIONAL ANALYSIS

A preliminary simplified design scheme was adopted in this study for each of the four UHPC mixes, which can be outlined as follows:

1. Select a preliminary UHPC column diameter and start with ~1.5% reinforcement ratio (as original case) to maintain a similar axial load ratio as conventional concrete;
2. Perform a cross-sectional analysis for the UHPC column while considering XTRACT, Concrete02, and Concrete04 as calibrated based on the given UHPC mechanical properties;
3. Compare the obtained UHPC column ultimate moment with the ultimate moment capacity of the conventional concrete design;
4. Change the column diameter in increments of 2 inches as needed to optimize the design at a close value for the moment capacity;
5. Try different reinforcement ratios (2.0-2.5%, 3.0-3.5%, and 5.0-6.0%) and optimize the section for each of the alternative reinforcement cases. This is to investigate whether increasing the reinforcement ratio can better utilize the inherent UHPC strength.

It is noted that once the column diameter is finalized, the bent cap beam width is finalized accordingly by adding two feet to the column diameter as recommended by AASHTO (2012) and Caltrans SDC (2013) and eventually checked to see if it remains virtually elastic when subjected to seismic forces. The design procedure shown above was adopted for XTRACT for the original conventional concrete case (as a validation to the values produced by OpenSees) and OpenSees (using Concrete02 and Concrete04) for both the original conventional concrete case and UHPC. Only the results from XTRACT are shown in this section for the original conventional concrete case and the main focus and finalized designs throughout the study are mainly using the OpenSees Concrete02 and Concrete04 models.

As discussed before, four UHPC mixes are selected and used throughout this study (Table 4-3). Mixes with full prescribed mechanical properties are selected so that the computational constitutive models can be defined accurately. The original NSC prototype bridge column (6 ft. diameter with ~1.5% reinforcement ratio) is also considered for the sectional analysis to determine its ultimate moment capacity from XTRACT and OpenSees and check it against the readily available value from the original design document (Caltrans 2006). The obtained ultimate moment capacity is the target for the UHPC design optimization trials. Table 4-4 tabulates the axial load applied, reinforcing steel, ultimate moment, and curvature at the ultimate moment as obtained from XTRACT and OpenSees. Moreover, Figure 4.3 compares the moment-curvature relationship from both XTRACT and OpenSees.

Table 4-4 Sectional Analysis Results Using Conventional Concrete

Column Diameter	6'-0"
Axial Load	1,694 kips
Longitudinal Reinforcement	26 #14
Transverse Reinforcement	#8 at 5"
Ultimate Moment	XTRACT: 173,700 kip-in.
	OpenSees: 175,905 kip-in
Curvature at Ultimate Moment	XTRACT: 0.001116 1/in.
	OpenSees: 0.0011 1/in.

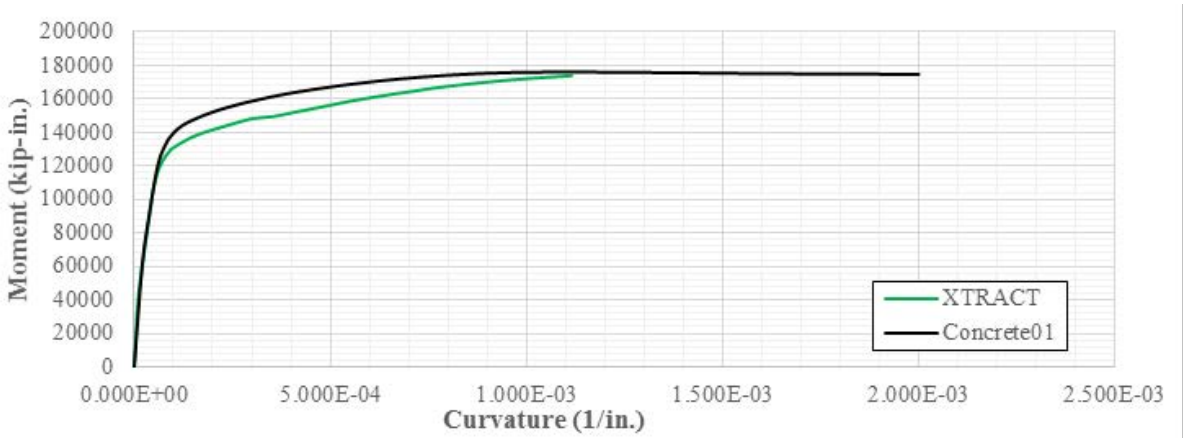

Figure 4.3 Moment-curvature results for XTRACT and OpenSees for the original conventional concrete design.

4.3.1 COLUMN DESIGN OPTIMIZATION

Using the design scheme explained before, the final optimized results of the sectional analysis for each UHPC mix design and for each varying longitudinal steel ratio when Concrete02 is used is listed in Table 4-5. Moreover, Figure 4.4 illustrates the obtained moment-curvature relationships

for all optimized UHPC sections as compared to the NSC original design (that used a nominal 4,000 psi concrete compressive strength). Four different ranges for the longitudinal steel ratios are considered as mentioned before (~1.5%, 2.0-2.5%, 3.0-3.5%, and 5.0-6.0%) and shown in the results. Similarly, Concrete04 was used to define the UHPC concrete material model and optimize the design cases for different UHPC mixes and varying reinforcement ratios. Table 4-6 summarizes the Concrete04-based designs and Figure 4.5 shows all its corresponding moment-curvature relationships. It should be noted that the different UHPC mixes are identified in the figures using their reported 28-day strength and that the figures feature the final optimized column diameter for all the different design cases. The results show that the original 6'-0" NSC column can be reduced to 4'-2" when UHPC is used with 3.0-3.5% steel reinforcement ratios. When reinforcement ratios between 5.0-6.0% is selected for Concrete02 and Concrete04, the column diameter reaches its most optimized value, averaging 4'-0" regardless of compressive strength. This would imply that the concrete no longer has any effect and that only the steel reinforcement is being utilized. The moment curvatures shown in Figure 4.4 and 4.5 display a post-peak degradation for the UHPC designs while the conventional concrete continuously hardens. This is due to the material model defined for UHPC which includes linear and exponential tensile softening for Concrete02 and Concrete04 respectively, a material property not defined for the conventional concrete case. It is suggested for future studies to further investigate higher reinforcement ratios in the 3.0-3.5% range (or even higher) for the most ideal reinforcement ratio for the most optimized results. UHPC is expected to provide strain compatibility up to higher strain levels than what is needed to rupture the reinforcing bars according to the current designs. Thus, much higher reinforcement ratios or potential use of high strength steel should be considered in future studies for further optimization.

Table 4-5 Optimized Concrete02 Column Design and Section Analysis Results

Property	Original	UHPC 1	UHPC 2	UHPC 3	UHPC 4
f'_c (psi)	4,000	17,260	21,147	28,900	36,360
f_t (psi)	-	1,300	1,500*	1,700	2,611
A_{st}≅1.5%					
Column Diameter	6’-0”	5’-2”	5’-0”	4’-10”	4’-6”
Bent Cap Width	8’-0”	7’-2”	7’-0”	6’-10”	6’-6”
Column Longitudinal Reinforcement	26 #14	28 #11	28 #11	28 #11	22 #11
Column Transverse Reinforcement	#8 at 5”	#5 at 5”	#5 at 5”	#5 at 5”	#5 at 5”
Actual Column Steel Percentage	1.44%	1.45%	1.54%	1.65%	1.50%
Ultimate Moment (kip-in)	176,911	178,136	177,013	178,473	177,536
Curvature at Ultimate Moment (1/in.)	0.001120	0.00016	0.00018	0.00018	0.00016
A_{st}≅2.0-2.5%					
Column Diameter	6’-0”	4’-10”	4’-8”	4’-8”	4’-4”
Bent Cap Width	8’-0”	6’-10”	6’-8”	6’-8”	6’-4”
Column Longitudinal Reinforcement	26 #14	26 #14	28 #14	24 #14	22 #14
Column Transverse Reinforcement	#8 at 5”	#5 at 5”	#5 at 5”	#5 at 5”	#5 at 5”
Actual Column Steel Percentage	1.44%	2.21%	2.56%	2.19%	2.33%
Ultimate Moment (kip-in)	176,911	182,065	179,394	179,508	180,684
Curvature at Ultimate Moment (1/in.)	0.001120	0.00024	0.00026	0.0002	0.0002
A_{st}≅3.0-3.5%					
Column Diameter	6’-0”	4’-8”	4’-6”	4’-4”	4’-2”
Bent Cap Width	8’-0”	6’-8”	6’-6”	6’-4”	6’-2”
Column Longitudinal Reinforcement	26 #14	32 #14	32 #14	32 #14	30 #14
Column Transverse Reinforcement	#8 at 5”	#5 at 5”	#5 at 5”	#5 at 5”	#5 at 5”
Actual Column Steel Percentage	1.44%	2.92%	3.14%	3.39%	3.44%
Ultimate Moment (kip-in)	176,911	182,773	179,553	178,426	186,882
Curvature at Ultimate Moment (1/in.)	0.001120	0.00026	0.0003	0.00028	0.00024
A_{st}≅5.0-6.0%					
Column Diameter	6’-0”	4’-0”	4’-0”	4’-0”	3’-10”
Bent Cap Width	8’-0”	6’-0”	6’-0”	6’-0”	5’-10”
Column Longitudinal Reinforcement	26 #14	26 #18	26 #18	24 #18	22 #18
Column Transverse Reinforcement	#8 at 5”	#5 at 5”	#5 at 5”	#5 at 5”	#5 at 5”
Actual Column Steel Percentage	1.44%	5.75%	5.75%	5.31%	5.30%
Ultimate Moment (kip-in)	176,911	184,758	187,347	182,755	180,330
Curvature at Ultimate Moment (1/in.)	0.001120	0.01792	0.01127	0.00798	0.00035

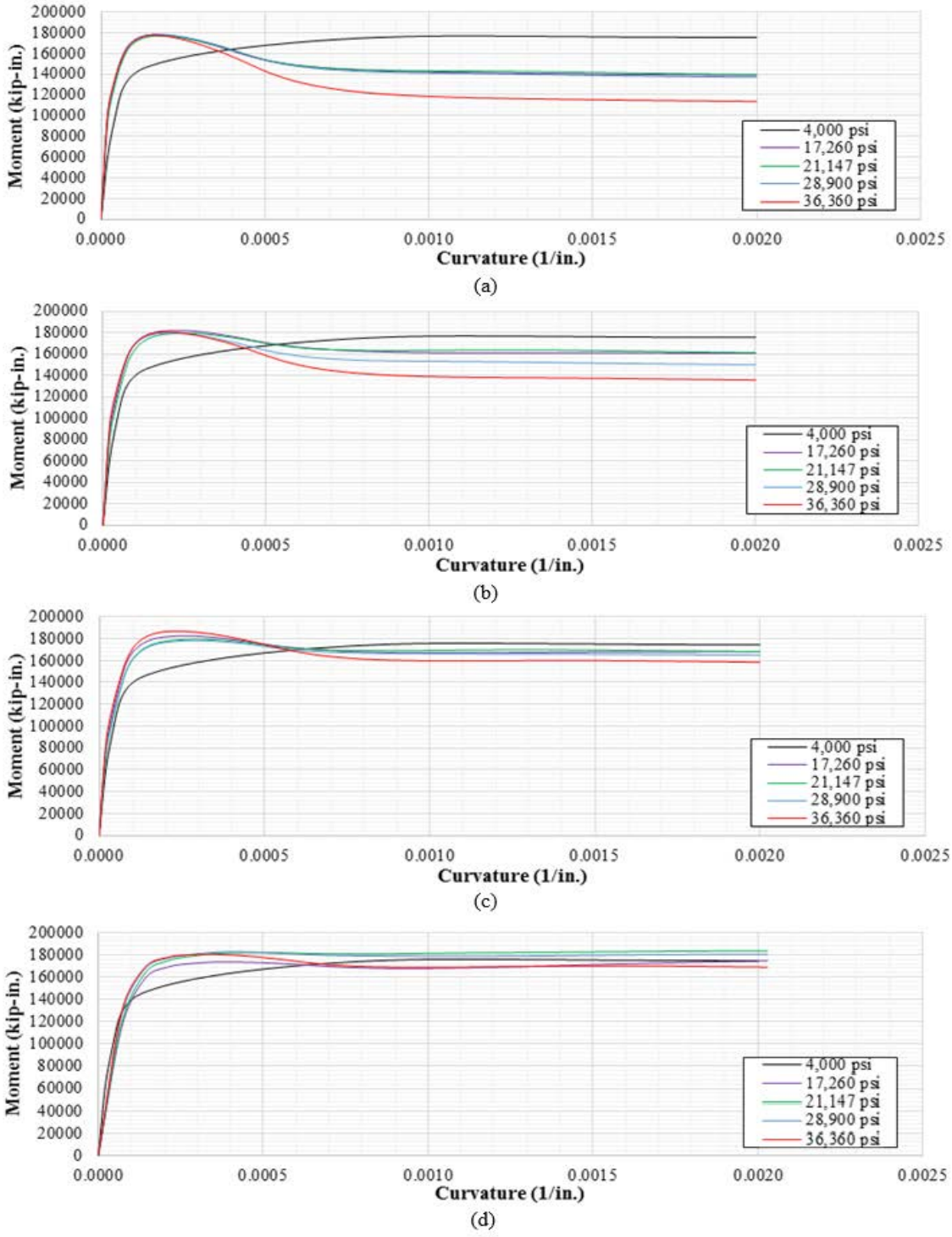

Figure 4.4 Concrete02-Based Moment Curvature Relationships for all UHPC Cases Along with Different Longitudinal Steel Ratios: (a) A_{st}≅1.5% (b) A_{st}≅2.0-2.5% (c) A_{st}≅3.0-3.5% (d) A_{st}≅5.0-6.0%.

Table 4-6 Optimized Concrete04 Column Design and Section Analysis Results

Property	Original	UHPC 1	UHPC 2	UHPC 3	UHPC 4
f'_c (psi)	4,000	17,260	21,147	28,900	36,360
f_t (psi)	-	1,300	1,500*	1,700	2,611
A_{st}≅1.5%					
Column Diameter	6’-0”	5’-8”	5’-6”	5’-4”	5’-0”
Bent Cap Width	8’-0”	7’-8”	7’-6”	7’-4”	7’-0”
Column Longitudinal Reinforcement	26 #14	24 #14	24 #14	22 #14	28 #11
Column Transverse Reinforcement	#8 at 5”	#5 at 5”	#5 at 5”	#5 at 5”	#5 at 5”
Actual Column Steel Percentage	1.44%	1.49%	1.58%	1.54%	1.54%
Ultimate Moment (kip-in)	176,911	184,828	183,081	177,339	181,267
Curvature at Ultimate Moment (1/in.)	0.001120	0.0001	0.0001	0.0001	0.00008
A_{st}≅2.0-2.5%					
Column Diameter	6’-0”	5’-2”	5’-0”	5’-0”	4’-8”
Bent Cap Width	8’-0”	7’-2”	7’-0”	7’-0”	6’-8”
Column Longitudinal Reinforcement	26 #14	32 #14	32 #14	30 #14	28 #14
Column Transverse Reinforcement	#8 at 5”	#5 at 5”	#5 at 5”	#5 at 5”	#5 at 5”
Actual Column Steel Percentage	1.44%	2.38%	2.55%	2.39%	2.56%
Ultimate Moment (kip-in)	176,911	181,132	183,302	182,797	177,676
Curvature at Ultimate Moment (1/in.)	0.001120	0.00014	0.00082	0.00088	0.00012
A_{st}≅3.0-3.5%					
Column Diameter	6’-0”	4’-10”	4’-8”	4’-8”	4’-6”
Bent Cap Width	8’-0”	6’-10”	6’-8”	6’-8”	6’-6”
Column Longitudinal Reinforcement	26 #14	22 #18	22 #18	20 #18	20 #18
Column Transverse Reinforcement	#8 at 5”	#5 at 5”	#5 at 5”	#5 at 5”	#5 at 5”
Actual Column Steel Percentage	1.44%	3.33%	3.57%	3.25%	3.49%
Ultimate Moment (kip-in)	176,911	184,961	188,215	184,778	183,678
Curvature at Ultimate Moment (1/in.)	0.001120	0.00046	0.00076	0.00082	0.00014
A_{st}≅5.0-6.0%					
Column Diameter	6’-0”	4’-4”	4’-2”	4’-2”	4’-0”
Bent Cap Width	8’-0”	6’-4”	6’-2”	6’-2”	6’-0”
Column Longitudinal Reinforcement	26 #14	28 #18	26 #18	26 #18	26 #18
Column Transverse Reinforcement	#8 at 5”	#5 at 5”	#5 at 5”	#5 at 5”	#5 at 5”
Actual Column Steel Percentage	1.44%	5.70%	5.30%	5.30%	5.75%
Ultimate Moment (kip-in)	176,911	186,077	178,214	184,979	182,399
Curvature at Ultimate Moment (1/in.)	0.001120	0.0004	0.0007	0.00068	0.00074

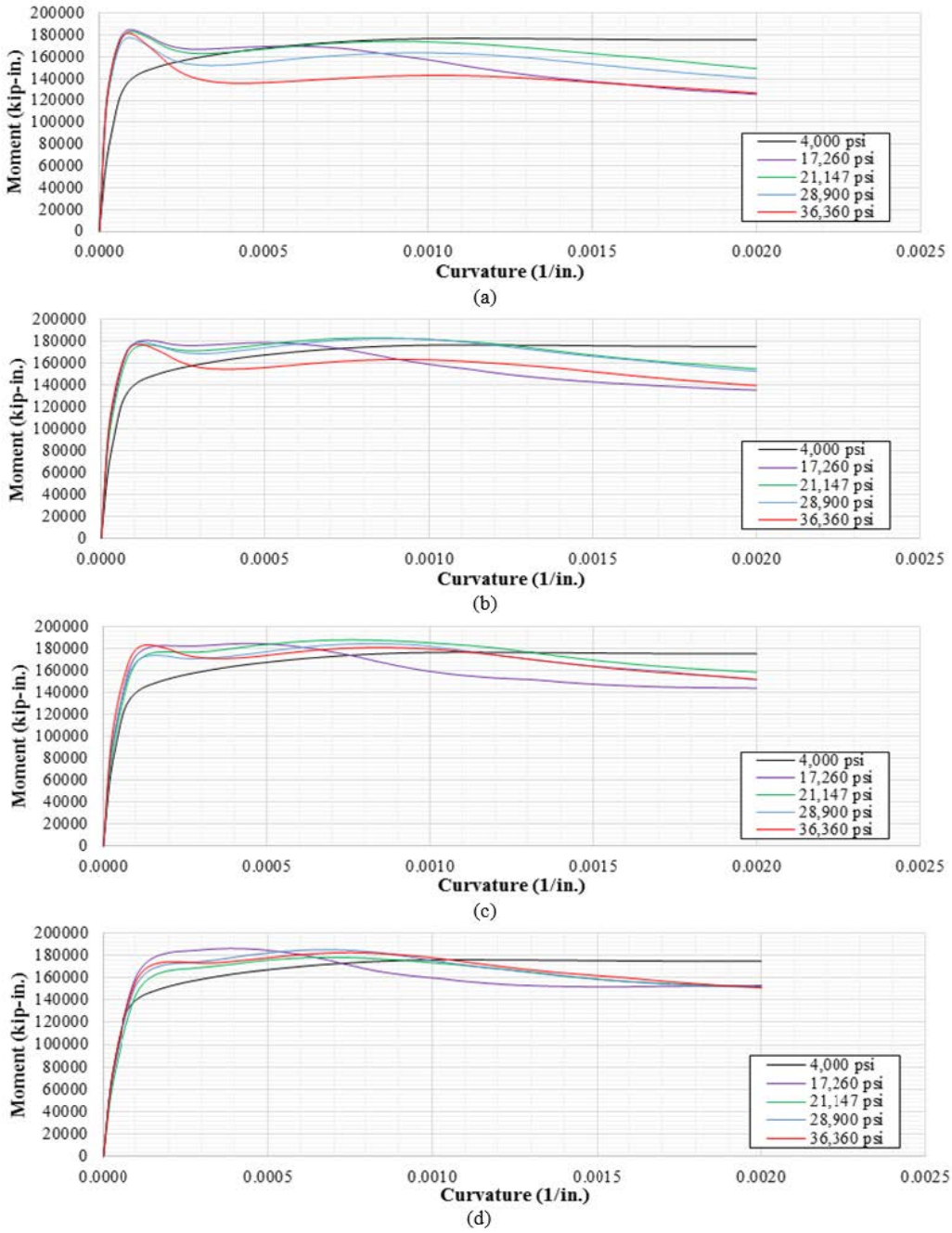

Figure 4.5 Concrete04-Based Moment Curvature Relationships for all UHPC Cases Along with Different Longitudinal Steel Ratios: (a) A_{st}≅1.5% (b) A_{st}≅2.0-2.5% (c) A_{st}≅3.0-3.5% (d) A_{st}≅5.0-6.0%.

4.3.2 CAP BEAM DESIGN OPTIMIZATION

Following the finalized UHPC column designs, the bent cap beam design width is finalized by adding 2.0 ft. to the column diameter. An iterative procedure was also used to check whether a slight reduction in the depth of the cap beam can be obtained while maintaining the same ultimate

moment capacity from the original NSC case. Table 4-7 and 4-8 summarizes the optimized sectional analysis results for Concrete02 and Concrete04, respectively, for the bent cap using the optimized values from Table 4-5 and 4-6. Longitudinal steel was kept to #11 along the top and bottom reinforcement and only the depth of the bent cap was optimized through section analysis. The results show that the original 8 ft. bent cap width and 6'-9" depth can be reduced to a 6'-2" width and 6'-0" depth along with reduction in the reinforcement ratio as well.

Table 4-7 Optimized Concrete02 Bent Cap Design and Section Analysis Results

Property	**Original**	**UHPC 1**	**UHPC 2**	**UHPC 3**	**UHPC 4**
f'_c (psi)	4,000	17,260	21,147	28,900	36,360
f_t (psi)	-	1,300	1,500*	1,700	2,611
A_{st}≅1.5%					
Column Diameter	6'-0"	5'-2"	5'-0"	4'-10"	4'-6"
Bent Cap Width	8'-0"	7'-2"	7'-0"	6'-10"	6'-6"
Bent Cap Depth	6'-9"	6'-0"	6'-0"	6'-0"	6'-0"
Longitudinal Reinforcement (Top and Bottom)	22 #11 24 #11	16 #11 16 #11	14 #11 14 #11	12 #11 12 #11	10 #11 12 #11
Ultimate Moment (kip-in.)	212,907	294,893	308,329	327,561	438,958
Curvature at Ult. Moment (1/in.)	0.004224	0.0001	0.00008	0.00008	0.00008
A_{st}≅2.0-2.5%					
Column Diameter	6'-0"	4'-10"	4'-8"	4'-8"	4'-4"
Bent Cap Width	8'-0"	6'-10"	6'-8"	6'-8"	6'-4"
Bent Cap Depth	6'-9"	6'-0"	6'-0"	6'-0"	6'-0"
Longitudinal Reinforcement (Top and Bottom)	22 #11 24 #11	16 #11 18 #11	14 #11 16 #11	14 #11 14 #11	12 #11 14 #11
Ultimate Moment (kip-in.)	212,907	290,261	301,556	330,967	438,565
Curvature at Ult. Moment (1/in.)	0.004224	0.0001	0.0001	0.00008	0.00008
A_{st}≅3.0-3.5%					
Column Diameter	6'-0"	4'-8"	4'-6"	4'-4"	4'-2"
Bent Cap Width	8'-0"	6'-8"	6'-6"	6'-4"	6'-2"
Bent Cap Depth	6'-9"	6'-0"	6'-0"	6'-0"	6'-0"
Longitudinal Reinforcement (Top and Bottom)	22 #11 24 #11	18 #11 18 #11	16 #11 16 #11	14 #11 16 #11	14 #11 14 #11
Ultimate Moment (kip-in.)	212,907	290,480	301,133	322,891	433,419
Curvature at Ult. Moment (1/in.)	0.004224	0.0001	0.0001	0.00008	0.00008
A_{st}≅5.0-6.0%					
Column Diameter	6'-0"	4'-0"	4'-0"	4'-0"	3'-10"
Bent Cap Width	8'-0"	6'-0"	6'-0"	6'-0"	5'-10"
Bent Cap Depth	6'-9"	6'-0"	6'-0"	6'-0"	6'-0"
Longitudinal Reinforcement (Top and Bottom)	22 #11 24 #11	20 #11 22 #11	20 #11 20 #11	18 #11 20 #11	16 #11 18 #11
Ultimate Moment (kip-in.)	212,907	286,048	304,819	330,628	427,779
Curvature at Ult. Moment (1/in.)	0.004224	0.0001	0.0001	0.0001	0.00008

Table 4-8 Optimized Concrete04 Bent Cap Design and Section Analysis Results

Property	Original	UHPC 1	UHPC 2	UHPC 3	UHPC 4
f'_c (psi)	4,000	17,260	21,147	28,900	36,360
f_t (psi)	-	1,300	1,500*	1,700	2,611
A_{st}≅1.5%					
Column Diameter	6'-0"	5'-8"	5'-6"	5'-4"	5'-0"
Bent Cap Width	8'-0"	7'-8"	7'-6"	7'-4"	7'-0"
Bent Cap Depth	6'-9"	6'-0"	6'-0"	6'-0"	6'-0"
Longitudinal Reinforcement (Top and Bottom)	22 #11 24 #11	22 #11 22 #11	18 #11 18 #11	16 #11 18 #11	16 #11 16 #11
Ultimate Moment (kip-in.)	212,907	248,489	249,943	267,694	357,959
Curvature at Ult. Moment (1/in.)	0.004224	0.00006	0.00006	0.00004	0.00004
A_{st}≅2.0-2.5%					
Column Diameter	6'-0"	5'-2"	5'-0"	5'-0"	4'-8"
Bent Cap Width	8'-0"	7'-2"	7'-0"	7'-0"	6'-8"
Bent Cap Depth	6'-9"	6'-0"	6'-0"	6'-0"	6'-0"
Longitudinal Reinforcement (Top and Bottom)	22 #11 24 #11	24 #11 24 #11	18 #11 18 #11	16 #11 18 #11	16 #11 16 #11
Ultimate Moment (kip-in.)	212,907	246,131	238,203	257,603	342,852
Curvature at Ult. Moment (1/in.)	0.004224	0.00006	0.00006	0.00004	0.00004
A_{st}≅3.0-3.5%					
Column Diameter	6'-0"	4'-10"	4'-8"	4'-8"	4'-6"
Bent Cap Width	8'-0"	6'-10"	6'-8"	6'-8"	6'-6"
Bent Cap Depth	6'-9"	6'-0"	6'-0"	6'-0"	6'-0"
Longitudinal Reinforcement (Top and Bottom)	22 #11 24 #11	26 #11 26 #11	22 #11 22 #11	20 #11 20 #11	16 #11 18 #11
Ultimate Moment (kip-in.)	212,907	247,051	245,893	260,871	337,636
Curvature at Ult. Moment (1/in.)	0.004224	0.00008	0.00006	0.00006	0.00004
A_{st}≅5.0-6.0%					
Column Diameter	6'-0"	4'-4"	4'-2"	4'-2"	4'-0"
Bent Cap Width	8'-0"	6'-4"	6'-2"	6'-2"	6'-0"
Bent Cap Depth	6'-9"	6'-0"	6'-0"	6'-0"	6'-0"
Longitudinal Reinforcement (Top and Bottom)	22 #11 24 #11	28 #11 28 #11	24 #11 24 #11	22 #11 22 #11	20 #11 20 #11
Ultimate Moment (kip-in.)	212,907	247,552	253,549	255,389	323,296
Curvature at Ult. Moment (1/in.)	0.004224	0.00008	0.00006	0.00006	0.00006

5 Seismic Analysis of UHPC Substructure

This chapter provides the seismic analysis results and discussion for the NSC and UHPC bridge piers. Nonlinear pushover and time history analyses are conducted to compare the seismic behavior of UHPC bridge piers against conventional NSC piers. The analysis also aims at finalizing the UHPC pier design, where a capacity check is required for the bent caps.

5.1 DESIGN PHILOSOPHY OF BRIDGES

AASHTO 3.10.1 (2012) states that, “Bridges shall be designed to have a low probability of collapse but may suffer significant damage and disruption to service when subject to earthquake ground motions.” This design philosophy keeps the costs of the bridge practical while keeping life safety at the highest priority. If higher levels of performance are required, the bridge owner must give the authorization for that design. The general design philosophy of bridges begins with selecting where you want the damage to occur under seismic loading. All other elements shall be shall be protected from failure and remain essentially elastic. Caltrans SDC 3.4 (2013) states that while damage is allowed in columns, capacity protected concrete components include footings, Type II shafts, bent cap beams, column joints at the footing and bent cap, and the superstructure. The columns shall have a ductile design (to resist smaller loads without having to do immediate repairs) and selected as the component where damage shall occur for larger seismic events. The bridge columns require a plastic hinging system to dissipate the earthquake energy when the columns begin to experience non-linear effects. Plastic hinging is required to form just beneath the bent cap at the column for multi-column bents, where columns are pinned at the footings. This is achieved by assuring that the bent cap and various capacity protected components remain essentially elastic. This location of the plastic hinge also allows for easy inspection of the columns after a large seismic event. If plastic hinging forms anywhere else such as the superstructure, the superstructure can lose jacking forces in its post-tensioned system, for instance, making the bridge susceptible to catastrophic failure. To guarantee the desired essentially elastic behavior during a severe earthquake event, the capacity protected members design is checked against an overstrength column moment capacity, which is 1.2 times the ultimate plastic moment of the column determined from sectional analysis. An alternative approach for the capacity check, which is adopted in this

study, is to perform a nonlinear pushover and/or time history analysis to verify that the bent cap remains elastic.

5.2 NONLINEAR PUSHOVER ANALYSIS

Using the results from Chapter 4, it is determined that longitudinal steel ratios between 3.0-3.5%, are the most practical to optimize cross-sections and still stay below the maximum limit set by the codes at 4%. Higher reinforcement ratio might lead to further optimization but requires more comprehensive research for future recommendations for UHPC design codes. Also, both Concrete02 and Concrete04 were used in the design optimization and didn't show significant difference. Thus, the seismic analysis presented here is limited to using Concrete02 for optimized sections with 3-3.5% steel reinforcement ratios.

A two-dimensional model was developed in OpenSees using nonlinear beam column elements for the original NSC and each of the selected four UHPC mix designs. The frame was first loaded using vertical loads that are calculated from the original bridge superstructure (dead weight of the concrete box-girder, Type 732 concrete barriers, and wearing surfaces at 35 psf). Next, a displacement-based lateral pushover was applied in the x direction and continued up to 30 inches. One objective of the nonlinear pushover analysis is to record the maximum force (base shear) capacity along with the equivalent displacement at first plastic hinge formulation. The overall force capacity is obtained by summing the column base shear results from the pushover analysis, and results are summarized in Table 5-1. It is noted that the equivalent yield displacement is defined according to the Caltrans SDC (2013) provisions. Caltrans defines this yield displacement as the displacement that corresponds to the first plastic hinge formulation in the pier. Figure 5.1 illustrates the pushover curve for all Concrete02-based UHPC mix designs using $A_{st} \cong$3.0-3.5%. For the UHPC cases, the equivalent displacement at first plastic hinge is approximately the value at the peak force. For the NSC pier, the yield displacement of 6.8 in. is interpreted from Figure 5.1 if a bilinear curve approximation is sought. It is observed that higher base shear capacities can be achieved using UHPC. Comparable base shear is also observed at higher deformation levels when UHPC piers are compared to the original conventional concrete design. Due to the over-turning moment effect, the two columns experience different axial loads during the lateral pushover. Figure 5.2 compares a sample moment-curvature relationship from both columns along with what

was obtained from the sectional analysis. This figure shows that the sectional analysis results is an average estimate of the two laterally loaded columns as expected.

Another objective of the pushover analysis is to finalize the design of the full pier by checking the optimized bent cap beam sections, i.e. satisfy the required Caltrans capacity check. It is observed for all UHPC design cases that the cap beam remains linear elastic while all the damage takes place in the columns as desired. Figure 5.3 shows a sample moment curvature response for UHPC 3 cap beam as resulting from the pushover analysis. The figure shows very small curvature values and the beam is essentially elastic as per Caltrans SDC provisions (2013).

Table 5-1 Final cross-sections and OpenSees pushover results using Concrete02 (A_{st}≅3.0-3.5%)

Property	Original	UHPC 1	UHPC 2	UHPC 3	UHPC 4
f'_c (psi)	4,000	17,260	21,147	28,900	36,360
Column Diameter	6'-0"	4'-8"	4'-6"	4'-4"	4'-2"
Bent Cap Width	8'-0"	6'-8"	6'-6"	6'-4"	6'-2"
Bent Cap Depth	6'-9"	6'-0"	6'-0"	6'-0"	6'-0"
Column Section Analysis Results					
Ultimate Moment (kip-in)	176,911	182,773	179,553	178,426	186,882
Bent Cap Section Analysis Results					
Ultimate Moment (kip-in)	212,907	290,480	301,133	322,891	433,419
Pushover Analysis Results					
Pier Maximum Force (kip)	577.50	712.17	695.31	693.08	734.94
Equivalent Yield Deformation, Δ_y (in.)	6.80	7.571	8.136	7.878	7.220

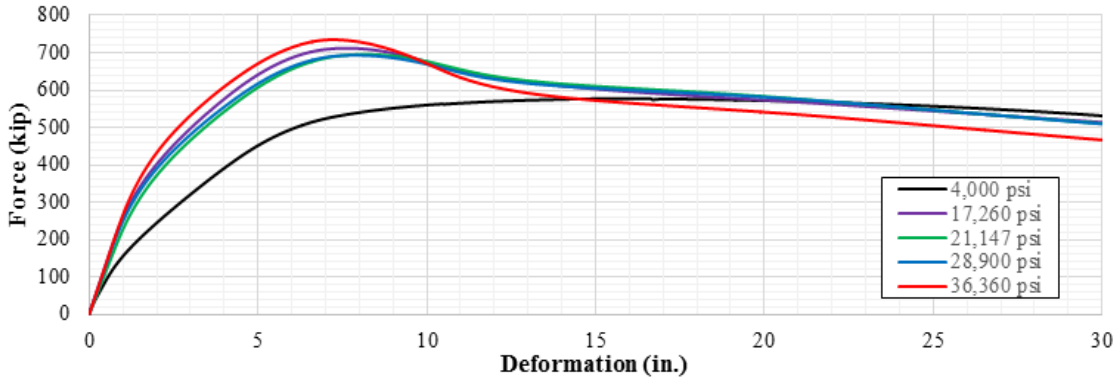

Figure 5.1 Pushover curve for NSC and UHPC bents with column reinforcement A_{st} ≅ 3.0-3.5%.

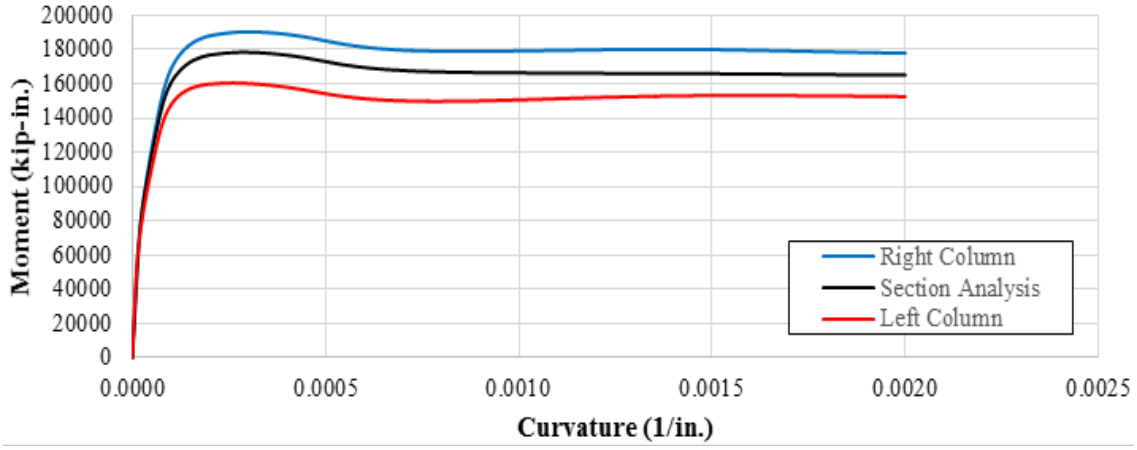

Figure 5.2 Sample moment-curvature relationship for UHPC 3 bent columns (A_{st} ≅3.0-3.5%) as obtained from the OpenSees pushover and sectional analysis using Concrete02.

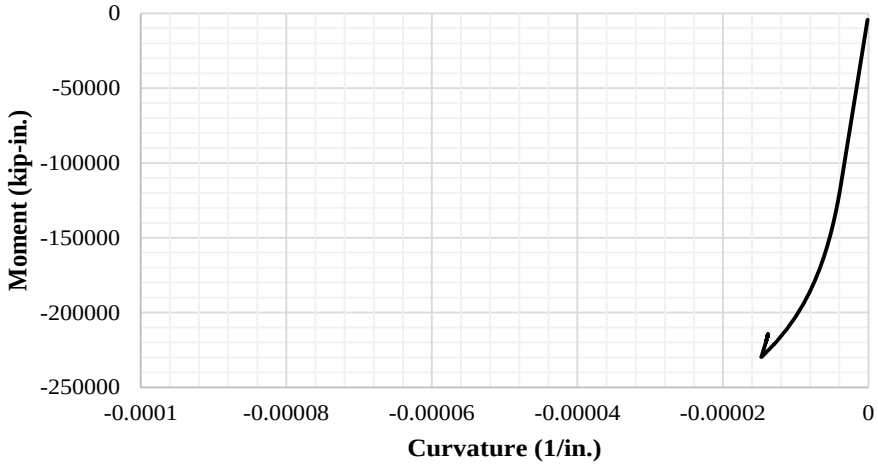

Figure 5.3 Sample moment-curvature relationship for UHPC 3 bent cap beam as obtained from the OpenSees pushover analysis using Concrete02.

5.3 NONLINEAR TIME HISTORY ANALYSIS

A nonlinear time history (response) analysis (NTHA) was performed and presented in this section for the cases that used Concrete02 with column reinforcement A_{st} ≅3.0-3.5%. The objective of NTHA is to investigate the actual dynamic and seismic behavior of UHPC piers in the transverse direction under actual ground motions. The longitudinal direction was not considered because the overall bridge designs will dictate the longitudinal force and reactions.

5.3.1 GROUND MOTIONS

The Caltrans design response spectrum used for the original conventional concrete prototype bridge design is utilized in this study to select four different ground motions for the NTHA. This design spectrum is inputted into the Pacific Earthquake Engineering Research Center (PEER) Ground Motion Database and NGA-2 tool (2015) to select ground motions that best match the input response spectrum. Table 5-2 shows the list of the selected ground motions for the NTHA that best match the Caltrans design level earthquake (DLE) spectrum. The conducted NTHA in this study also considered the maximum considered earthquake (MCE) level ground motions, which is 1.5 times the corresponding DLE ground motions. Figure 5.4 plots the response spectra of the selected DLE ground motions along with their mean spectrum and the inputted Caltrans design spectrum (used for the original prototype bridge design).

Table 5-2 Selected Ground Motion Records for NTHAs

Earthquake Name	Year	Magnitude	Record Sequence Number	Station Name	Scale Factor (DLE)	Scale Factor (MCE)	Duration (sec)
Imperial Valley-02	1940	6.95	RSN 6	El Centro Array #9	2.393	3.590	54
San Fernando	1971	6.61	RSN 68	LA – Hollywood Store FF	3.195	4.792	80
San Fernando	1971	6.61	RSN 77	Pacoima Dam (Upper Left Abut)	0.902	1.353	42
Managua_Nicaragua-02	1972	5.2	RSN 96	Managua_ESSO	3.570	5.354	48

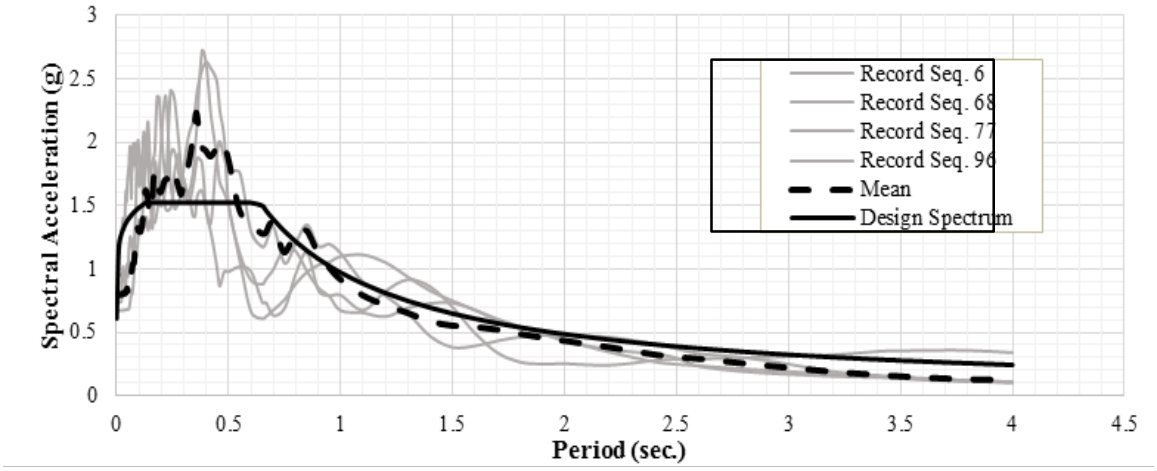

Figure 5.4 Response spectra of the selected records and Caltrans design spectrum (5% damping).

5.3.2 RESPONSE QUANTITIES

For the NTHA, the max deformation (Δ_{max}), residual displacement, columns base shear, and columns moments and curvatures are recorded for all analysis cases. A total of 40 analysis cases are considered which include the NSC and four UHPC piers, each analyzed twice under the four selected ground motions when applied at the design level and the maximum considered earthquake level. The obtained Δ_{max} from each NTHA case is used to calculate two important response quantities: the target displacement ductility demand and the maximum drift ratio. The target displacement ductility demand (μ_D) is calculated using Caltrans SDC (2013) Equation 2.2.3-1, which states that $\mu_D = \Delta_{max} / \Delta_y$, where Δ_{max} is the maximum obtained displacement and Δ_y is the equivalent yield displacement obtained from the pushover analysis (Table 5-1). The ductility demands calculated from NTHA are not necessarily the capacity values for the UHPC bents, where the full ductility capacity can be higher. In other words, the bridge columns develop plastic hinges but might still accommodate higher deformations, rotations, and curvatures. Current computational tools are not sufficient to determine displacement (or ductility) capacities of UHPC columns, and future experimental work is needed to find these values. For this study, the displacement ductility demands for each of the NTHA cases are checked against limits specified in Caltrans SDC 2.2.4 (2013) at the design level (See Figure 5.5). The other important response quantity considered is the maximum drift ratio which is calculated by dividing the max deformation of the pier by the column clear height (44 ft.) and expressed as a percentage.

Single Column Bents supported on fixed foundation	$\mu_D \leq 4$
Multi-Column Bents supported on fixed or pinned footings	$\mu_D \leq 5$
Pier Walls (weak direction) supported on fixed or pinned footings	$\mu_D \leq 5$
Pier Walls (strong direction) supported on fixed or pinned footings	$\mu_D \leq 1$

Figure 5.5 Excerpt from Caltrans SDC (2013) specifying limits of the target displacement ductility demands with the considered component type identified.

5.3.3 SUMMARY OF NTHA RESULTS

Different response histories are presented and discussed for the DLE and MCE analyses in the next subsections. However, a tabular summary of the obtained peak key response quantities is presented in this subsection. Tables 5-3, 5-4, 5-5, 5-6, and 5-7 summarize the peak (maximum)

displacements, ductility demands, maximum drift ratios, residual displacements, and maximum base shears, respectively, generated for all NTHA (DLE and MCE) cases. The overall observation is that UHPC piers experience less peak displacements and have less ductility demands. The maximum obtained base shear is the same as the pier's force capacity determined from pushover analysis (Table 5-1) for all the cases, which means that the NSC and UHPC bridge piers reaches its capacity for all DLE and MCE cases. However, the DLE cases show lower displacement values, less residual displacement, and lower ductility demands than the MCE for NSC and all UHPC cases as expected. For a force-based design approach, all NSC and UHPC pier columns are expected to reach their force capacity, which does not favor UHPC seismic behavior to NSC. However, the lower displacements demands on UHPC promises favorable seismic response if bridge piers are designed using a displacement-based or a performance-based approach. If so, future research will be needed to properly determine UHPC pier displacement capacities to enable accurate prospect performance-based design.

Table 5-3 Summary of NTHA Maximum Displacements (in.)

	RSN 6		**RSN 68**		**RSN 77**		**RSN 96**	
	DLE	MCE	DLE	MCE	DLE	MCE	DLE	MCE
Original	16.394	19.986	10.719	19.111	12.683	21.427	14.766	26.494
UHPC 1	11.941	19.250	9.827	18.228	12.280	18.900	11.068	21.383
UHPC 2	12.972	19.043	9.521	17.738	12.620	19.080	11.912	22.993
UHPC 3	12.959	18.701	9.533	17.741	12.473	19.052	11.371	21.942
UHPC 4	12.265	18.853	9.492	18.346	13.059	18.870	10.721	20.953

Table 5-4 Summary of NTHA Ductility Demands

	RSN 6		**RSN 68**		**RSN 77**		**RSN 96**	
	DLE	MCE	DLE	MCE	DLE	MCE	DLE	MCE
Original	2.411	2.939	1.576	2.810	1.865	3.151	2.171	3.896
UHPC 1	1.577	2.543	1.298	2.408	1.622	2.496	1.462	2.824
UHPC 2	1.594	2.341	1.170	2.180	1.551	2.345	1.464	2.826
UHPC 3	1.645	2.374	1.210	2.252	1.583	2.418	1.443	2.785
UHPC 4	1.699	2.611	1.315	2.541	1.809	2.614	1.485	2.902

Table 5-5 Summary of NTHA Maximum Drift Ratios

	RSN 6		**RSN 68**		**RSN 77**		**RSN 96**	
	DLE	MCE	DLE	MCE	DLE	MCE	DLE	MCE
Original	3.10%	3.79%	2.03%	3.62%	2.40%	4.06%	2.80%	5.02%
UHPC 1	2.26%	3.65%	1.86%	3.45%	2.33%	3.58%	2.10%	4.05%
UHPC 2	2.46%	3.61%	1.80%	3.36%	2.39%	3.61%	2.26%	4.35%
UHPC 3	2.45%	3.54%	1.81%	3.36%	2.36%	3.61%	2.15%	4.16%
UHPC 4	2.32%	3.57%	1.80%	3.47%	2.47%	3.57%	2.03%	3.97%

Table 5-6 Summary of NTHA Residual Displacements (in.)

	RSN 6		RSN 68		RSN 77		RSN 96	
	DLE	MCE	DLE	MCE	DLE	MCE	DLE	MCE
Original	3.519	6.478	2.022	1.757	0.877	7.016	0.270	7.177
UHPC 1	0.881	3.971	0.489	1.033	0.456	3.570	0.017	2.378
UHPC 2	1.100	4.644	0.536	0.551	0.547	3.407	0.092	3.008
UHPC 3	1.079	4.551	0.473	0.593	0.562	3.329	0.163	2.451
UHPC 4	1.012	4.918	0.399	0.998	0.807	3.683	0.314	1.977

Table 5-7 Summary of NTHA Maximum Base Shears (kip)

25	RSN 6		RSN 68		RSN 77		RSN 96	
	DLE	MCE	DLE	MCE	DLE	MCE	DLE	MCE
Original	574.05	575.60	559.69	585.42	566.68	577.01	574.05	582.08
UHPC 1	707.83	696.40	697.48	709.63	712.54	710.87	710.80	711.60
UHPC 2	690.48	685.61	684.90	691.57	695.78	694.02	693.92	694.30
UHPC 3	687.30	678.04	677.92	688.26	693.50	691.89	691.80	692.07
UHPC 4	726.653	721.55	725.33	721.75	735.66	734.41	733.01	732.34

5.3.4 DETAILED ANALYSIS RESULTS: DESIGN LEVEL EARTHQUAKE

This subsection presents the different response histories of the different UHPC piers as compared to the NSC under the four DLE ground motions. Figures 5.6 through 5.9 show the displacement history for each of the four ground motions. Figures 5.10 through 5.13 show the force-displacement (hysteresis) relationships for each DLE ground motion. As shown from the displacement histories, the maximum displacements for the UHPC designs are consistently lower when compared to the original conventional concrete design with lower residual displacements overall. The displacement ductility demands all satisfied the limits specified in SDC 2.2.4 ($\mu_D \leq 5$) and the drift ratios for each DLE ground motion averaged between 2-3%. The forces from the hysteresis diagrams are also consistent with the results from the pushover analysis, i.e. indicating the bridge pier reaching its capacity.

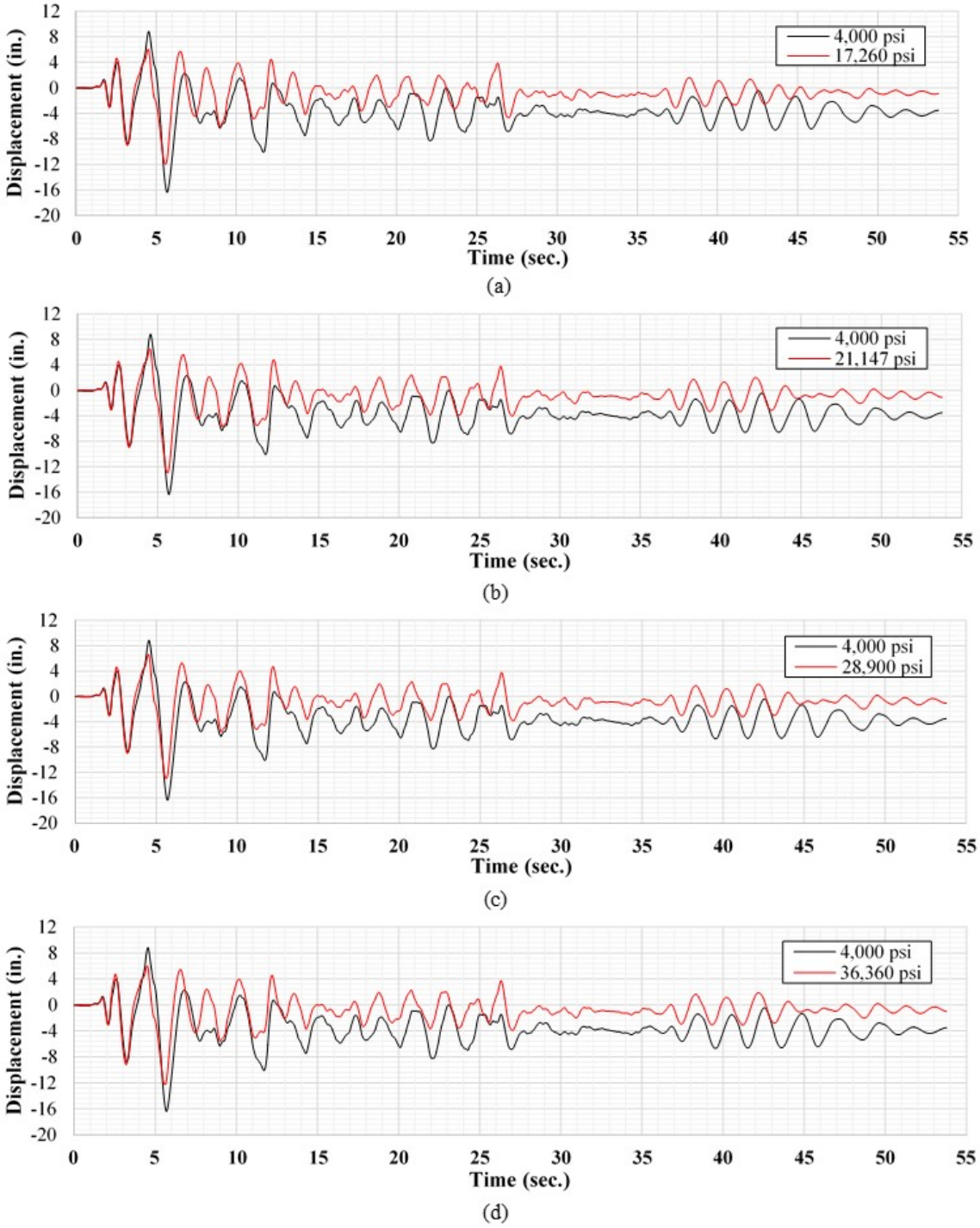

Figure 5.6 Displacement history for RSN 6 (Design Level) for (a) UHPC 1, (b) UHPC 2, (c) UHPC 3, and (d) UHPC 4

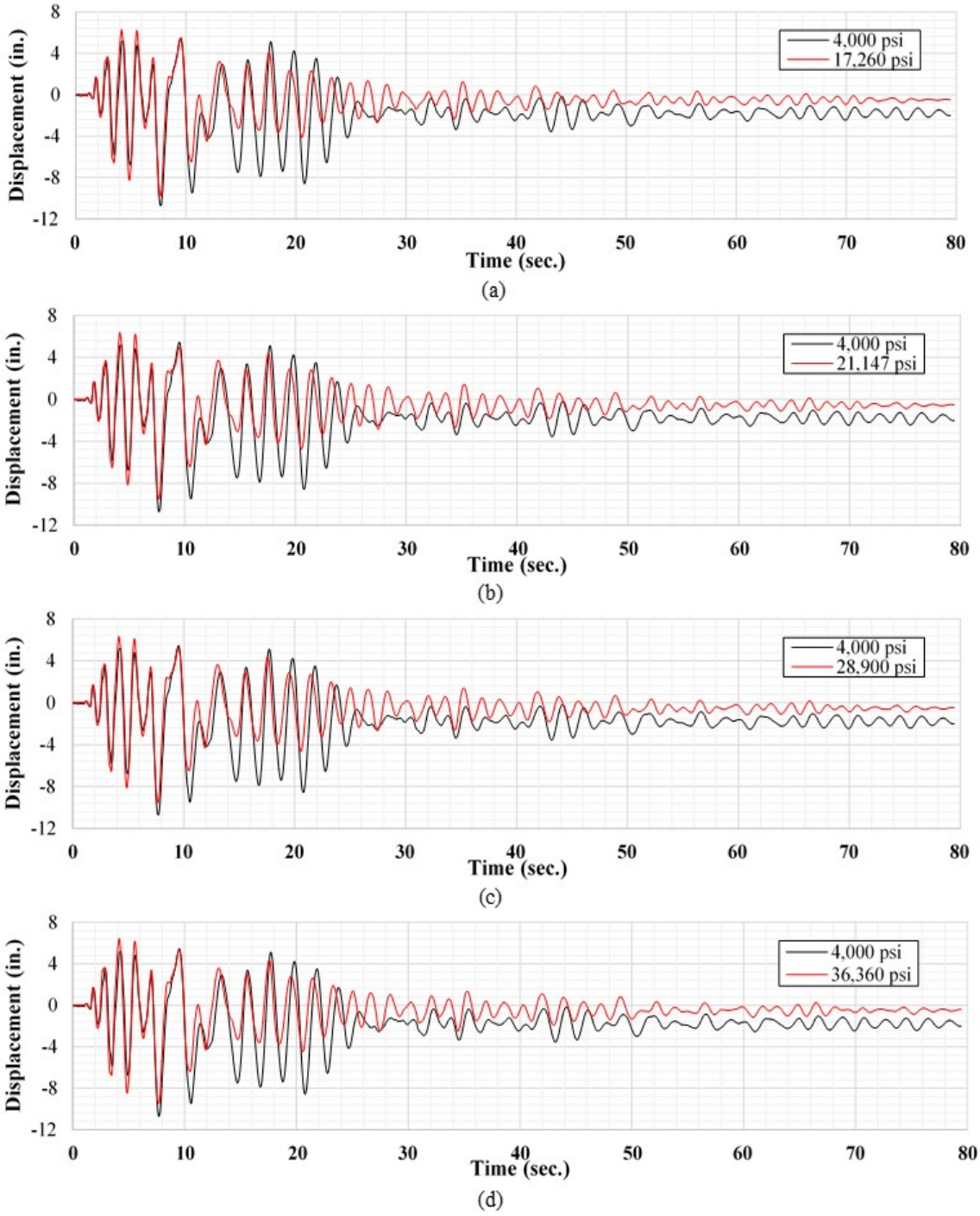

Figure 5.7 Displacement history for RSN 68 (Design Level) for (a) UHPC 1, (b) UHPC 2, (c) UHPC 3, and (d) UHPC 4

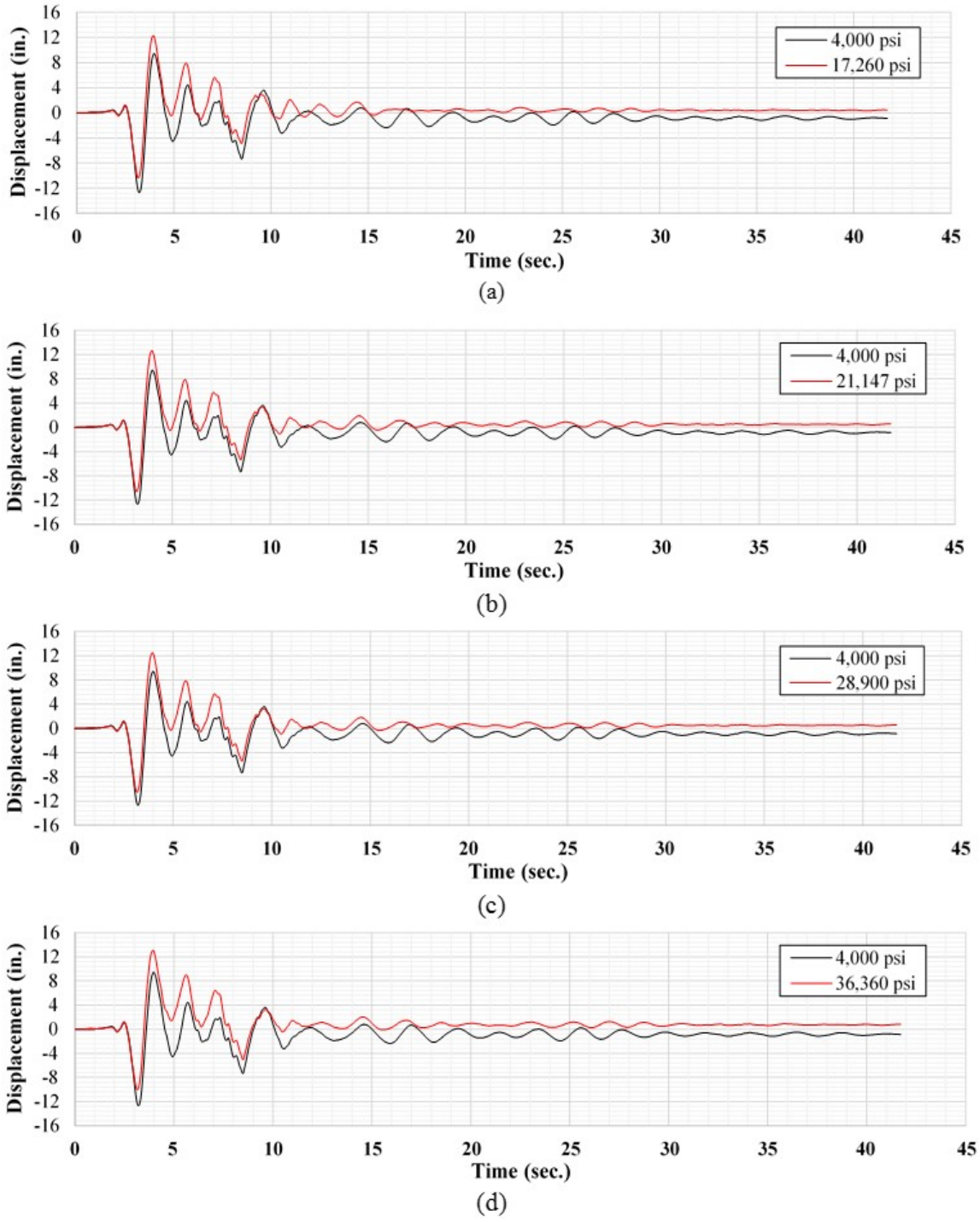

Figure 5.8 Displacement history for RSN 77 (Design Level) for (a) UHPC 1, (b) UHPC 2, (c) UHPC 3, and (d) UHPC 4

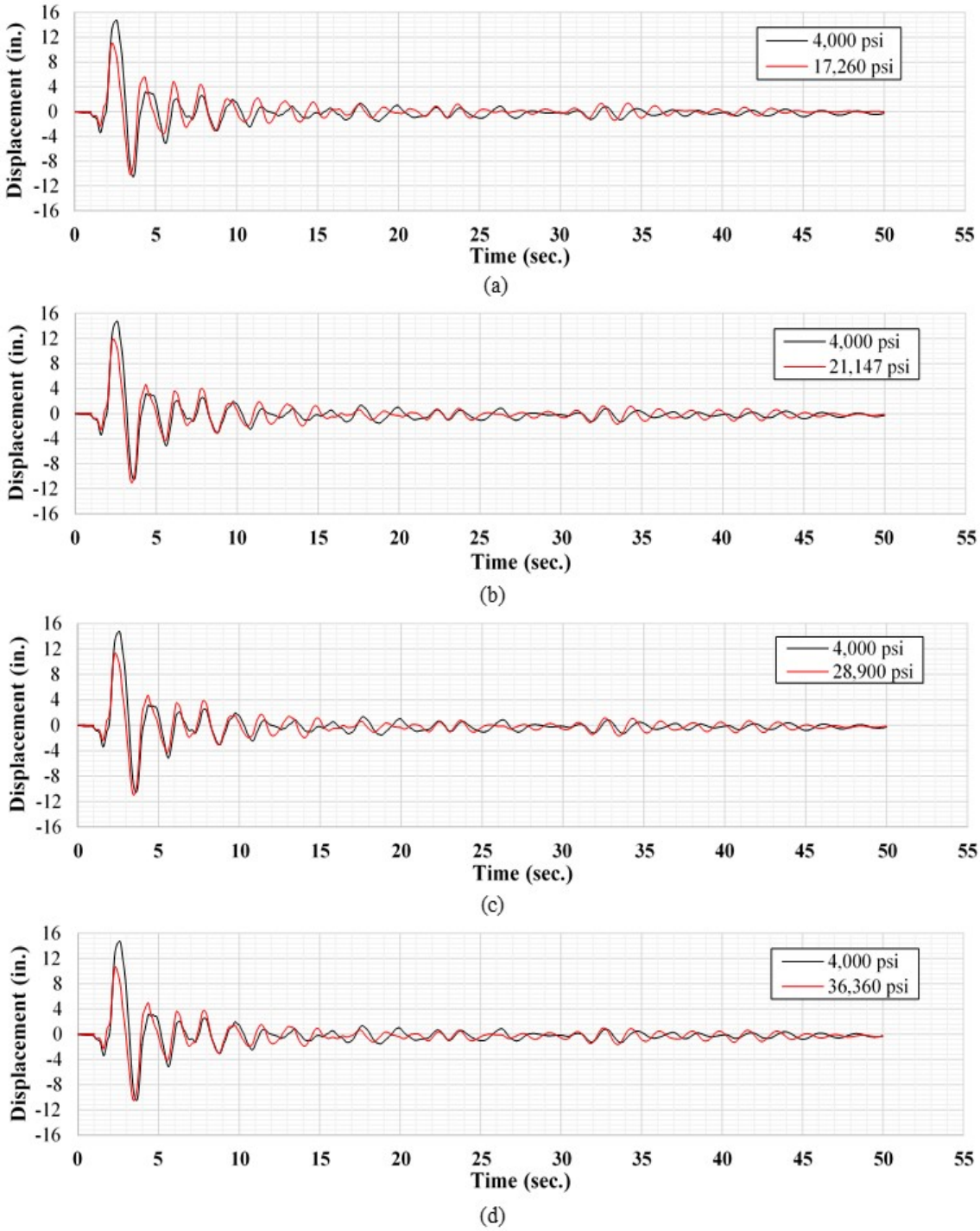

Figure 5.9 Displacement history for RSN9 6 (Design Level) for (a) UHPC 1, (b) UHPC 2, (c) UHPC 3, and (d) UHPC 4.

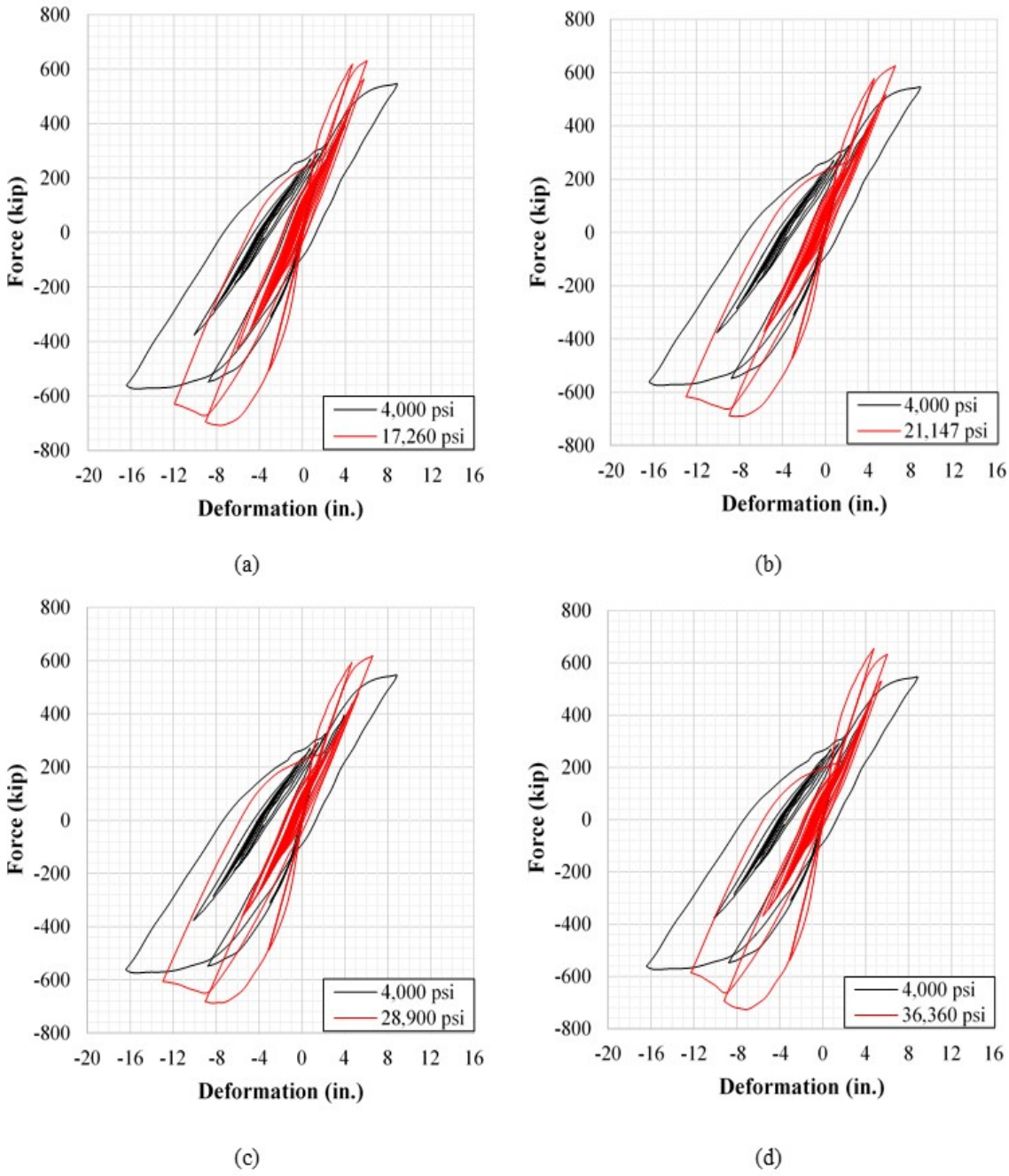

Figure 5.10 Force-displacement (hysteresis) relationship for (a) UHPC 1, (b) UHPC 2, (c) UHPC 3, and (d) UHPC 4 piers under RSN 6 (Design Level) ground motion.

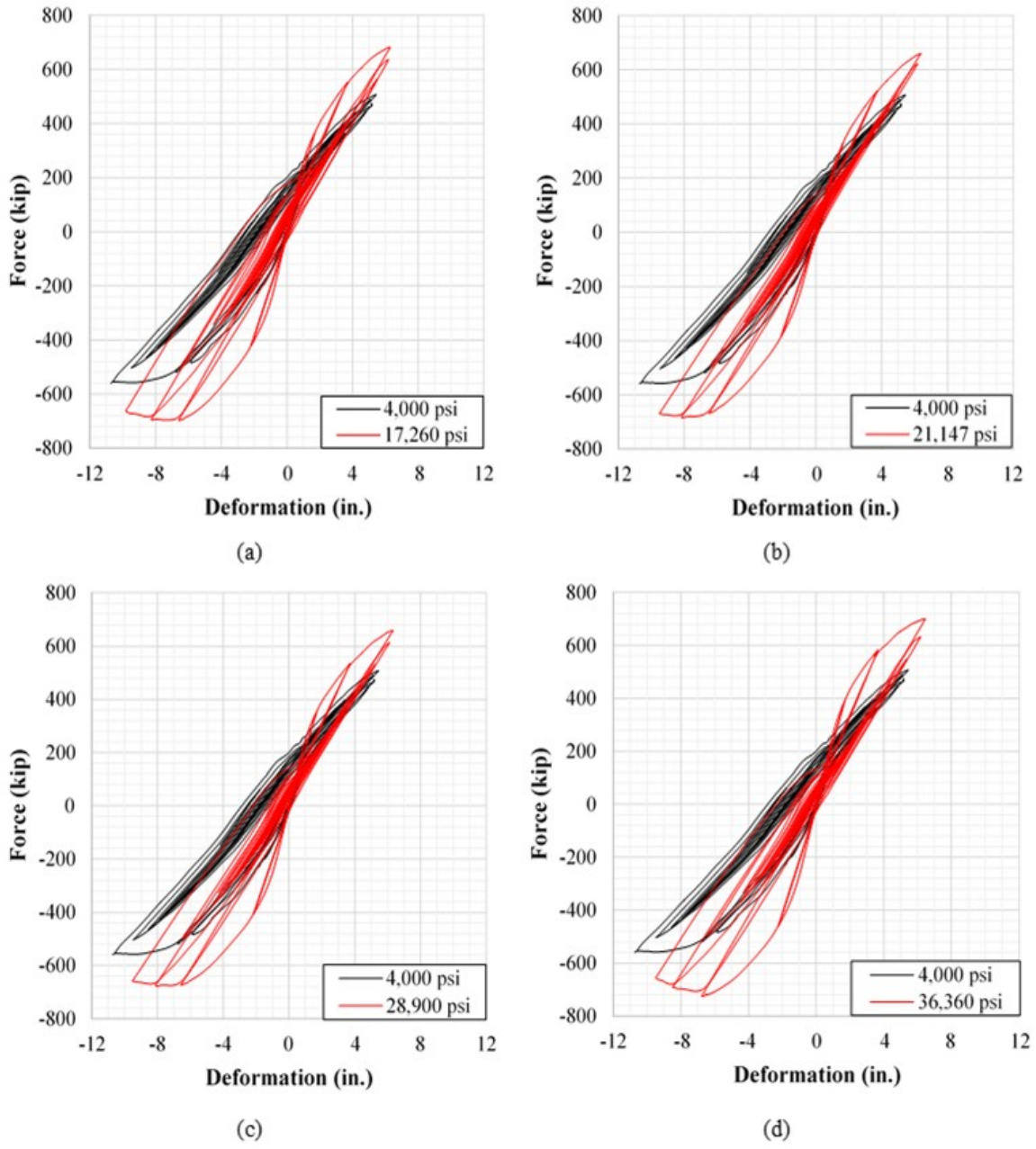

Figure 5.11 Force-displacement (hysteresis) relationship for (a) UHPC 1, (b) UHPC 2, (c) UHPC 3, and (d) UHPC 4 piers under RSN 68 (Design Level) ground motion.

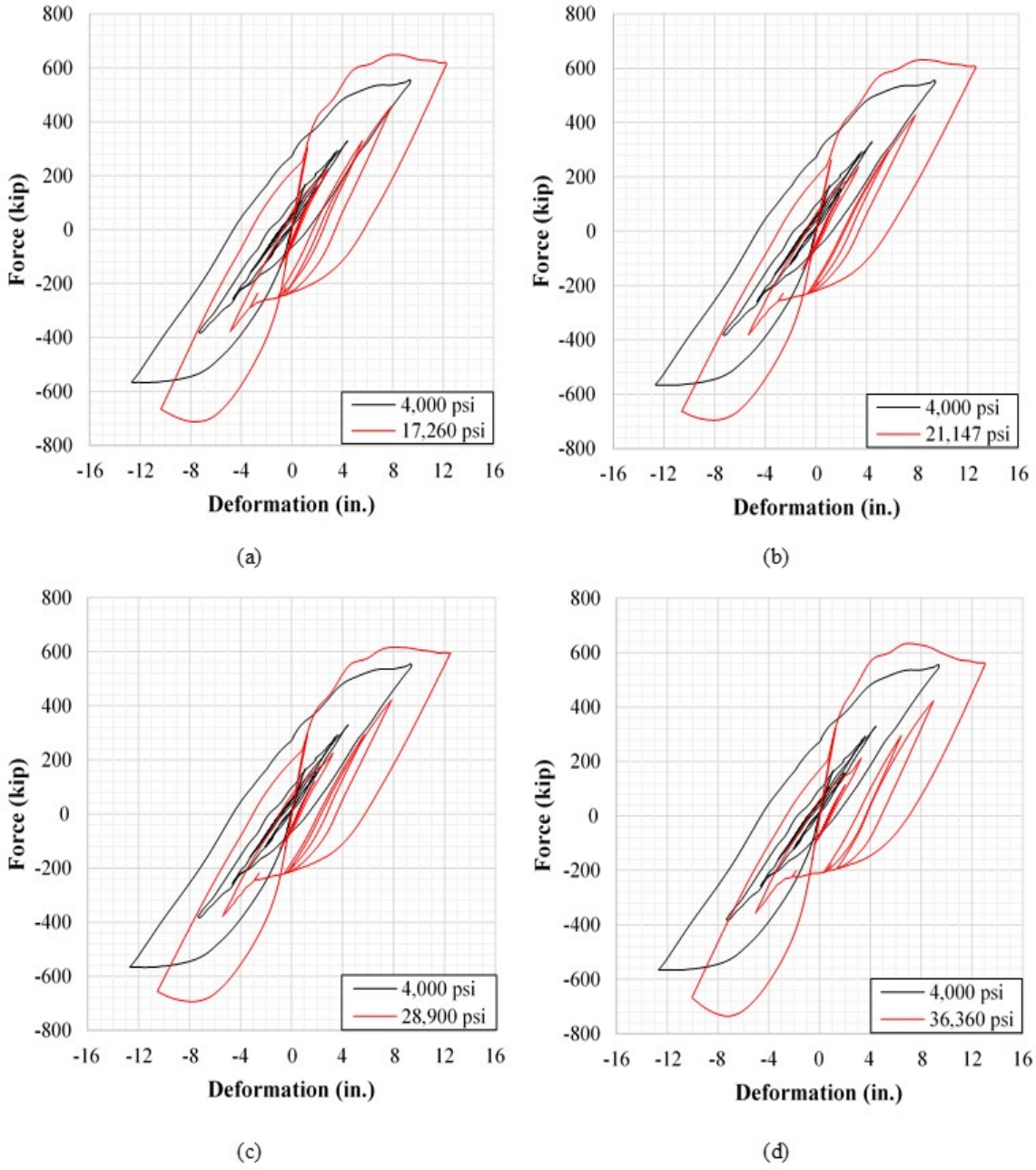

Figure 5.12 Force-displacement (hysteresis) relationship for (a) UHPC 1, (b) UHPC 2, (c) UHPC 3, and (d) UHPC 4 piers under RSN 77 (Design Level) ground motion.

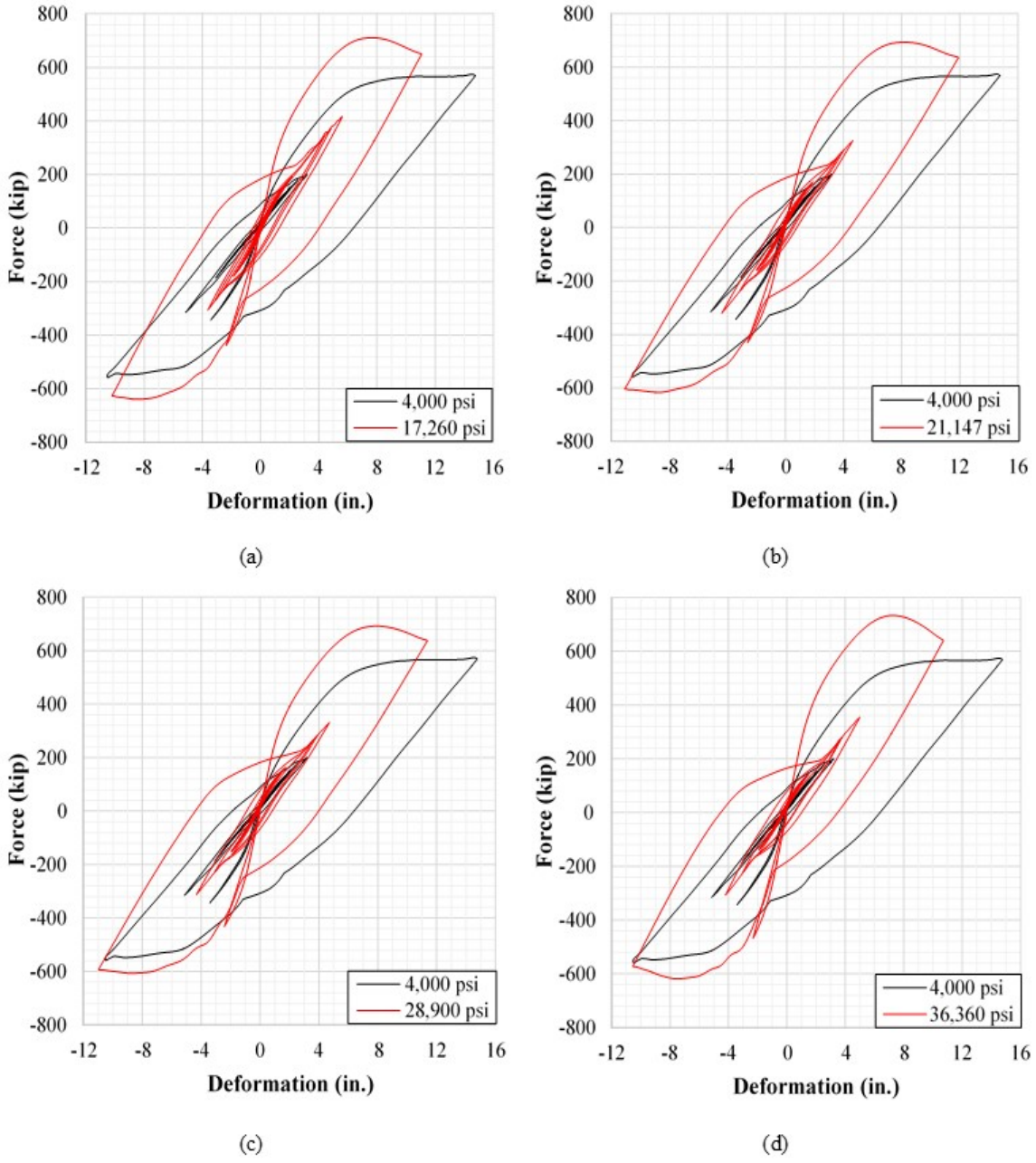

Figure 5.13 Force-displacement (hysteresis) relationship for (a) UHPC 1, (b) UHPC 2, (c) UHPC 3, and (d) UHPC 4 piers under RSN 96 (Design Level) ground motion.

Moreover, Figure 5.14 shows a sample of the moment-curvature relationships for the two bridge columns but only for the first selected ground motion (RSN 6 from Table 5-2). The figure suggests that the UHPC experience much higher curvatures demands than NSC. Accurate estimates of displacement, curvature, and/or rotation capacities of UHPC columns are not available yet due to

the lack of experimental research in this relatively new field. Thus, it is hard to tell whether the higher UHPC curvature demands, compared to the original conventional concrete case, is a drawback. However, from a different perspective, the higher UHPC curvatures might be attributed to the nature of the moment-curvature behavior associated with UHPC OpenSees modeling assumptions. In Figure 4.4c from Chapter 4, the UHPC column moment-curvature relationship does not follow the same usual trend as NSC, i.e. the moment is not monotonically increasing as curvatures increase. On the contrary, after the UHPC column moment capacity is reached, the moment values start dropping as curvatures increase. This might suggest that after a typical UHPC column reaches its capacity, it becomes sensitive to curvatures increase (descending or softening branch of the moment-curvature curve). Figure 5.14 also show that two pier columns have consistently different moment capacities (~200,000 kip-in versus ~150,000 kip-in) for all cases. This is because of the fluctuating axial load level associated with the seismic overturning moments, which leads to one column experiencing higher compression forces, and in turn, demonstrate a higher moment capacity.

Similar to the capacity check performed using the nonlinear pushover analysis, the bent cap beam moment-curvature response is checked to verify that the bent cap remains essentially elastic due to seismic loading. Figure 5.15 shows a sample moment-curvature response of the bent cap for one of the design cases (UHPC 3 with 3-3.5% reinforcement) due to design level RSN 6 ground motion. The figure demonstrates that the cap beam remains essentially elastic and all damage occur in the columns as desired.

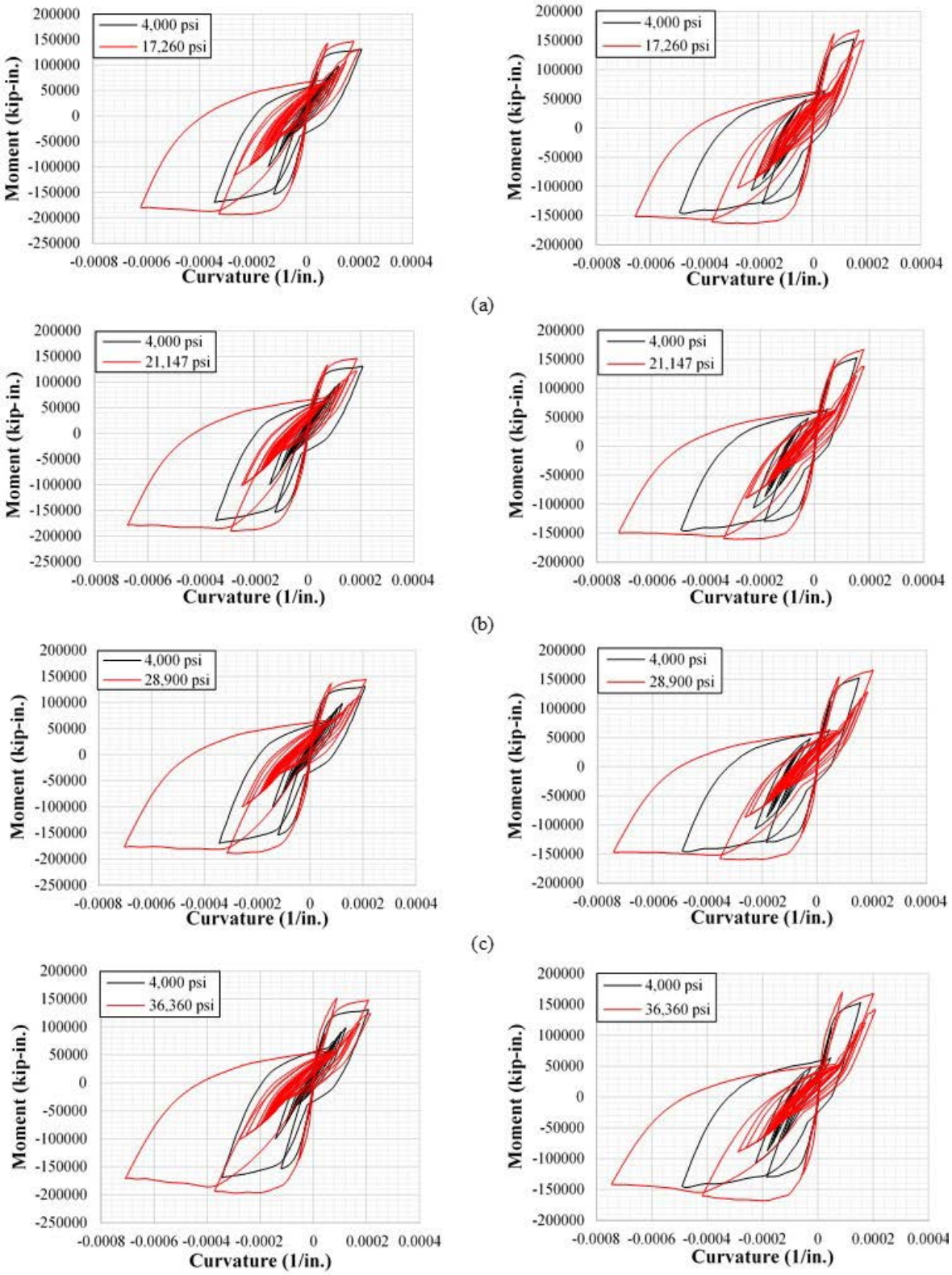

Figure 5.14 Moment-curvature response of the two pier columns for RSN 6 (Design Level) using (a) UHPC 1, (b) UHPC 2, (c) UHPC 3, and (d) UHPC 4.

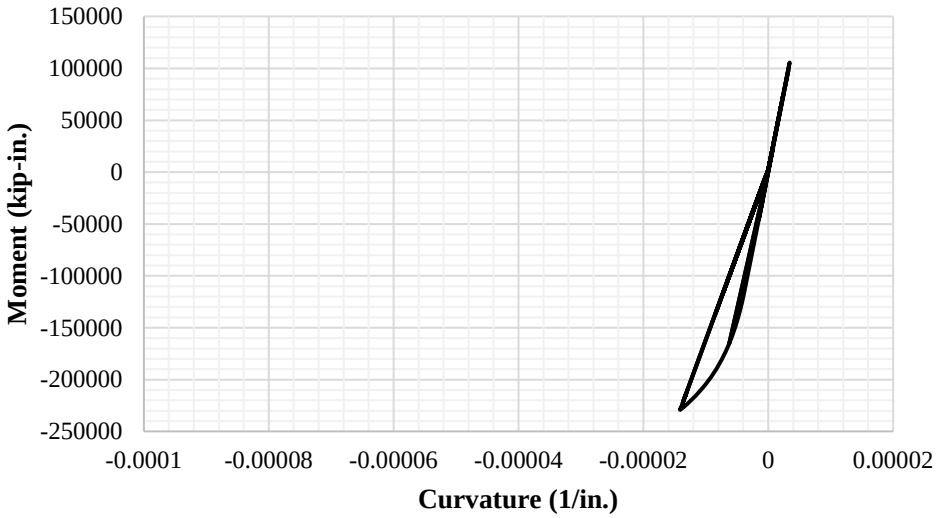

Figure 5.15 Sample moment-curvature response of the bent cap beam under RSN 6 (Design Level) for both conventional concrete and UHPC 3 bridge piers.

To conclude the discussion of the DLE NTHA cases, Figures 5.16, 5.17, and 5.18 summarize the maximum displacements, residual displacements, and base shears for each UHPC design as compared with the original conventional concrete design. These figures provide the same observations as before. It illustrates in a more convenient visual display that UHPC piers have higher force capacities and experience overall less displacements and residual (permanent) damage.

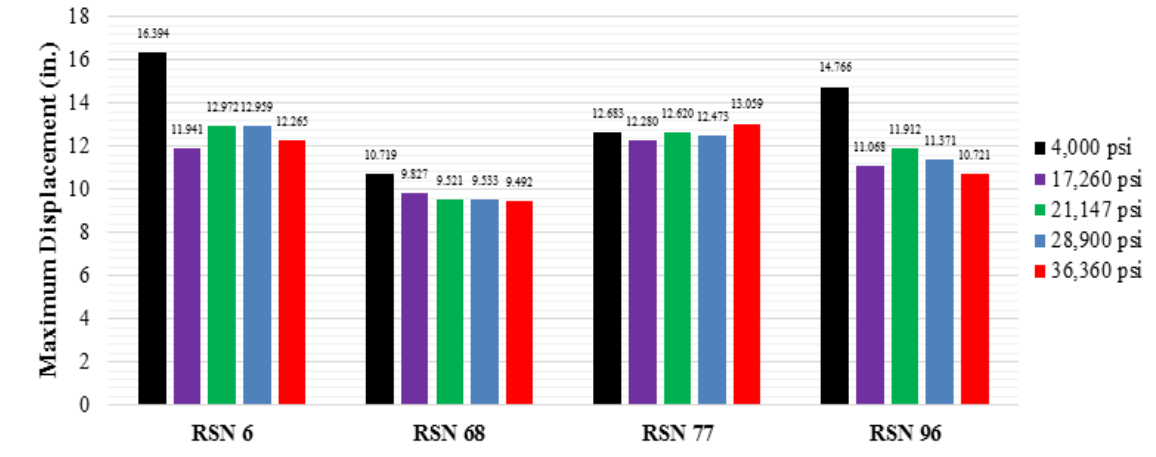

Figure 5.16 Maximum displacements for each ground motion case at the Design Level.

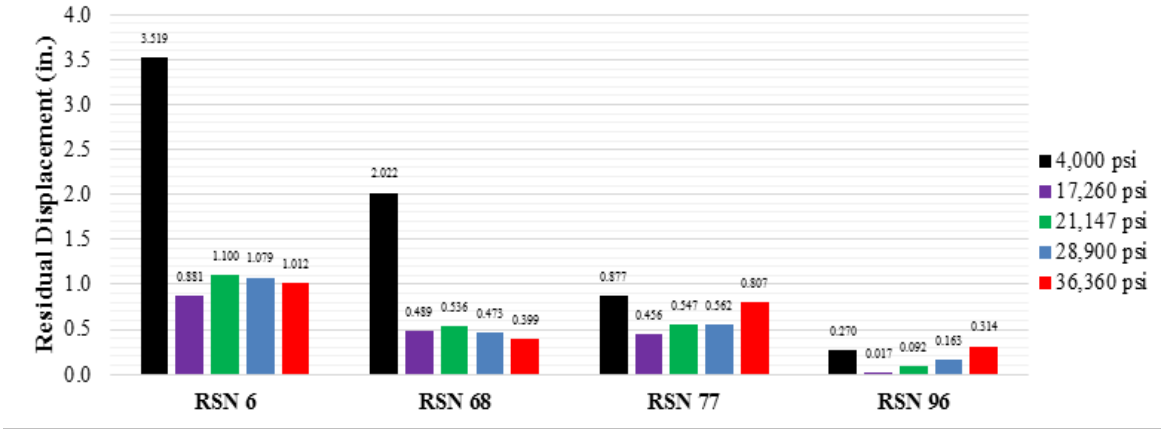

Figure 5.17 Residual displacements for each ground motion case at the Design Level.

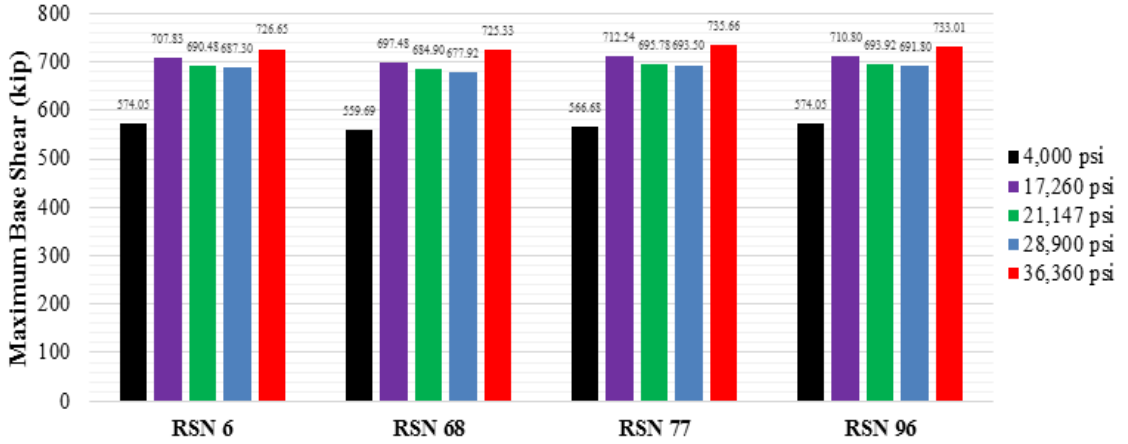

Figure 5.18 Maximum base shear for each ground motion case at the Design Level.

5.3.5 DETAILED ANALYSIS RESULTS: MAXIMUM CONSIDERED EARTHQUAKES

A similar framework as DLE is shown here to present the MCE analysis cases. Figures 5.19 through 5.22 show the displacement history, while Figures 5.23 through 5.26 show the hysteresis force-displacement response for all four ground motions, respectively. Figure 5.27 presents a sample of moment-curvature responses of each UHPC column under the RSN 6 ground motion. While the maximum and residual displacements for the UHPC designs are still lower than the original conventional concrete design, the maximum displacements have closer values since all the NCS and UHPC columns are well into the nonlinear behavior and at elevated damage states. The drift ratios increased on average by 1-2% higher than DLE cases, with the maximum base shear remaining nearly the same (dictated by the column capacities). Figures 5.28, 5.29, and 5.30

again summarize the maximum displacements, residual displacements, and base shears for each UHPC design, respectively, as compared with the original conventional concrete design at the MCE level. In summary, the optimized UHPC piers have demonstrated an overall comparable, or even superior, seismic response when compared to conventional concrete with higher force capacities and lower deformations and displacement demands.

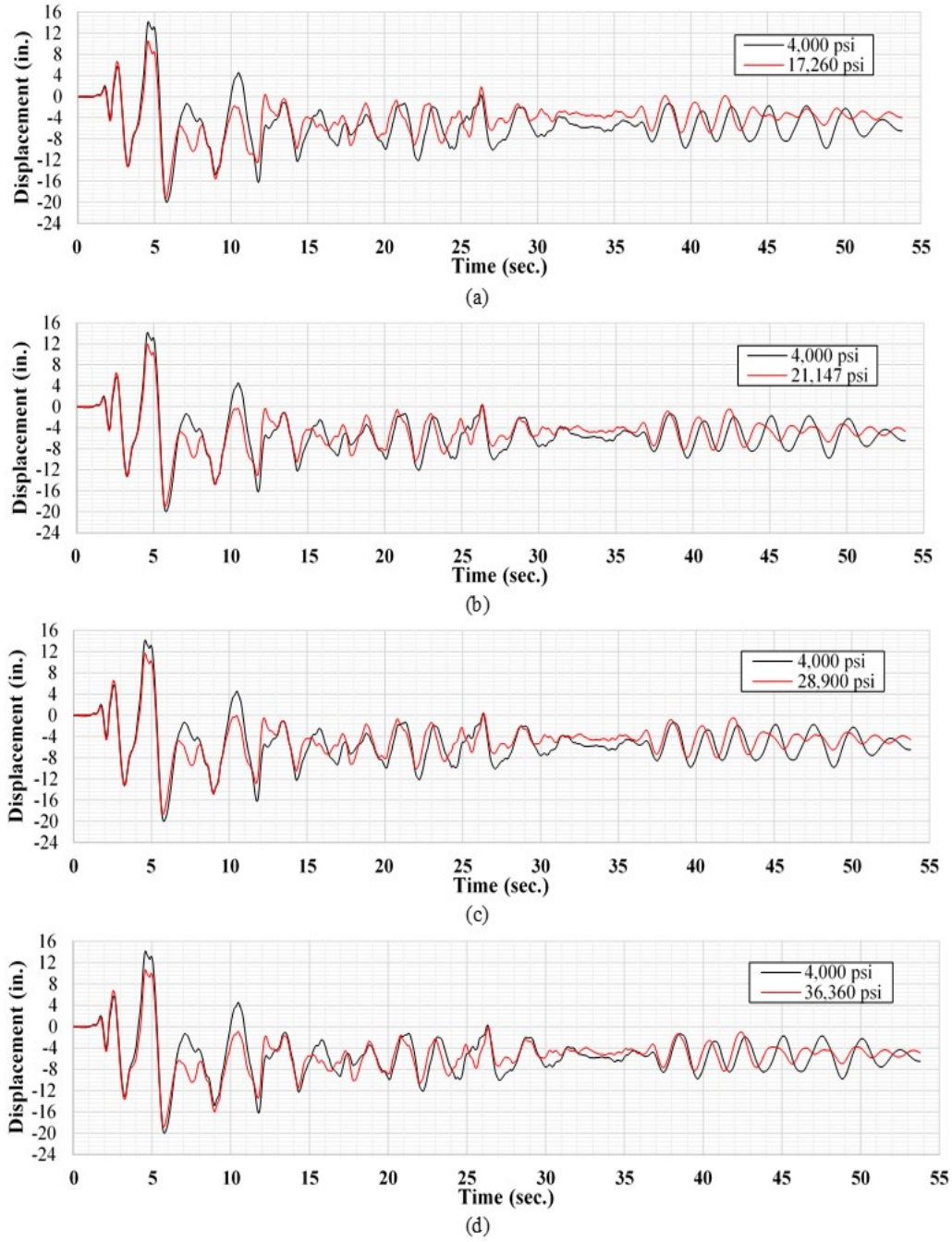

Figure 5.19 Displacement history for RSN 6 (MCE) for (a) UHPC 1, (b) UHPC 2, (c) UHPC 3, and (d) UHPC 4.

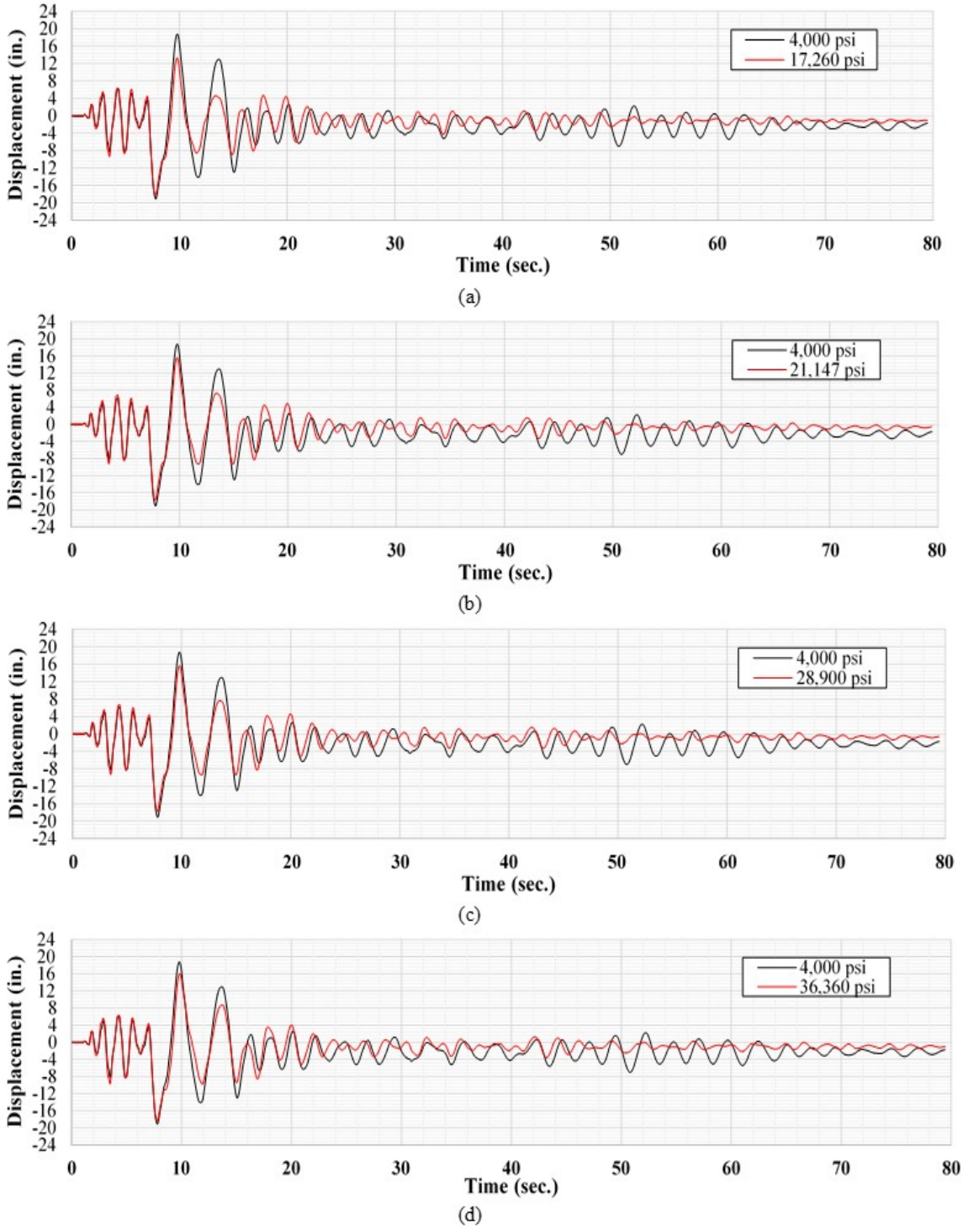

Figure 5.20 Displacement history for RSN 68 (MCE) for (a) UHPC 1, (b) UHPC 2, (c) UHPC 3, and (d) UHPC 4.

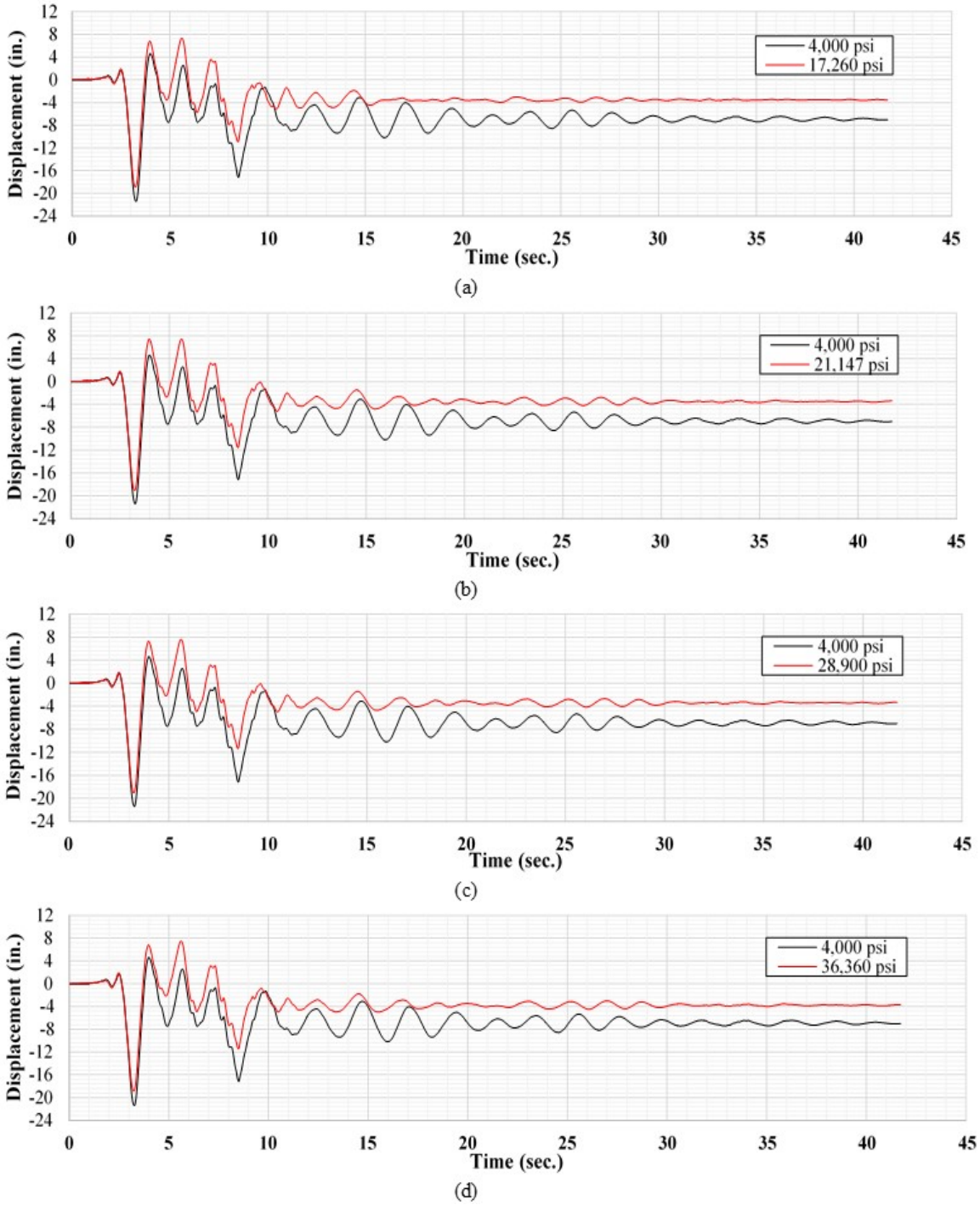

Figure 5.21 Displacement history for RSN 77 (MCE) for (a) UHPC 1, (b) UHPC 2, (c) UHPC 3, and (d) UHPC 4.

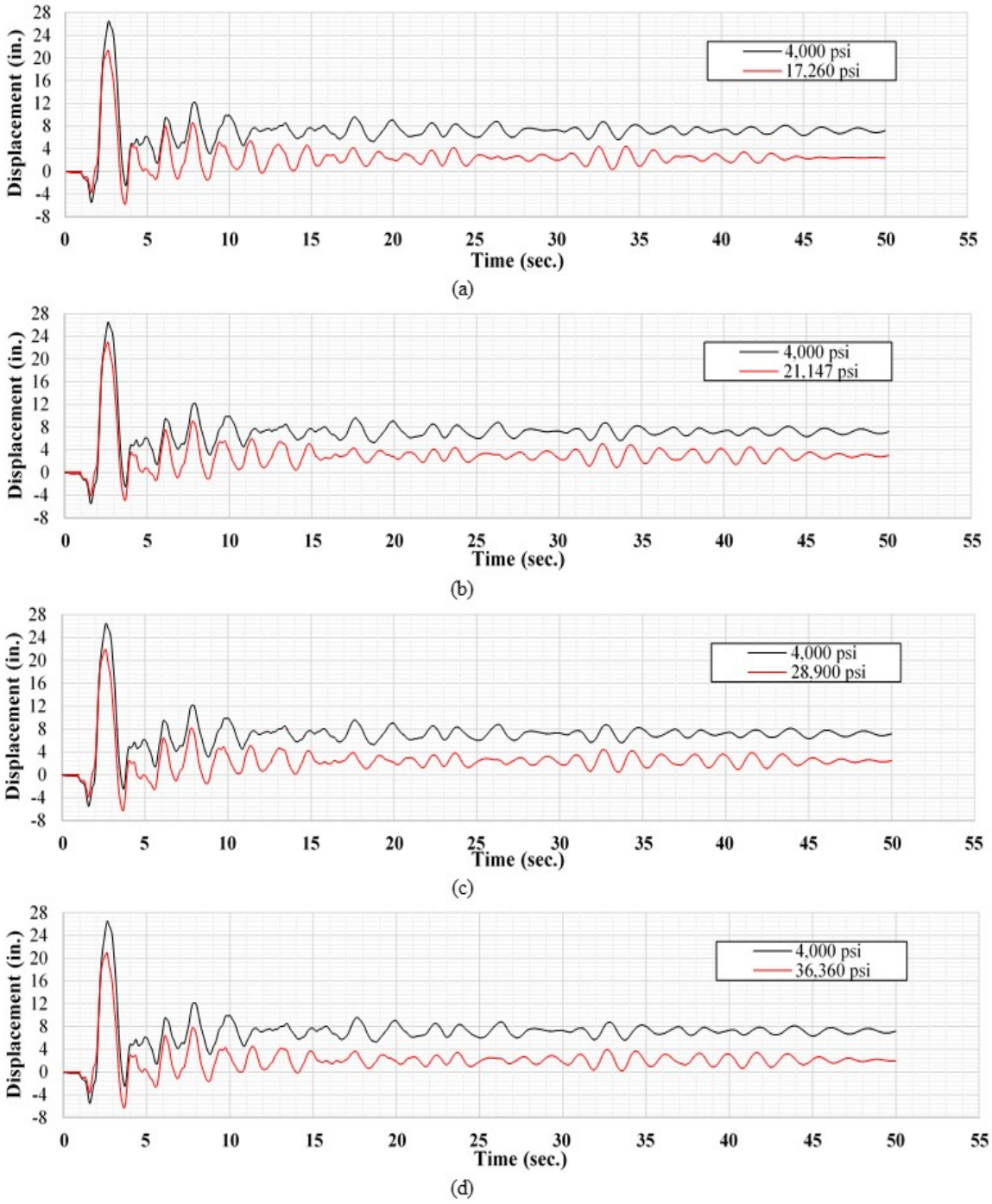

Figure 5.22 Displacement history for RSN 96 (MCE) for (a) UHPC 1, (b) UHPC 2, (c) UHPC 3, and (d) UHPC 4.

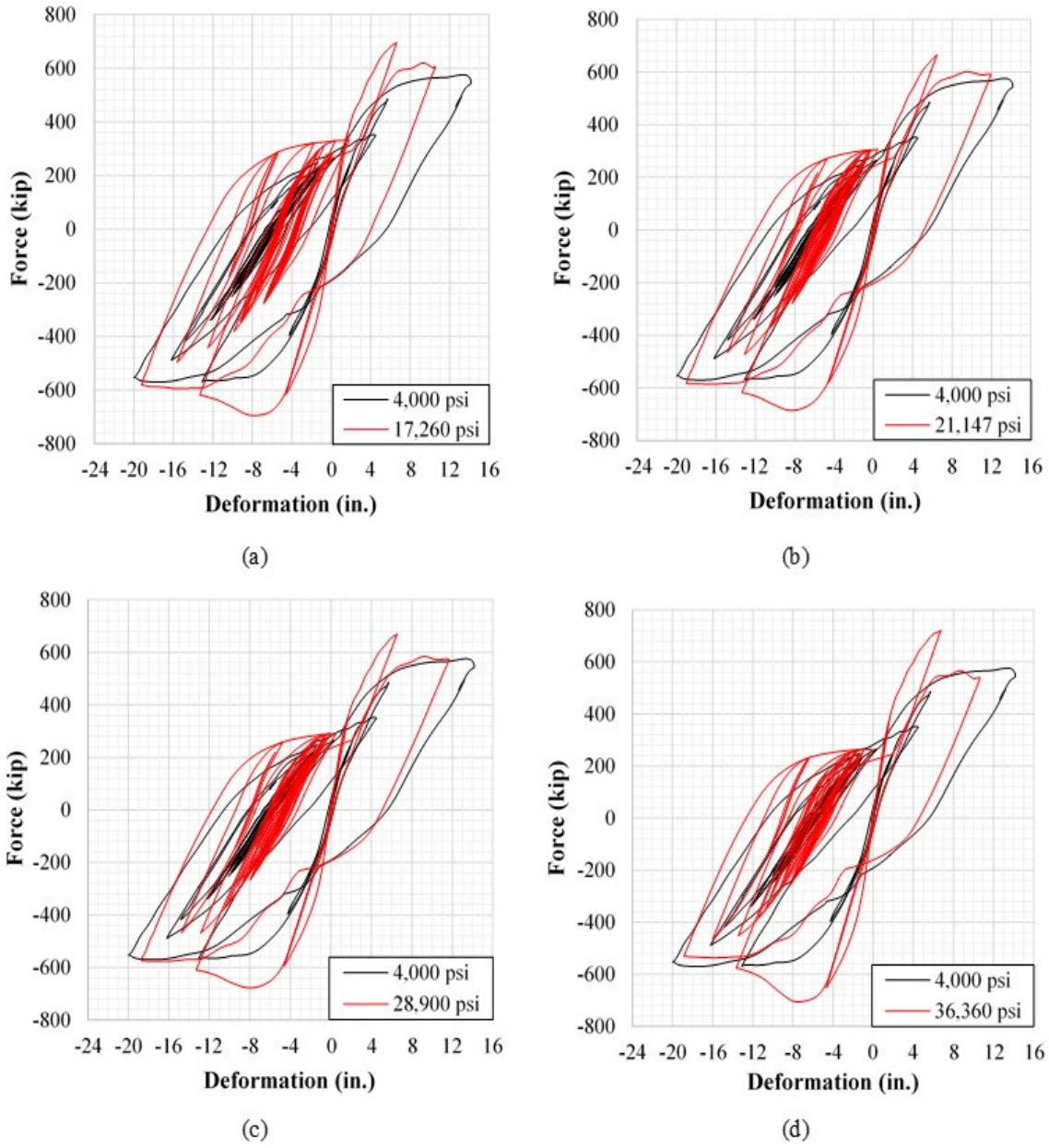

Figure 5.23 Force-displacement (hysteresis) relationship for (a) UHPC 1, (b) UHPC 2, (c) UHPC 3, and (d) UHPC 4 piers under RSN 6 (MCE level) ground motion.

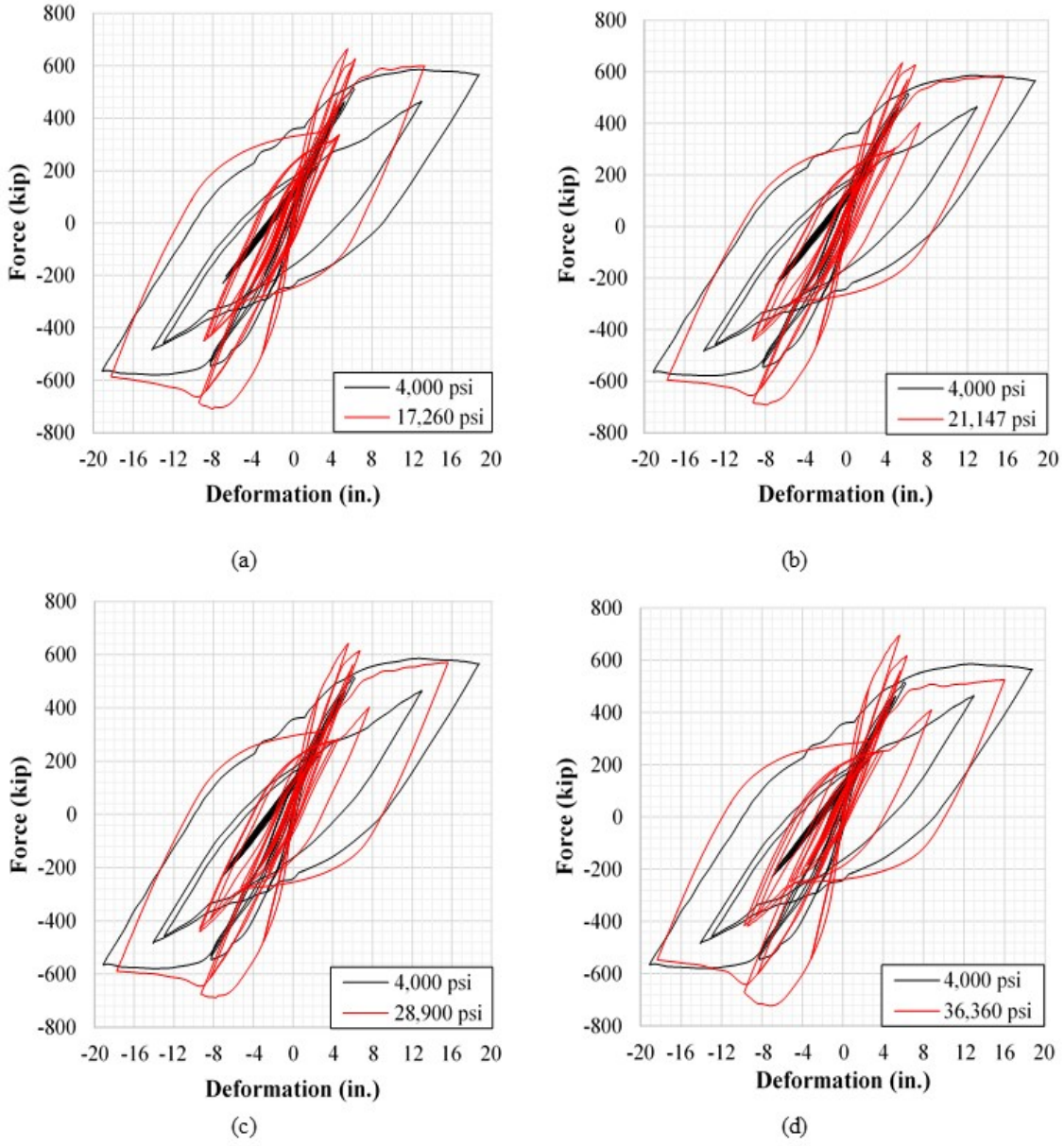

Figure 5.24 Force-displacement (hysteresis) relationship for (a) UHPC 1, (b) UHPC 2, (c) UHPC 3, and (d) UHPC 4 piers under RSN 68 (MCE level) ground motion.

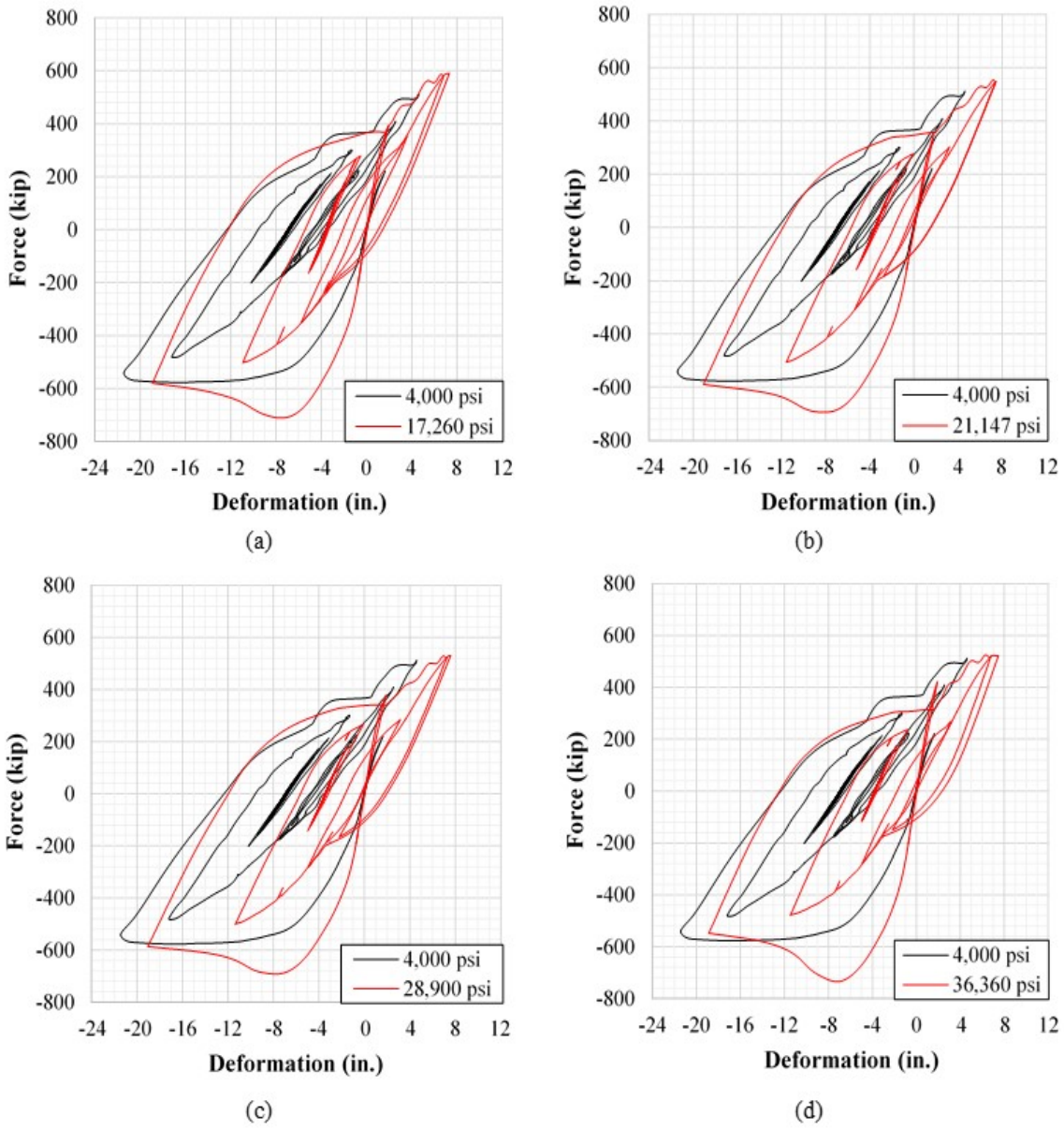

Figure 5.25 Force-displacement (hysteresis) relationship for (a) UHPC 1, (b) UHPC 2, (c) UHPC 3, and (d) UHPC 4 piers under RSN 77 (MCE level) ground motion.

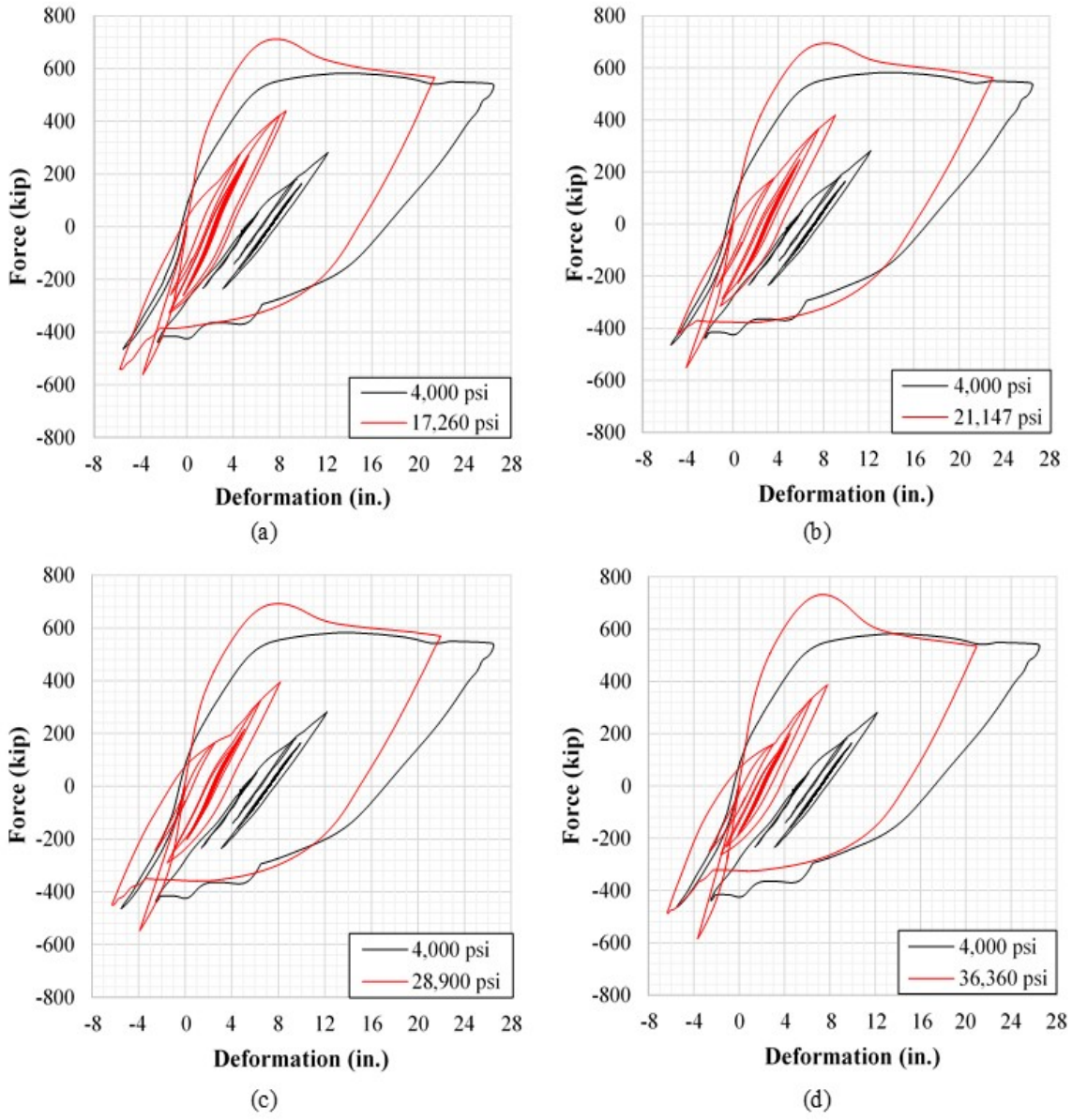

Figure 5.26 Force-displacement (hysteresis) relationship for (a) UHPC 1, (b) UHPC 2, (c) UHPC 3, and (d) UHPC 4 piers under RSN 96 (MCE level) ground motion.

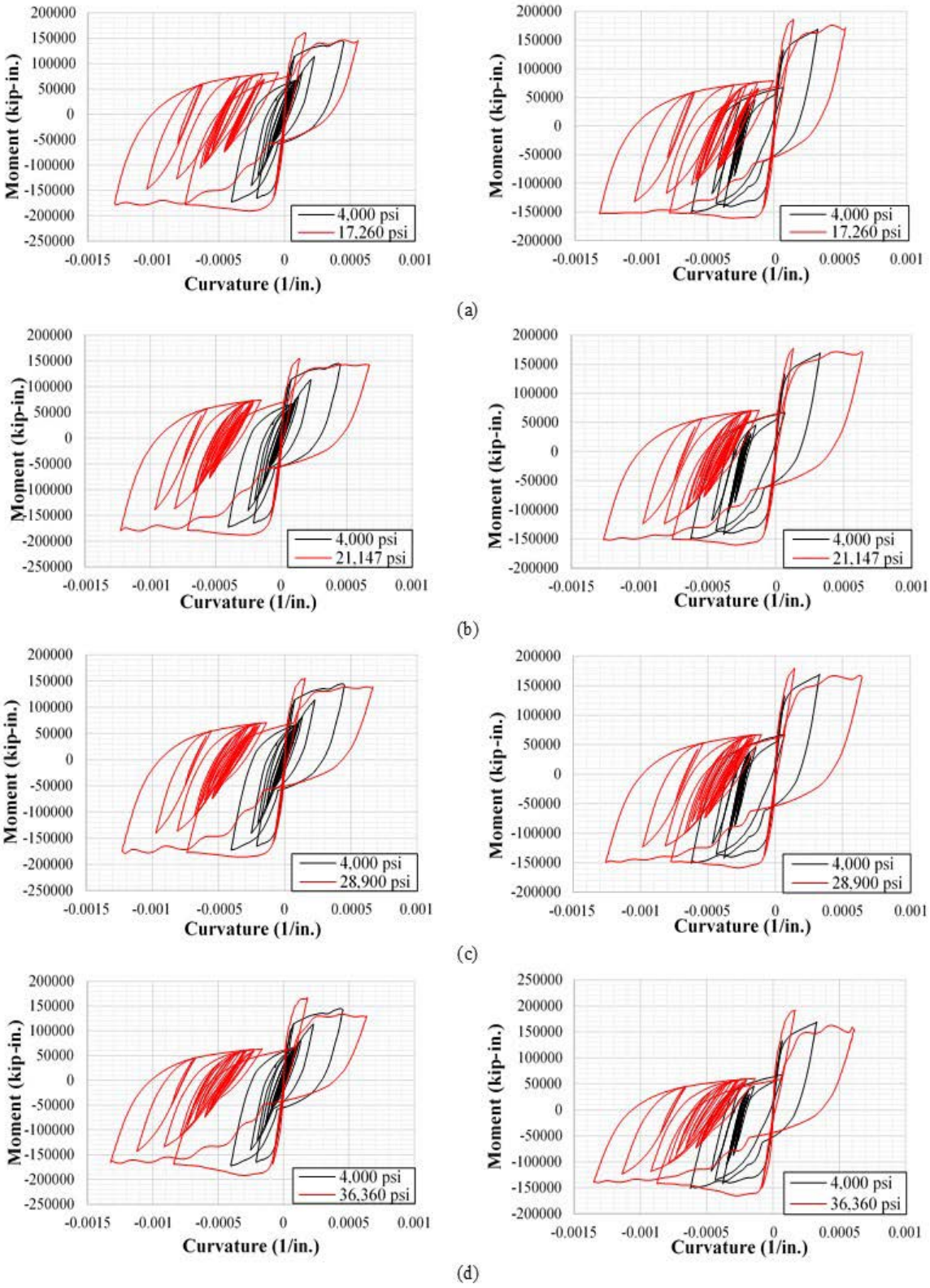

Figure 5.27 Moment-curvature response of the two pier columns for RSN 6 (MCE) using (a) UHPC 1, (b) UHPC 2, (c) UHPC 3, and (d) UHPC 4.

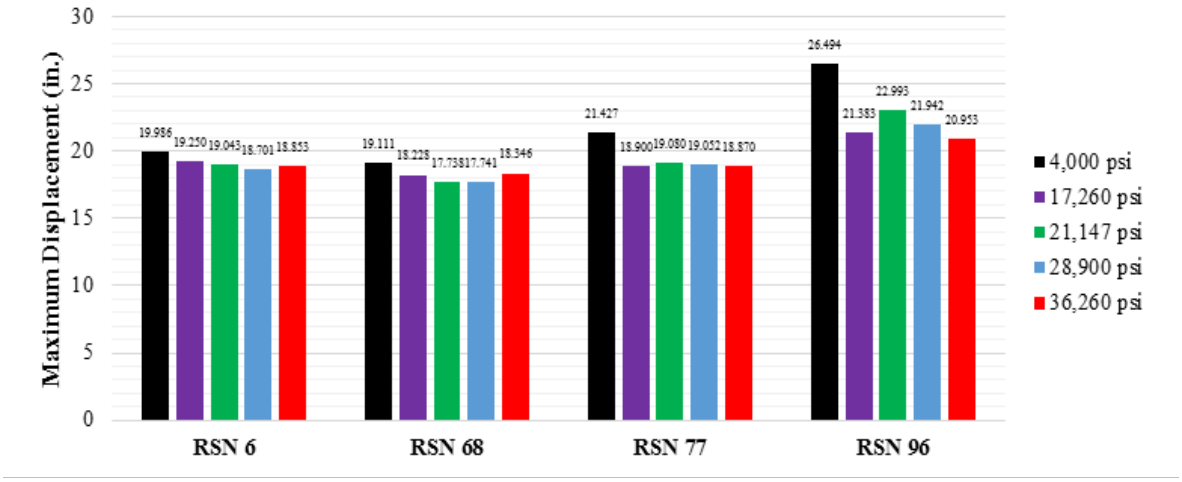

Figure 5.28 Maximum displacements for each ground motion at the MCE level.

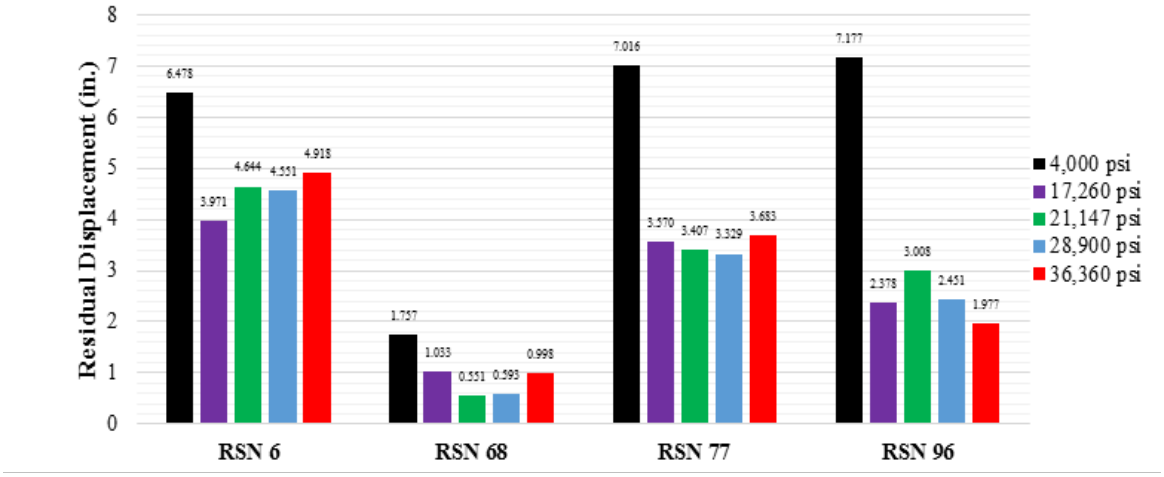

Figure 5.29 Residual displacements for each ground motion at the MCE level.

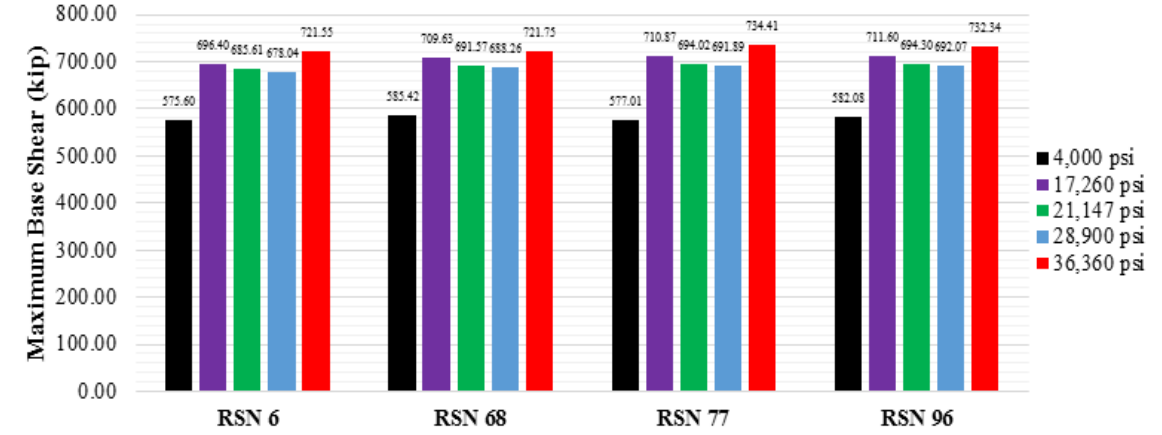

Figure 5.30 Maximum base shear for each ground motion at the MCE level.

6 Cost Analysis

6.1 BILLS OF QUANTITIES

Using the optimized column designs from Chapter 4 for each varying longitudinal steel reinforcement ratio (~1.5%, 2.0-2.5%, 3.0-3.5%, and 5.0-6.0%) and associated bent cap designs, volumetric and weight calculations per full bridge pier are performed. Tables 6-1 and 6-2 summarize the concrete and reinforcement bill of quantities based on the Concrete02 and Concrete04 optimized designs, respectively. The estimated material consumption metrics, based on bills of quantities, include cement, water, superplasticizer, steel fibers, and reinforcement steel. Tables 6-3 and 6-4 present the consumed material estimates for the Concrete02 and Concrete04 designs, respectively. As demonstrated in Chapter 4, the importance of increasing the longitudinal steel reinforcement ratios is to better utilize the UHPC superior mechanical properties, and in turn, allow the decrease in column diameter and bent cap width.

The steep costs of steel fibers in the UHPC mix designs contribute immensely to the costs of each design. The cost of manufacturing the steel fibers is high due to the lack of multiple domestic manufacturers and low demands. According to Voort et al. (2008), as the utilization of UHPC increases across North America, the manufacturing costs of steel fibers will decrease as more orders of steel fibers are placed. The cost of UHPC in North America was approximately $\$2{,}000/yd^3$ in the year 2000 and has since decreased (Voort et al., 2008), especially for non-proprietary mixes. Current costs of UHPC have been reported as low as $\$1{,}500/yd^3$ and will hopefully decrease to an amount as low as $\$570/yd^3$, which is the current estimate in Europe where UHPC is more widely utilized (Aïtcin, 2000).

Table 6-1 Total Concrete and Steel Volumes for Concrete02-Based Designs

Property	Original	UHPC 1	UHPC 2	UHPC 3	UHPC 4
f'_c (psi)	4,000	17,260	21,147	28,900	36,360
f_t (psi)	-	1,300	1,500*	1,700	2,611
A_{st}≅1.5%					
Total Column Concrete Volume (yd^3)	92.15	68.33	64.00	59.80	51.84
Total Bent Cap Concrete Volume (yd^3)	98.88	78.74	76.91	75.08	71.41
Total Column Rebar Weight (ton)	10.75	8.26	8.20	8.14	6.63
Total Bent Cap Rebar Weight (ton)	6.04	4.20	3.68	3.15	2.89
Total Rebar Weight (ton)	16.79	12.46	11.88	11.29	9.51
Total Concrete Volume (yd^3)	191.03	147.07	140.90	134.88	123.25
% Decrease of Total Volume	-	23.01%	26.24%	29.39%	35.48%
A_{st}≅2.0-2.5%					
Total Column Concrete Volume (yd^3)	92.15	59.80	55.75	55.75	48.07
Total Bent Cap Concrete Volume (yd^3)	98.88	75.08	73.24	73.24	69.58
Total Column Rebar Weight (ton)	10.75	10.35	10.97	9.62	8.83
Total Bent Cap Rebar Weight (ton)	6.04	4.46	3.94	3.68	3.41
Total Rebar Weight (ton)	16.79	14.82	14.91	13.30	12.25
Total Concrete Volume (yd^3)	191.03	134.88	128.99	128.99	117.65
% Decrease of Total Volume	-	29.39%	32.48%	32.48%	38.41%
A_{st}≅3.0-3.5%					
Total Column Concrete Volume (yd^3)	92.15	55.75	51.84	48.07	44.44
Total Bent Cap Concrete Volume (yd^3)	98.88	73.24	71.41	69.58	67.75
Total Column Rebar Weight (ton)	10.75	12.31	12.26	12.20	11.47
Total Bent Cap Rebar Weight (ton)	6.04	4.73	4.20	3.94	3.68
Total Rebar Weight (ton)	16.79	17.04	16.46	16.14	15.15
Total Concrete Volume (yd^3)	191.03	128.99	123.25	117.65	112.19
% Decrease of Total Volume	-	32.48%	35.48%	38.41%	41.27%
A_{st}≅5.0-6.0%					
Total Column Concrete Volume (yd^3)	92.15	40.96	40.96	40.96	37.62
Total Bent Cap Concrete Volume (yd^3)	98.88	65.92	65.92	65.92	64.09
Total Column Rebar Weight (ton)	10.75	16.87	16.87	15.68	14.42
Total Bent Cap Rebar Weight (ton)	6.04	5.51	5.25	4.99	4.46
Total Rebar Weight (ton)	16.79	22.39	22.12	20.66	18.89
Total Concrete Volume (yd^3)	191.03	106.88	106.88	106.88	101.70
% Decrease of Total Volume	-	44.05%	44.05%	44.05%	46.76%

Table 6-2 Total Concrete and Steel Volumes for Concrete04-Based Designs

Property	Original	UHPC 1	UHPC 2	UHPC 3	UHPC 4
f'_c (psi)	4,000	17,260	21,147	28,900	36,360
f_t (psi)	-	1,300	1,500*	1,700	2,611
A_{st}≅1.5%					
Total Column Concrete Volume (yd^3)	92.15	82.20	77.43	72.81	64.00
Total Bent Cap Concrete Volume (yd^3)	98.88	84.23	82.40	80.57	76.91
Total Column Rebar Weight (ton)	10.75	9.97	9.91	9.18	8.20
Total Bent Cap Rebar Weight (ton)	6.04	5.78	4.73	4.46	4.20
Total Rebar Weight (ton)	16.79	15.74	14.63	13.64	12.40
Total Concrete Volume (yd^3)	191.03	166.43	159.83	153.38	140.90
% Decrease of Total Volume	-	12.88%	16.33%	19.71%	26.24%
A_{st}≅2.0-2.5%					
Total Column Concrete Volume (yd^3)	92.15	68.33	64.00	64.00	55.75
Total Bent Cap Concrete Volume (yd^3)	98.88	78.74	76.91	76.91	73.24
Total Column Rebar Weight (ton)	10.75	12.49	12.43	11.76	10.97
Total Bent Cap Rebar Weight (ton)	6.04	6.30	4.73	4.46	4.20
Total Rebar Weight (ton)	16.79	18.79	17.15	16.22	15.17
Total Concrete Volume (yd^3)	191.03	147.07	140.90	140.90	128.99
% Decrease of Total Volume	-	23.01%	26.24%	26.24%	32.48%
A_{st}≅3.0-3.5%					
Total Column Concrete Volume (yd^3)	92.15	59.80	55.75	55.75	51.84
Total Bent Cap Concrete Volume (yd^3)	98.88	75.08	73.24	73.24	71.41
Total Column Rebar Weight (ton)	10.75	14.77	14.71	13.51	13.45
Total Bent Cap Rebar Weight (ton)	6.04	6.83	5.78	5.25	4.46
Total Rebar Weight (ton)	16.79	21.59	20.48	18.76	17.92
Total Concrete Volume (yd^3)	191.03	134.88	128.99	128.99	123.25
% Decrease of Total Volume	-	29.39%	32.48%	32.48%	35.48%
A_{st}≅5.0-6.0%					
Total Column Concrete Volume (yd^3)	92.15	48.07	44.44	44.44	40.96
Total Bent Cap Concrete Volume (yd^3)	98.88	69.58	67.75	67.75	65.92
Total Column Rebar Weight (ton)	10.75	18.18	16.93	16.93	16.87
Total Bent Cap Rebar Weight (ton)	6.04	7.35	6.30	5.78	5.25
Total Rebar Weight (ton)	16.79	25.54	23.23	22.71	22.12
Total Concrete Volume (yd^3)	191.03	117.65	112.19	112.19	106.88
% Decrease of Total Volume	-	38.41%	41.27%	41.27%	44.05%

Table 6-3 Total Material Consumption for Concrete02-Based Designs

Property	Original	UHPC 1	UHPC 2	UHPC 3	UHPC 4
Mix No.	-	#1	#81	#1	#87
f'_c (psi)	4,000	17,260	21,147	28,900	36,360
f_t (psi)	-	1,300	1,500*	1,700	2,611
Cement (lb/yd^3)	675	1,200	1,153	1,200	1,002
Water (lb/yd^3)	335	184	196	184	190
Superplasticizer (lb/yd^3)	-	51.8	28.8	51.8	11.0
Steel Fibers (lb/yd^3)	-	263	288	263	271
A_{st}≅1.5%					
Total Cement Consumed (ton)	64.47	88.24	81.23	80.93	61.75
Total Water Consumed (gallons)	8,608	3,640	3,715	3,338	3,150
Total Superplasticizer Consumed (ton)	-	3.81	2.03	3.49	0.68
Total Steel Fibers Consumed (ton)	-	19.34	20.29	17.74	16.70
Total Rebar Consumed (ton)	16.79	12.46	11.88	11.29	9.51
A_{st}≅2.0-2.5%					
Total Cement Consumed (ton)	64.47	80.93	74.36	77.39	58.94
Total Water Consumed (gallons)	8,608	3,338	3,401	3,192	3,007
Total Superplasticizer Consumed (ton)	-	3.49	1.86	3.34	0.65
Total Steel Fibers Consumed (ton)	-	17.74	18.57	16.96	15.94
Total Rebar Consumed (ton)	16.79	14.82	14.91	13.30	12.25
A_{st}≅3.0-3.5%					
Total Cement Consumed (ton)	64.47	77.39	71.05	70.59	56.21
Total Water Consumed (gallons)	8,608	3,192	3,249	2,912	2,867
Total Superplasticizer Consumed (ton)	-	3.34	1.77	3.05	0.62
Total Steel Fibers Consumed (ton)	-	16.96	17.75	15.47	15.20
Total Rebar Consumed (ton)	16.79	17.04	16.46	16.14	15.15
A_{st}≅5.0-6.0%					
Total Cement Consumed (ton)	64.47	64.13	61.62	64.13	50.95
Total Water Consumed (gallons)	8,608	2,645	2,818	2,645	2,599
Total Superplasticizer Consumed (ton)	-	2.77	1.54	2.77	0.56
Total Steel Fibers Consumed (ton)	-	14.05	15.39	14.05	13.78
Total Rebar Consumed (ton)	16.79	22.39	22.12	20.66	18.89

Table 6-4 Total Material Consumption for Concrete04-Based Designs

Property	Original	UHPC 1	UHPC 2	UHPC 3	UHPC 4
Mix No.	-	#1	#81	#1	#87
f'_c (psi)	4,000	17,260	21,147	28,900	36,360
f_t (psi)	-	1,300	1,500*	1,700	2,611
Cement (lb/yd^3)	675	1,200	1,153	1,200	1,002
Water (lb/yd^3)	335	184	196	184	190
Superplasticizer (lb/yd^3)	-	51.8	28.8	51.8	11.0
Steel Fibers (lb/yd^3)	-	263	288	263	271
A_{st}≅1.5%					
Total Cement Consumed (ton)	64.47	99.86	92.14	92.03	70.59
Total Water Consumed (gallons)	8,608	4,119	4,214	3,796	3,601
Total Superplasticizer Consumed (ton)	-	4.31	2.30	3.97	0.77
Total Steel Fibers Consumed (ton)	-	21.89	23.02	20.17	19.09
Total Rebar Consumed (ton)	16.79	15.74	14.63	13.64	12.40
A_{st}≅2.0-2.5%					
Total Cement Consumed (ton)	64.47	88.24	81.23	84.54	64.62
Total Water Consumed (gallons)	8,608	3,640	3,715	3,487	3,296
Total Superplasticizer Consumed (ton)	-	3.81	2.03	3.65	0.71
Total Steel Fibers Consumed (ton)	-	19.34	20.29	18.53	17.48
Total Rebar Consumed (ton)	16.79	18.79	17.15	16.22	15.17
A_{st}≅3.0-3.5%					
Total Cement Consumed (ton)	64.47	80.93	74.36	77.39	61.75
Total Water Consumed (gallons)	8,608	3,338	3,401	3,192	3,150
Total Superplasticizer Consumed (ton)	-	3.49	1.86	3.34	0.68
Total Steel Fibers Consumed (ton)	-	17.74	18.57	16.96	16.70
Total Rebar Consumed (ton)	16.79	21.59	20.48	18.76	17.92
A_{st}≅5.0-6.0%					
Total Cement Consumed (ton)	64.47	70.59	64.68	67.31	53.55
Total Water Consumed (gallons)	8,608	2,912	2,958	2,777	2,731
Total Superplasticizer Consumed (ton)	-	3.05	1.62	2.91	0.59
Total Steel Fibers Consumed (ton)	-	15.47	16.16	14.75	14.48
Total Rebar Consumed (ton)	16.79	25.54	23.23	22.71	22.12

6.2 MONETARY COST ESTIMATES

Using the calculated volumes of concrete and the weight of the steel fibers and reinforcement (Tables 6-1 through 6-4), the total costs of each UHPC design case are estimated using four different estimates that range as follows: \$550/yd^3, \$1,500/yd^3, \$2,000/yd^3, and \$2,500/yd^3. These estimations include the costs of curing and mixing the various UHPC components such as cement, steel fibers, fine sand, ground quartz, silica fume, high range water reducers, and accelerators. As a side calculation to a percent contribution of the total costs due to the steel fibers, the cost of an equivalent 2% steel fibers is estimated to be \$1,000 for one cubic yard of UHPC using estimates provided by KPM Industries, a Canadian UHPC manufacturer (2016). Note that this estimate is only for current typical costs in Northern America. Thus, such percentage for cost contribution from the steel fiber cost is not valid, and not calculated, for the \$550/yd^3 European estimate. The cost of steel reinforcement was estimated to be \$441 per metric ton of reinforcing steel (SteelBenchmarker, 2016). The cost of the original conventional concrete design (f'_c = 4,000 psi) is estimated to be \$130/yd^3 of concrete (Paragon Ready Mix Inc., 2016).

While all Concrete02 and Concrete04-based designs result in significant savings in volume (compared to the original conventional concrete design), UHPC 4 achieved the highest savings of cement in each level of steel reinforcement ratio. Despite the increasing compressive strengths and Young's Moduli across UHPC 1, 2, 3, and 4, cases using the 5.0-6.0% steel reinforcement ratios result in nearly similar column dimensions. Since each design performs equally well, mechanical properties beyond UHPC 1 would not be necessary to achieve the most optimized dimensions. Overall, the largest percent decrease in volume achieved for Concrete02 and Concrete04-based designs, when compared to the original conventional concrete design, are 46.76% and 44.05%, respectively (refer to Table 4-8 and 4-9 in Chapter 4 for the tabulated column and bent dimensions for the NSC and each UHPC design case).

An estimate of the material costs of a single bridge pier for each of the considered design cases is calculated and summarized in Table 6-5 and 6-6 for the designs based on Concrete02 and Concrete04, respectively. When the assumed unit cost of UHPC is equal to the highest estimate at \$2,500/yd^3, immediate cost savings, relative to the original conventional design, are achieved at A_{st} = 3.0-3.5% for UHPC 3 and 4, and for all designs at A_{st}=5.0-6.0%. When the assumed cost of UHPC is equal to \$2,000/yd^3, immediate cost savings are achieved at every design except for

UHPC 1 at A_{st} = ~1.5%. Estimations at \$550/yd^3 and \$1,500/yd^3 of UHPC were able to achieve cost savings for every design with respect to the original conventional concrete design.

For a meaningful cost comparison, the UHPC piers construction costs are integrated within an overall cost estimate for the full prototype bridge. For this purpose, the bridge superstructure is always considered a NSC box-girder and only the piers are considered to be made of UHPC. Using values provided by the Florida Department of Transportation (FDOT, 2009), a cost estimate for a concrete bridge (continuous span) is approximately \$211/ft^2 making the overall construction cost estimate of the original conventional concrete bridge approximately \$4,297,918 (~\$4.3 million). If the \$2,500 UHPC unit cost (highest estimate) is considered along with the highlighted pier construction costs in Tables 6-5 and 6-6, the increase for UHPC columns as a percentage of overall bridge cost ranges from 10.7%-15.9% and 11.4%-18.2% for both Concrete02 and Concrete04-based designs, respectively. This cost increase range depends on which UHPC mix is used and what reinforcement ratios are used to optimize the design. For the \$550 UHPC unit cost estimate, the percent increase in bridge cost ranges from 1.5%-2.5% and 1.7%-3.1% for both Concrete02 and Concrete04-based designs, respectively. Thus, if UHPC unit material cost drops in the future to be within the current price range as in Europe, building UHPC bridge piers will lead to only a very small increase in the construction costs based on the prototype bridge considered in this study. This small increase in cost is worth considering for a better life expectancy, seismic performance, and minimal maintenance.

Table 6-5 Cost of Optimized Concrete02-Based Pier Design

Cost of UHPC ($550/yd^3)					
A_{st}	**Case**	**Cost of Concrete ($)**	**% Total Cost of Steel Fibers**	**Cost of Steel Reinforcement ($)**	**Total ($)**
≅1.5%	Original	$24,899.90	-	$7,404.39	$32,304.29
	UHPC 1	$80,888.50	N/A	$5,494.86	$86,383.36
	UHPC 2	$77,495.00	N/A	$5,239.08	$82,734.08
	UHPC 3	$74,184.00	N/A	$4,978.89	$79,162.89
	UHPC 4	$67,787.50	N/A	$4,193.91	$71,981.41
2.0-2.5%	UHPC 1	$74,184.00	N/A	$6,535.62	$80,719.62
	UHPC 2	$70,944.50	N/A	$6,575.31	$77,519.81
	UHPC 3	$70,944.50	N/A	$5,865.30	$76,809.80
	UHPC 4	$64,707.50	N/A	$5,402.25	$70,109.75
3.0-3.5%	UHPC 1	$70,944.50	N/A	$7,514.64	$78,459.14
	UHPC 2	$67,787.50	N/A	$7,258.86	$75,046.36
	UHPC 3	$64,707.50	N/A	$7,117.74	$71,825.24
	UHPC 4	$61,704.50	N/A	$6,681.15	$68,385.65
5.0-6.0%	UHPC 1	$58,784.00	N/A	$9,873.99	$68,657.99
	UHPC 2	$58,784.00	N/A	$9,754.92	$68,538.92
	UHPC 3	$58,784.00	N/A	$9,111.06	$67,895.06
	UHPC 4	$55,935.00	N/A	$8,330.49	$64,265.49
Cost of UHPC ($1500/yd^3)					
A_{st}	**Case**	**Cost of Concrete ($)**	**% Total Cost of Steel Fibers**	**Cost of Steel Reinforcement ($)**	**Total ($)**
≅1.5%	Original	$24,899.90	-	$7,404.39	$32,304.29
	UHPC 1	$220,605.00	65.05%	$5,494.86	$226,099.86
	UHPC 2	$211,350.00	65.05%	$5,239.08	$216,589.08
	UHPC 3	$202,320.00	65.07%	$4,978.89	$207,298.89
	UHPC 4	$184,875.00	65.19%	$4,193.91	$189,068.91
2.0-2.5%	UHPC 1	$202,320.00	64.58%	$6,535.62	$208,855.62
	UHPC 2	$193,485.00	64.48%	$6,575.31	$200,060.31
	UHPC 3	$193,485.00	64.71%	$5,865.30	$199,350.30
	UHPC 4	$176,475.00	64.69%	$5,402.25	$181,877.25
3.0-3.5%	UHPC 1	$193,485.00	64.17%	$7,514.64	$200,999.64
	UHPC 2	$184,875.00	64.15%	$7,258.86	$192,133.86
	UHPC 3	$176,475.00	64.08%	$7,117.74	$183,592.74
	UHPC 4	$168,285.00	64.12%	$6,681.15	$174,966.15
5.0-6.0%	UHPC 1	$160,320.00	62.80%	$9,873.99	$170,193.99
	UHPC 2	$160,320.00	62.84%	$9,754.92	$170,074.92
	UHPC 3	$160,320.00	63.08%	$9,111.06	$169,431.06
	UHPC 4	$152,550.00	63.21%	$8,330.49	$160,880.49

Table 6-5 Cost of Optimized Concrete02-Based Pier Design (Continued)

Cost of UHPC ($2000/yd^3)					
A_{st}	**Case**	**Cost of Concrete ($)**	**% Total Cost of Steel Fibers**	**Cost of Steel Reinforcement ($)**	**Total ($)**
≅1.5%	Original	$24,899.90	-	$7,404.39	$32,304.29
	UHPC 1	$294,140.00	49.08%	$5,494.86	$299,634.86
	UHPC 2	$281,800.00	49.09%	$5,239.08	$287,039.08
	UHPC 3	$269,760.00	49.09%	$4,978.89	$274,738.89
	UHPC 4	$246,500.00	49.16%	$4,193.91	$250,693.91
2.0-2.5%	UHPC 1	$269,760.00	48.82%	$6,535.62	$276,295.62
	UHPC 2	$257,980.00	48.76%	$6,575.31	$264,555.31
	UHPC 3	$257,980.00	48.89%	$5,865.30	$263,845.30
	UHPC 4	$235,300.00	48.88%	$5,402.25	$240,702.25
3.0-3.5%	UHPC 1	$257,980.00	48.58%	$7,514.64	$265,494.64
	UHPC 2	$246,500.00	48.57%	$7,258.86	$253,758.86
	UHPC 3	$235,300.00	48.53%	$7,117.74	$242,417.74
	UHPC 4	$224,380.00	48.55%	$6,681.15	$231,061.15
5.0-6.0%	UHPC 1	$213,760.00	47.79%	$9,873.99	$223,633.99
	UHPC 2	$213,760.00	47.82%	$9,754.92	$223,514.92
	UHPC 3	$213,760.00	47.96%	$9,111.06	$222,871.06
	UHPC 4	$203,400.00	48.03%	$8,330.49	$211,730.49
Cost of UHPC ($2500/yd^3)					
A_{st}	**Case**	**Cost of Concrete ($)**	**% Total Cost of Steel Fibers**	**Cost of Steel Reinforcement ($)**	**Total ($)**
≅1.5%	Original	$24,899.90	-	$7,404.39	$32,304.29
	UHPC 1	$367,675.00	39.41%	$5,494.86	$373,169.86
	UHPC 2	$352,250.00	39.41%	$5,239.08	$357,489.08
	UHPC 3	$337,200.00	39.42%	$4,978.89	$342,178.89
	UHPC 4	$308,125.00	39.46%	$4,193.91	$312,318.91
2.0-2.5%	UHPC 1	$337,200.00	39.24%	$6,535.62	$343,735.62
	UHPC 2	$322,475.00	39.20%	$6,575.31	$329,050.31
	UHPC 3	$322,475.00	39.29%	$5,865.30	$328,340.30
	UHPC 4	$294,125.00	39.28%	$5,402.25	$299,527.25
3.0-3.5%	UHPC 1	$322,475.00	39.09%	$7,514.64	$329,989.64
	UHPC 2	$308,125.00	39.08%	$7,258.86	$315,383.86
	UHPC 3	$294,125.00	39.05%	$7,117.74	$301,242.74
	UHPC 4	$280,475.00	39.07%	$6,681.15	$287,156.15
5.0-6.0%	UHPC 1	$267,200.00	38.57%	$9,873.99	$277,073.99
	UHPC 2	$267,200.00	38.59%	$9,754.92	$276,954.92
	UHPC 3	$267,200.00	38.68%	$9,111.06	$276,311.06
	UHPC 4	$254,250.00	38.73%	$8,330.49	$262,580.49

Table 6-6 Cost of Optimized Concrete04-Based Pier Design

Cost of UHPC ($550/yd^3)					
A_{st}	**Case**	**Cost of Concrete ($)**	**% Total Cost of Steel Fibers**	**Cost of Steel Reinforcement ($)**	**Total ($)**
≅1.5%	Original	$24,899.90	-	$7,404.39	$32,304.29
	UHPC 1	$91,536.50	N/A	$6,941.34	$98,477.84
	UHPC 2	$87,906.50	N/A	$6,451.83	$94,358.33
	UHPC 3	$84,359.00	N/A	$6,015.24	$90,374.24
	UHPC 4	$77,495.00	N/A	$5,468.40	$82,963.40
2.0-2.5%	UHPC 1	$80,888.50	N/A	$8,286.39	$89,174.89
	UHPC 2	$77,495.00	N/A	$7,563.15	$85,058.15
	UHPC 3	$77,495.00	N/A	$7,153.02	$84,648.02
	UHPC 4	$70,944.50	N/A	$6,689.97	$77,634.47
3.0-3.5%	UHPC 1	$74,184.00	N/A	$9,521.19	$83,705.19
	UHPC 2	$70,944.50	N/A	$9,031.68	$79,976.18
	UHPC 3	$70,944.50	N/A	$8,273.16	$79,217.66
	UHPC 4	$67,787.50	N/A	$7,902.72	$75,690.22
5.0-6.0%	UHPC 1	$64,707.50	N/A	$11,263.14	$75,970.64
	UHPC 2	$61,704.50	N/A	$10,244.43	$71,948.93
	UHPC 3	$61,704.50	N/A	$10,015.11	$71,719.61
	UHPC 4	$58,784.00	N/A	$9,754.92	$68,538.92
Cost of UHPC ($1500/yd^3)					
A_{st}	**Case**	**Cost of Concrete ($)**	**% Total Cost of Steel Fibers**	**Cost of Steel Reinforcement ($)**	**Total ($)**
≅1.5%	Original	$24,899.90	-	$7,404.39	$32,304.29
	UHPC 1	$249,645.00	64.86%	$6,941.34	$256,586.34
	UHPC 2	$239,745.00	64.92%	$6,451.83	$246,196.83
	UHPC 3	$230,070.00	64.97%	$6,015.24	$236,085.24
	UHPC 4	$211,350.00	64.99%	$5,468.40	$216,818.40
2.0-2.5%	UHPC 1	$220,605.00	64.25%	$8,286.39	$228,891.39
	UHPC 2	$211,350.00	64.36%	$7,563.15	$218,913.15
	UHPC 3	$211,350.00	64.48%	$7,153.02	$218,503.02
	UHPC 4	$193,485.00	64.44%	$6,689.97	$200,174.97
3.0-3.5%	UHPC 1	$202,320.00	63.67%	$9,521.19	$211,841.19
	UHPC 2	$193,485.00	63.69%	$9,031.68	$202,516.68
	UHPC 3	$193,485.00	63.93%	$8,273.16	$201,758.16
	UHPC 4	$184,875.00	63.93%	$7,902.72	$192,777.72
5.0-6.0%	UHPC 1	$176,475.00	62.67%	$11,263.14	$187,738.14
	UHPC 2	$168,285.00	62.84%	$10,244.43	$178,529.43
	UHPC 3	$168,285.00	62.92%	$10,015.11	$178,300.11
	UHPC 4	$160,320.00	62.84%	$9,754.92	$170,074.92

Table 6-6 Cost of Optimized Concrete04-Based Pier Design (Continued)

Cost of UHPC ($2000/yd^3)					
A_{st}	**Case**	**Cost of Concrete ($)**	**% Total Cost of Steel Fibers**	**Cost of Steel Reinforcement ($)**	**Total ($)**
≅1.5%	Original	$24,899.90	-	$7,404.39	$32,304.29
	UHPC 1	$332,860.00	48.98%	$6,941.34	$339,801.34
	UHPC 2	$319,660.00	49.01%	$6,451.83	$326,111.83
	UHPC 3	$306,760.00	49.04%	$6,015.24	$312,775.24
	UHPC 4	$281,800.00	49.05%	$5,468.40	$287,268.40
2.0-2.5%	UHPC 1	$294,140.00	48.63%	$8,286.39	$302,426.39
	UHPC 2	$281,800.00	48.69%	$7,563.15	$289,363.15
	UHPC 3	$281,800.00	48.76%	$7,153.02	$288,953.02
	UHPC 4	$257,980.00	48.74%	$6,689.97	$264,669.97
3.0-3.5%	UHPC 1	$269,760.00	48.30%	$9,521.19	$279,281.19
	UHPC 2	$257,980.00	48.31%	$9,031.68	$267,011.68
	UHPC 3	$257,980.00	48.45%	$8,273.16	$266,253.16
	UHPC 4	$246,500.00	48.45%	$7,902.72	$254,402.72
5.0-6.0%	UHPC 1	$235,300.00	47.72%	$11,263.14	$246,563.14
	UHPC 2	$224,380.00	47.82%	$10,244.43	$234,624.43
	UHPC 3	$224,380.00	47.86%	$10,015.11	$234,395.11
	UHPC 4	$213,760.00	47.82%	$9,754.92	$223,514.92
Cost of UHPC ($2500/yd^3)					
A_{st}	**Case**	**Cost of Concrete ($)**	**% Total Cost of Steel Fibers**	**Cost of Steel Reinforcement ($)**	**Total ($)**
≅1.5%	Original	$24,899.90	-	$7,404.39	$32,304.29
	UHPC 1	$416,075.00	39.34%	$6,941.34	$423,016.34
	UHPC 2	$399,575.00	39.36%	$6,451.83	$406,026.83
	UHPC 3	$383,450.00	39.38%	$6,015.24	$389,465.24
	UHPC 4	$352,250.00	39.39%	$5,468.40	$357,718.40
2.0-2.5%	UHPC 1	$367,675.00	39.12%	$8,286.39	$375,961.39
	UHPC 2	$352,250.00	39.16%	$7,563.15	$359,813.15
	UHPC 3	$352,250.00	39.20%	$7,153.02	$359,403.02
	UHPC 4	$322,475.00	39.19%	$6,689.97	$329,164.97
3.0-3.5%	UHPC 1	$337,200.00	38.90%	$9,521.19	$346,721.19
	UHPC 2	$322,475.00	38.91%	$9,031.68	$331,506.68
	UHPC 3	$322,475.00	39.00%	$8,273.16	$330,748.16
	UHPC 4	$308,125.00	39.00%	$7,902.72	$316,027.72
5.0-6.0%	UHPC 1	$294,125.00	38.52%	$11,263.14	$305,388.14
	UHPC 2	$280,475.00	38.59%	$10,244.43	$290,719.43
	UHPC 3	$280,475.00	38.62%	$10,015.11	$290,490.11
	UHPC 4	$267,200.00	38.59%	$9,754.92	$276,954.92

7 Ecological Assessment

This chapter presents the ecological assessment and environmental impact analysis conducted for the different UHPC and NSC bridge pier cases. A detailed background section for energy consumption and global warming potential associated with concrete industries is presented first. This background section is included here for convenience as it provides the necessary data used in the ecological assessment.

7.1 ENERGY CONSUMPTION AND GLOBAL WARMING POTENTIAL

Cement production accounted for 9.5% of global carbon dioxide (CO_2) emissions in 2013. These high emissions are caused by a combination of carbonate oxidation during the cement clinker production process and fuel combustion during the general cement production within the kiln (Olivier et al., 2014). Limestone, a primary component of cement production, is made up of calcium carbonate. When heated to approximately 2700^{o}F, the limestone breaks down into calcium oxide and CO_2 contributing to roughly 50% of all CO_2 emissions from cement production (Rubenstein, 2012). Unfortunately, concrete is still the second most consumed substance on Earth next to water and will continually contribute to the global CO_2 emissions. In 2013, China's cement use contributed to approximately 57.8% of global cement emissions with India and the European Union following at 6.1% and 5.0% respectively. United States, Turkey, Russia, Japan, Iran, and Brazil followed next with each country contributing between 1.5% and 2.09% in global cement emissions (Olivier et al., 2014).

The four main steps of manufacturing portland cement include the following:

Quarry and Crush: Raw materials are extracted from the earth and are crushed into two inch pieces stockpiled.

Raw Meal Preparation: Materials are moved from stockpiles, proportioned to the right chemical composition, ground, and blended.

Pyroprocess: The materials are processed to remove water, calcinating limestone and causing the mix components to react.

Clinker, a stony residue from a furnace or burned coal, is produced, cooled, and stored.

Finishing Grind: The clinker is extracted from storage, gypsum is added, and the mix is round to a fine powder. The final product is then moved to storage and prepped for shipping. (Portland Cement Association, 2006)

Table 7-1 summarizes the fuel and electricity input for four cement plant processes (wet, long dry, dry with preheater, and dry with preheater and precalciner) and the weighted production average in the United States. Each process creates the same product but differs mostly in energy consumption. The wet process feeds raw material directly into the kiln as a slurry and averages 5.5 MBTu (million British thermal unit)/ton of concrete compared to the dry process (powder) with preheater and precalciner which averages 3.6 MBTu/ton of concrete. Approximately 55% of cement plants utilize post-consumer or industrial waste products as a fuel for combustion processes during cement production. A few types of these waste products include tire-derived wastes, waste oil, and solvents and are sometimes even combined by a few cement plants (PCA, 2006). Table 7-2 summarizes the energy input by cement plant process type.

Table 7-1 Fuel and Electricity Input by Cement Process Type (Portland Cement Association, 2006)

	Wet	Long Dry	Preheater	Precalciner	Average
Fuel and Electricity	**Fuel or Electricity Unit/Ton of Cement**				
Coal (ton)	0.121	0.106	0.117	0.101	0.107
Gasoline (gallon)	0.0834	0.0118	0.0255	0.0233	0.0319
Liquefied Petroleum Gas (gallon)	0	0.0096	0.001	0.0035	0.0034
Middle Distillates (gallon)	0.171	0.16	0.193	0.326	0.255
Natural Gas (ft^3)	0.066	0.171	0.12	0.232	0.178
Petroleum Coke (ton)	0.0326	0.0528	0.0139	0.0134	0.0223
Residual Oil (gallon)	0.0043	0.0131	0	0.015	0.0106
Wastes (ton)	0.0634	0.008	0.0037	0.0103	0.0177
Electricity (kWh)	125	136	136	130	131

Table 7-2 Energy Input by Cement Process Type (Portland Cement Association, 2006)

	Wet	Long Dry	Preheater	Precalciner	Average
Energy Source	**MBtu/Metric Ton of Cement**				
Coal	2.719	2.388	2.633	2.283	2.425
Gasoline	0.0104	0.0015	0.0032	0.0029	0.004
Liquefied Petroleum Gas	0	0.0009	0.0001	0.0003	0.0003
Middle Distillates	0.0238	0.0222	0.0267	0.0452	0.0354
Natural Gas	0.0676	0.174	0.123	0.237	0.182
Petroleum Coke	0.983	1.59	0.419	0.404	0.673
Residual Oil	0.0006	0.002	0	0.0022	0.0016
Wastes	1.269	0.161	0.075	0.206	0.354
Electricity	0.425	0.465	0.464	0.444	0.447
Total	5.499	4.804	3.743	3.626	4.122

In order to produce a ton of concrete, nearly 400 pounds of coal (4.7 MBTu of energy) is required producing nearly one ton of CO_2 (UNEP, 2010). According to a survey performed by the Portland Cement Association, an average of 2,044 lb of CO_2 is produced for every 2,205 lb of portland cement produced in the United States (Portland Cement Association, 2006). This translates to 1 lb of CO_2 produced for every 1.08 lb of portland cement produced. Table 7-3 summarizes the pyroprocess emissions from fuel combustion and calcination during cement production for four cement plant processes. It should be noted that CO_2 emissions cannot be consistently directly proportional to cement production since the clinker fractions in cement decreases over time. Clinker fractions in global cement production decreased on average to between 70% and 80% in 2013 compared to 95% in the past. Purnell stressed that using a single value for embodied carbon dioxide of concrete can lead to "gross over-simplifications". This can be costly for future projects if local/legislative measures eventually implement an economic environment taxing each metric ton of CO_2 emitted (Purnell, 2013). Concrete reinforcement produces CO_2 mostly through its iron and steel production processes in coke ovens, blast furnaces, and oxygen steel furnaces (WSA, 2014). Water, on the other hand, requires energy to treat and transport and holds its own contribution to carbon emissions. Furthermore, with drought stricken states such as Nevada, Texas, and California, water is becoming increasingly valuable and expensive. Table 7-4 summarizes the total emissions of particulates, fuel combustion gases, and CO_2 to the air from cement calcination processes.

Table 7-3 Pyroprocess Emissions from Fuel Combustion and Calcination (Portland Cement Association, 2006)

	Wet	Long Dry	Preheater	Precalciner	Average
Emission	**lb/Ton of Cement**				
Particulate Matter (Total)	0.561	0.694	0.295	0.304	0.401
Carbon Dioxide (CO_2)	2,180	2,000	1,691	1,726	1,835
Sulfur Dioxide (SO_2)	7.74	9.58	0.523	1.05	3.3
Nitrogen Oxides	6.99	5.75	4.57	4.01	4.84
Volatile Organic Compounds	0.11	0.0198	0.00608	0.101	0.0759
Carbon Monoxide (CO)	0.125	0.206	0.938	3.53	2.08
Methane (CH_4)	0.109	0.0193	0.00538	0.1	0.075
Ammonia (NH_3)	0.00943	0.00958	0.0095	0.00952	0.00951
Hydrogen Chloride (HCl)	0.086	0.11	0.26	0.13	0.14
Mercury (Hg)	1.10E-04	1.67E-04	5.38E-05	1.39E-04	1.25E-04
Dioxins and Furans (TEQ)	1.90E-07	1.10E-06	7.10E-09	2.00E-07	2.98E-07

Another study conducted by Feiz et al. (2015) evaluated the global warming potential of clinker and three common cement products produced by various cement production plants.

- CEM I 42.5 – Also known as portland cement with approximately 92% clinker content.
- CEM III/A 42.5 – A blended cement type with approximately 50% clinker content.
- CEM III/B 42.5 – A blended cement with GGBFS as a supplementary cementitious material that has approximately 27% clinker content.

Table 7-4 Total Emissions to the Air (Portland Cement Association, 2006)

	Wet	Long Dry	Preheater	Precalciner	Average
Emission	**lb/Ton of Cement**				
Particulate Matter (Total)	5.25	4.92	4.14	4.64	4.7
Particulate Matter (PM-10*)	0.648	0.575	0.531	0.598	0.593
Particulate Matter (PM-2.5*)	1.98E-04	1.82E-04	1.69E-04	1.81E-04	1.82E-04
Carbon Dioxide (CO_2)	2,200	2,010	1,700	1,750	1,850
Sulfur Dioxide (SO_2)	7.76	9.60	0.544	1.08	3.32
Nitrogen Oxides	7.16	5.87	4.7	4.2	5.01
Volatile Organic Compounds	0.132	0.0372	0.0256	0.13	0.1
Carbon Monoxide (CO)	0.249	0.293	1.04	3.68	2.21
Methane (CH_4)	0.112	0.0222	0.00859	0.105	0.0791
Ammonia (NH_3)	0.00943	0.00958	0.0095	0.00952	0.00951
Hydrogen Chloride (HCl)	0.086	0.11	0.26	0.13	0.14
Mercury (Hg)	1.10E-04	1.67E-04	5.38E-05	1.39E-04	1.25E-04
Dioxins and Furans (TEQ)	1.90E-07	1.10E-06	7.10E-09	2.00E-07	2.98E-07

**PM-10 is particulate matter with a median mass aerodynamic diameter of 10 micrometers or less*
**PM-2.5 is particulate matter with a median mass aerodynamic diameter of 2.5 micrometers or less*

The CO_2 emissions and various ratios for clinker, each cement product from three different cement plants, and the average is summarized in Table 7-5. The cement plants are located in Germany and include Kollenbach (Beckum), Dortmund (Dortmund), and Schwelgern (Duisburg). Feiz et al. (2015) found that nearly 90% of the CO_2 emissions for clinker wre connected to the Kollenbach plant with 64% due to calcination, 10% due to the combustion of kiln coal, and 8% due to the refused derived fuels (RDF). Table 7-6 is an excerpt from the Feiz et al. (2015) study breaking down the life cycle and energy consumption of clinker in the Kollenbach plant.

Table 7-5 Unit CO_2 Emissions for Clinker and Various Cement Products (Feiz et al., 2015)

Cement Products	Production Plant	Clinker-to-Cement Ratio (%)	GBFS-to-Cement Ratio (%)	Other Contents (%)	Clinker Substitution Rate (%)	Unit CO_2 Emissions (lb CO_2/ton)
Clinker	Kollenbach	100	0	0	0	1874
CEM I 42.5	Kollenbach	90	0	10	10	1717
CEM III/A 42.5	Dortmund	47	45	8	53	996
CEM III/B 42.5	Schwelgern	25	70	5	75	584
Average	-	40	53	7	60	849

Table 7-6 Life Cycle of Clinker in the Kollenbach Plant (Feiz et al., 2015)

Life cycle phase	Process	Consumed unit / tonne clinker		Emissions kg CO_2-eq / tonne clinker	Share %
Raw material extraction Cradle-to-gate (entrance)	Electricity (German mix)	kWh	68.5	45.5	5.4%
	Upgrading of animal meal	kg	60.8	39.1	4.6%
	Kiln coal	kg	35.4	12.2	1.4%
	Transport (rail and road)	tonne.km	58.1	3.6	0.4%
	Crushed marly limestone	kg	1002.1	2.1	0.2%
	Upgrading of RDF-fluff (silo)	kg	58.2	1.2	0.1%
	High grade limestone	kg	501.9	0.9	0.1%
	Refractory waste	kg	0.5	0.6	0.1%
	Light fuel oil	kg	0.4	0.3	0.04%
	Lignite	kg	14.4	0.2	0.02%
	Upgrading of RDF fluff (kiln)	kg	3.5	0.1	0.01%
	Upgrading of tires	kg	2.6	0.1	0.01%
	Upgrading of RDF fluff (agglomerate)	kg	1.4	0.0	0.00%
	Total raw material extraction phase			**106**	**12%**
Production Gate-to-gate	Calcination of raw materials			541	64%
	Combustion of kiln coal			89	11%
	Combustion of RDF fluff (silo)			71	8.0%
	Combustion of lignite			31	4.0%
	Combustion of tires			4.7	0.60%
	Combustion of RDF fluff (agglomerate)			3.2	0.40%
	Combustion of RDF fluff (kiln)			2.0	0.20%
	Combustion of light fuel oil			1.3	0.20%
	Total production phase			**744**	**88%**
Total clinker cradle to gate life cycle				**850**	**100%**

For this chapter, embodied carbon dioxide (eCO_2), measured by lb CO_2 per lb of cement, steel, water, and superplasticizer, is estimated for each mix design. While Purcell recommended not to use his embodied carbon dioxide metrics as an accurate value to each material component, this chapter will utilize those metrics to observe whether or not UHPC will have any immediate environmental benefits compared to the original conventional concrete design. Embodied carbon dioxide metrics for each material are summarized in Table 7-7. Note that the carbon dioxide emissions for cement is lower compared to the previous 2006 Portland Cement Association estimate (1 lb of CO_2 produced for every 1.08 lb of portland cement produced) due to improved production methods over time. Tables 7-8 and 7-9 summarize the embodied carbon dioxide resulting from the cement, water, superplasticizer, and rebar consumed for each Concrete02 and Concrete04-based design.

As seen in the results in Tables 7-8 and 7-9, cement is the material component that produces the most CO_2 in each mix design. As the steel reinforcement ratio increases, the embodied carbon dioxide for each design decreases for both Concrete02 and Concrete04-based designs due to decreasing column diameters and bent cap widths. Total embodied carbon dioxide for designs using UHPC 1, 2, and 3 saw very similar values, while UHPC 4 saw the largest percent difference when compared to the original conventional concrete design. The lowest total embodied carbon dioxide came from UHPC 4, equating to 60.24 tons and 64.86 tons for Concrete02 and Concrete04-based designs, respectively. Lower embodied carbon dioxide values are made possible by decreasing the diameter of the column, the width and depth of the bent cap, and by directly decreasing the cement, steel reinforcement, water, and superplasticizer consumed.

Table 7-7 Embodied Carbon Dioxide Metrics per Material (Purnell et al., 2012)

Material	Embodied Carbon Dioxide (lb CO_2 per lb of Material)
Cement	0.93
Steel	0.68
Water	0.001
Superplasticizer	0.01

Table 7-8 Embodied Carbon Dioxide for Concrete02-Based Designs

Property	Original	UHPC 1	UHPC 2	UHPC 3	UHPC 4
Mix No.	-	#1	#81	#1	#87
Cement (lb/yd^3)	675	1,200	1,153	1,200	1,002
Water (lb/yd^3)	335	184	196	184	190
Superplasticizer (lb/yd^3)	-	51.8	28.8	51.8	11.0
A_{st}≅1.5%					
eCO_2 of Cement (ton)	59.96	82.06	75.54	75.26	57.43
eCO_2 of Water (ton)	0.032	0.014	0.014	0.012	0.012
eCO_2 of Superplasticizer (ton)	-	0.038	0.020	0.035	0.007
eCO_2 of Rebar (ton)	11.42	8.47	8.08	7.68	6.47
Total eCO_2	71.41	90.59	83.66	82.99	63.91
A_{st}≅2.0-2.5%					
eCO_2 of Cement (ton)	59.96	75.26	69.15	71.97	54.81
eCO_2 of Water (ton)	0.032	0.012	0.013	0.012	0.011
eCO_2 of Superplasticizer (ton)	-	0.035	0.019	0.033	0.007
eCO_2 of Rebar (ton)	11.42	10.08	10.14	9.04	8.33
Total eCO_2	71.41	85.39	79.32	81.06	63.16
A_{st}≅3.0-3.5%					
eCO_2 of Cement (ton)	59.96	71.97	66.08	65.65	52.28
eCO_2 of Water (ton)	0.032	0.012	0.012	0.011	0.011
eCO_2 of Superplasticizer (ton)	-	0.033	0.018	0.031	0.0062
eCO_2 of Rebar (ton)	11.42	11.59	11.19	10.98	10.30
Total eCO_2	71.41	83.61	77.30	76.67	62.59
A_{st}≅5.0-6.0%					
eCO_2 of Cement (ton)	59.96	59.64	57.31	59.64	47.38
eCO_2 of Water (ton)	0.032	0.0098	0.010	0.0098	0.0097
eCO_2 of Superplasticizer (ton)	-	0.028	0.015	0.028	0.0056
eCO_2 of Rebar (ton)	11.42	15.23	15.04	14.05	12.85
Total eCO_2	71.41	74.90	72.37	73.73	60.24

Table 7-9 Embodied Carbon Dioxide for Concrete04-Based Designs

Property	Original	UHPC 1	UHPC 2	UHPC 3	UHPC 4
Mix No.	-	#1	#81	#1	#87
Cement (lb/yd^3)	675	1,200	1,153	1,200	1,002
Water (lb/yd^3)	335	184	196	184	190
Superplasticizer (lb/yd^3)	-	51.8	28.8	51.8	11.0
A_{st}≅1.5%					
eCO_2 of Cement (ton)	59.96	92.87	85.69	85.59	65.65
eCO_2 of Water (ton)	0.032	0.015	0.016	0.014	0.013
eCO_2 of Superplasticizer (ton)	-	0.043	0.023	0.040	0.0077
eCO_2 of Rebar (ton)	11.42	10.70	9.95	9.28	8.43
Total eCO_2	71.41	103.63	95.68	94.92	74.10
A_{st}≅2.0-2.5%					
eCO_2 of Cement (ton)	59.96	82.06	75.54	78.62	60.10
eCO_2 of Water (ton)	0.032	0.014	0.014	0.013	0.012
eCO_2 of Superplasticizer (ton)	-	0.038	0.020	0.037	0.0071
eCO_2 of Rebar (ton)	11.42	12.78	11.66	11.03	10.32
Total eCO_2	71.41	94.89	87.24	89.70	70.43
A_{st}≅3.0-3.5%					
eCO_2 of Cement (ton)	59.96	75.26	69.15	71.97	57.43
eCO_2 of Water (ton)	0.032	0.012	0.013	0.012	0.012
eCO_2 of Superplasticizer (ton)	-	0.035	0.019	0.033	0.0068
eCO_2 of Rebar (ton)	11.42	14.68	13.93	12.76	12.19
Total eCO_2	71.41	89.99	83.11	84.77	69.63
A_{st}≅5.0-6.0%					
eCO_2 of Cement (ton)	59.96	65.65	60.15	62.60	49.80
eCO_2 of Water (ton)	0.032	0.011	0.011	0.010	0.010
eCO_2 of Superplasticizer (ton)	-	0.031	0.016	0.029	0.0059
eCO_2 of Rebar (ton)	11.42	17.37	15.80	15.44	15.04
Total eCO_2	71.41	83.06	75.98	78.08	64.86

The percent difference of total embodied carbon dioxide of the original conventional concrete design relative to the total embodied carbon dioxide of each UHPC design for Concrete02 and Concrete04-based designs are summarized in Table 7-10. Negative percent differences in Table 7-10 means there are net reductions in embodied carbon dioxide in UHPC designs compared to the original conventional concrete design. Embodied carbon dioxide values for Concrete02 and Concrete04-based designs saw a maximum, possible percent difference of -15.64% and -9.17% respectively for steel reinforcement ratios at 5.0-6.0% due to having the smallest cross-sections achieved.

Table 7-10 Percent Difference of Total eCO_2 of Conventional Concrete Design with Total eCO_2 of UHPC

A_{st}	Concrete02				Concrete04			
	UHPC 1	UHPC 2	UHPC 3	UHPC 4	UHPC 1	UHPC 2	UHPC 3	UHPC 4
≅1.5%	26.86%	17.15%	16.22%	-10.50%	45.12%	33.99%	32.92%	3.77%
≅2.0-2.5%	19.58%	11.08%	13.51%	-11.55%	32.88%	22.17%	25.61%	-1.37%
≅3.0-3.5%	17.08%	8.25%	7.37%	-12.35%	26.02%	16.38%	18.71%	-2.49%
≅5.0-6.0%	4.89%	1.34%	3.25%	-15.64%	16.31%	6.40%	9.34%	-9.17%

7.2 WATER SAVINGS TO COMBAT DROUGHT CONCERNS

One major benefit of utilizing UHPC for bridge piers is the low water-to-cementitious materials ratio. Due to the recent dry weather, many states have been stricken with drought complications making water a very valuable and expensive resource. Purchasing and transporting water for construction sites where water is not readily available can also be costly and inconvenient. Water reducing admixtures allows UHPC to reach water-to-cementitious materials ratios as low as 0.115 while normal conventional concrete ranges between 0.32-0.48 (NPCA, 2014). Tables 7-11 and 7-12 summarize the total water consumption and percent savings of each UHPC pier (compared to the original conventional concrete design) for all Concrete02 and Concrete04-based designs. As observed in Tables 7-11 and 7-12, each design saw immediate water savings over 50% compared to the original conventional concrete design, regardless of the steel reinforcement ratio. It should be noted that while each mix design between UHPC 1, 2, 3 and 4 increases in strength respectively, the water savings do not necessarily increase with increasing strength because of varying mix proportions. The highest percent savings of water consumption is 69.81% and 68.27% for Concrete02 and Concrete04-based designs, saving a total of 6,009 gallons and 5,877 gallons of water respectively.

Table 7-11 Total Water Consumption and Savings for Concrete02-Based Designs

Property	Original	UHPC 1	UHPC 2	UHPC 3	UHPC 4
Mix No.	-	#1	#81	#1	#87
f'_c (psi)	4,000	17,260	21,147	28,900	36,360
f_t (psi)	-	1,300	1,500*	1,700	2,611
Water (lb/yd^3)	335	184	196	184	190
A_{st}≅1.5%					
Total Water Consumed (gallons)	8,608	3,640	3,715	3,338	3,150
Total Water Saved (gallons)	-	4,968	4,893	5,270	5,458
Percent Savings	-	57.71%	56.84%	61.22%	63.41%
A_{st}≅2.0-2.5%					
Total Water Consumed (gallons)	8,608	3,338	3,401	3,192	3,007
Total Water Saved (gallons)	-	5,270	5,207	5,416	5,601
Percent Savings	-	61.22%	60.49%	62.92%	65.07%
A_{st}≅3.0-3.5%					
Total Water Consumed (gallons)	8,608	3,192	3,249	2,912	2,867
Total Water Saved (gallons)	-	5,416	5,359	5,696	5,741
Percent Savings	-	62.92%	62.26%	66.17%	66.69%
A_{st}≅5.0-6.0%					
Total Water Consumed (gallons)	8,608	2,645	2,818	2,645	2,599
Total Water Saved (gallons)	-	5,963	5,790	5,963	6,009
Percent Savings	-	69.27%	67.26%	69.27%	69.81%

Table 7-12 Total Water Consumption and Savings for Concrete04-Based Designs

Property	Original	UHPC 1	UHPC 2	UHPC 3	UHPC 4
Mix No.	-	#1	#81	#1	#87
f'_c (psi)	4,000	17,260	21,147	28,900	36,360
f_t (psi)	-	1,300	1,500*	1,700	2,611
Water (lb/yd^3)	335	184	196	184	190
A_{st}≅1.5%					
Total Water consumed (gallons)	8,608	4,119	4,214	3,796	3,601
Total Water Saved (gallons)	-	4,489	4,394	4,812	5,007
Percent Savings	-	52.15%	51.05%	55.90%	58.17%
A_{st}≅2.0-2.5%					
Total Water Consumed (gallons)	8,608	3,640	3,715	3,487	3,296
Total Water Saved (gallons)	-	4,968	4,893	5,121	5,312
Percent Savings	-	57.71%	56.84%	59.49%	61.71%
A_{st}≅3.0-3.5%					
Total Water Consumed (gallons)	8,608	3,338	3,401	3,192	3,150
Total Water Saved (gallons)	-	5,270	5,207	5,416	5,458
Percent Savings	-	61.22%	60.49%	62.92%	63.41%
A_{st}≅5.0-6.0%					
Total Water Consumed (gallons)	8,608	2,912	2,958	2,777	2,731
Total Water Saved (gallons)	-	5,696	5,650	5,831	5,877
Percent Savings	-	66.17%	65.64%	67.74%	68.27%

8 Summary and Conclusions

This study examined the effectiveness of substituting conventional concrete in a multi-column bent of a typical California highway bridge with UHPC. The investigation began by exploring various published UHPC mix designs and selecting four designs to use, each with increasing strength. The four UHPC mix designs were used to optimize column and bent cap dimensions using existing and slightly modified concrete material models in OpenSees with actual UHPC mechanical properties. The objective was to find an overall design that performed equivalently (columns that form plastic hinges with bent caps that are virtually elastic under seismic loading), if not better, than the original conventional concrete design. Four ranges of reinforcement ratios (A_{st} = ~1.5%, 2.0-2.5%, 3.0-3.5%, and 5.0-6.0%) were also considered to investigate its effect on optimal utilization of the superior UHPC mechanical strength.

A two-dimensional OpenSees model was developed for each of the UHPC two-column bents, and nonlinear pushover and time history (response) seismic analyses were performed. The seismic analysis provided a final design check for each bent. The finalized designs were used to conduct a monetary and ecological cost analysis and assessment. The cost per bridge pier for each UHPC design was estimated using the following range of values: \$550/yd^3, \$1,500/yd^3, \$2,000/yd^3, and \$2,500/yd^3 of UHPC Moreover, the expected increase in the overall bridge construction cost due replacing conventional concrete with UHPC was estimated. Finally, an environmental assessment was conducted to estimate the global warming potential associated with UHPC bridge piers and potential savings in water as a result of the lower water-to-cement ratios adopted in UHPC mixes. This can potentially justify the use of UHPC from an ecological point of view given that UHPC consumes more cement than conventional concretes. According to the study presented in this report and briefly summarized above, the following conclusions can be drawn:

- Using UHPC for bridge columns and bent caps led to much more compact cross-sections with column diameter and overall volume reductions, relative to using conventional concrete, as high as 36% and 47%, respectively. Using varying longitudinal steel reinforcement ratios for optimizing the UHPC designs, higher steel ratios were found to lead to further reductions in cross-section dimensions. The 5-6% reinforcement ratio produced the most compact cross-sections. However, design codes currently limit columns maximum reinforcement ratio to 4%

to avoid over-reinforced concrete sections that might lead to brittle modes of failure. Thus, for UHPC sections, a 3.5%-4% reinforcement ratio may be most practical unless future research can demonstrate the value of higher ratios.

- The UHPC bridge piers showed acceptable seismic performance under the four different ground motions used in this study, which were applied at the design level and maximum considered earthquake. The overall structural and seismic response of the UHPC piers was comparable or even superior to conventional concrete piers by consistently achieving lower residual displacements and peak deformations.
- Naturally, by reducing the cross-sections of the UHPC bridge columns and bent cap, less materials are consumed. However, due to the higher UHPC unit material costs relative to conventional concrete, the cost of an optimized UHPC pier was found to be much higher than conventional concrete. If this additional material cost is accounted for in the overall cost of the full prototype bridge, the use of UHPC in bridge piers is estimated to increase the bridge cost by 10.7% to 18.2% based on a cost of \$2,500/yd^3 of UHPC. For the \$550/yd^3 of UHPC estimate, the bridge cost is estimated to increase by 1.5% to 3.1%. These ranges are lower and upper bounds based on UHPC mix design, reinforcement ratio, and modeling assumptions used in design optimization. Thus, if UHPC unit material cost drops in the future to be within the current price range as in Europe (\$550/yd^3), only a small increase in construction costs happens, which is worth considering for a better structural life expectancy, seismic performance, and minimal maintenance.
- Savings in cement consumption was made possible through some of the considered UHPC mixes for the steel ratios ~1.5%, 2.0-2.5%, and 3.0-3.5%, and for all considered mix designs using steel ratios between 5.0-6.0%. When savings in cement are achieved, the total embodied carbon dioxide (eCO_2) of the bridge bent can reach savings as high as 11.17 tons of eCO_2 relative to the conventional concrete bent. One more major benefit of utilizing UHPC over conventional concrete is the low water-to-cement ratio. All UHPC designs achieved a percent savings in water above 50% and reached savings as high as 70%, which can benefit many drought stricken states such as California and Nevada.
- Overall, using UHPC for structural members has been demonstrated through this study to achieve reduced cross sections, comparable (if not better) seismic performance, savings in

cement, water, and overall CO_2 emissions, and reasonable-to-justify additional costs. It is anticipated that further environmental and cost benefits can be demonstrated when using UHPC at larger scales if more accurate computational models are used in future studies. Due to the inability of modelling the UHPC strain hardening behavior using existing computational tools, the resulting UHPC dimensions, and in turn, material quantities and environmental metrics are considered conservative. However, all conclusions drawn here with respect to monetary and ecological costs are valid because the relaxed UHPC tensile strain hardening effects will only lead to smaller column dimensions.

- Finally, this study rendered several research needs to further develop confidence in using UHPC. Extensive experimental testing of UHPC structural members in flexure and shear and under monotonic and cyclic loading is needed to validate material property assumptions out to large strains. Seismic dynamic tests should be conducted to investigate the damage response of UHPC and behavior in plastic hinge zones. Such tests can provide new knowledge pertaining to displacements, curvatures, and/or rotation capacity of UHPC members for future performance-based design using UHPC. Accurate constitutive modeling of UHPC is also needed to calibrate existing material models readily implemented in general purpose finite element software or develop new numerical models.

REFERENCES

Ahlborn, T.M., Peuse, E.J., and Misson, D.L., "Ultra-High Performance Concrete for Michigan Bridges, Material Performance – Phase I, Final Report – November 2008." Michigan Department of Transportation (2008)

Ahlborn, T.M., Harris, D.K., Misson, D.L., and Peuse, E.J., "Strength and Durability Characterization of Ultra-High Performance Concrete Under Variable Curing Conditions." (2011)

Amato, I., "Green Cement: Concrete Solutions." Nature, International Weekly Journal of Science (2013)

American Coal Ash Association, "Fly Ash 101." *The Concrete Producer* (2006)

"AASHTO LRFD Bridge Design Specifications, 6th Ed." Customary U.S. Units (2012)

Bentz, D.P., Jones, S.Z., and Snyder, K.A., "Design and Performance of Ternary Blend High-Volume Fly Ash Concretes of Moderate Slump." (2015)

Bilodeau, A. and Malholtra, M.V., "High-Volume Fly Ash System: Concrete Solution for Sustainable Development." *ACI Materials Journal*, Jan-Feb (2000)

Bouzoubaâ, N., Fournier, B., Malholtra, M.V., and Golden, D.M., "Mechanical Properties and Durability of Concrete made with HVFA Blended Cement Produced in a Cement Plant." Materials Technology Laboratory (2001)

Bradley, D., "TR10: Green Concrete." MIT Technology Review. Web. (2010)

Caltrans Seismic Design Criteria, Version 1.7 (2013)

Cavill, B., "Ductal® - An Ultra-High Performance Material for Resistance to Blasts and Impacts." 1st Specialty Conference on Disaster Mitigation (2006)

Chadwell, C. B., and R. A. Imbsen. "XTRACT: A Tool for Axial Force-Ultimate Curvature Interactions." Struct. ASCE Library (2004).

Cheyrezy, M. and Behloul, M., "Creep and Shrinkage of Ultra-High Performance Concrete." (2001)

ChunPing, G., Guang, Y., and Wei, S., "Ultrahigh Performance Concrete-Properties, Applications, and Perspectives." (2015)

Crouch, L.K., Hewitt, R., and Byard, B., "High Volume Fly Ash Concrete." (2007)

DeCristofaro, N. and Sahu, S., "CO_2 – Reducing Cement" Solidia Technologies® – World Cement (2014)

Department of Homeland Security, Science and Technology, "UHPC, Ultra High Performance Concrete, Pathway to Commercialization." Web. (2011)

Ductal® Solutions, "Ductal® Façades: A New Adventure in Technology." (2011)

Ductal®, "Completed Projects." Web. (n.d.)

Dumne, S.M., "Effect of Superplasticizer on Fresh and Hardened Properties of Self-Compacting Concrete Containing Fly Ash." *American Journal of Engineering Research* (2014)

Feiz, R., Ammenberg, J., Baas, L., Eklund, M., Helgstrand, A., and Marshall, R., "Improving the CO_2 Performance of Cement, Part I: Utilizing Life-Cycle Assessment and Key Performance Indicators to Assess Development Within the Cement Industry." (2015)

Flietstra, J.C., "Creep and Shrinkage Behavior of Ultra High Performance Concrete under Compressive Loading with Varying Curing Regimes." Michigan Technological University (2011)

Florida Department of Transportation (FDOT), "BDR Cost Estimating." Structures Design Guidelines. Web. (2009)

Gauff, N., "Rubberized Asphalt Concrete (RAC)." CalRecycle. Web. (2012)

Garder, J.A., "Use of UHPC Piles in Integral Abutment Bridges." Iowa State University (2012)

Graybeal, B.A. and Hartmann, J.L., "Strength and Durability of Ultra-High Performance Concrete." 2003 Concrete Bridge Conference (2003)

Graybeal, B.A., "Material Property Characterization of Ultra-High Performance Concrete." Federal Highway Administration. (2006)

Graybeal, B.A., "Structural Behavior of Ultra-High Performance Concrete Prestressed I-Griders.) Federal Highway Administration. (2006)

Graybeal, B.A., "Compressive Behavior of Ultra-High-Performance Fiber-Reinforced Concrete." ACI Materials Journal, Title no. 104-M17. (2007)

Graybeal, B.A., "Structural Behavior of a 2nd Generation UHPC Pi-Girder." Federal Highway Administration. (2009)

Graybeal, B.A., "Simultaneous Structural and Environmental Loading of an Ultra-High Performance Concrete Component." Federal Highway Administration. (2010)

Graybeal, B.A. and Baby, F., "Development of Direct Tension Test Method for Ultra-High Performance Fiber-Reinforced Concrete." (2013)

Graybeal, B.A. and Davis, M., "Cylinder or Cube: Strength Testing of 80 to 200 MPa (11.6 to 29 ksi) Ultra-High-Performance Fiber-Reinforced Concrete." *ACI Materials Journal,* Nov-Dec (2008)

Imbsen, R.A., "AASHTO Guide Specifications for LRFD Seismic Bridge Design" (2007)

Hanson, K., "UHPC Offers Endless Possibilities." NPCA (2014)

Heinz, D., Urbonas, L., and Gerlicher, T., "Effect of Heat Treatment Method on the Properties of UHPC." 3rd International Symposium on UHPC and Nanotechnology for High Performance Construction Materials. (2012)

Huntzinger, D.N. and Eatmon, T.D., "A Life-Cycle Assessment of Portland Cement Manufacturing: Comparing the Traditional Process with Alternative Technologies." (2008)

Khayat, K.H. and Meng, W., "Design and Performance of Stay-in-Place UHPC Prefabricated Panels for Infrastructure Construction." (2014)

Kühne, H.C. and Müller, U., "Properties of Heat and Steam Cured Ultra High Performance Concrete (UHPC)." BAM (n.d.)

Li, G., “Properties of High-Volume Fly Ash Concrete Incorporating nano-SiO_2.” (2003)

Malhotra, V.M. and Mehta, P.K., “*High-Performance, High-Volume Fly Ash Concrete for Building Sustainable and Durable Structures. Third Edition.”* (2008)

Mander, J. B., Priestley, M. J., & Park, R. (1988). Theoretical stress-strain model for confined concrete. Journal of structural engineering, 114(8), 1804-1826.

Marceau, M.L., Nisbet, M.A., and VanGeem, M.G., “Life Cycle Inventory of Portland Cement Manufacture.” Portland Cement Association (2006)

Mehta, P.K., “High-Performance, High-Volume Fly Ash Concrete for Sustainable Development.” University of California, Berkeley (n.d.)

Mehta, P.K., “Greening of the Concrete Industry for Sustainable Development.” (2001)

Moore, B.P., “Little Cedar Creek Bridge – Big Innovation.” Creative Concrete Construction (2012)

Naaman, A.E., “Toughness, Ductility, Surface Energy and Deflection-Hardening FRC Composites.” Proceedings of JCI International Workshop on Ductile Fiber Reinforced Cementitious Composites (DFRCC) – Application and Evaluation (DFRCC-02). (2002)

Naaman, A.E. and Wille, K., “The Path to Ultra-High Performance Fiber Reinforced Concrete (UHP-FRC): Five Decades of Progress.” 3rd International Symposium of UHPC and Nanotechnology for High Performance Construction Materials. (2012)

National Ready Mixed Concrete Association (NRMCA), “CIP 36 – Structural Lightweight Concrete” (2004)

Naik, T.R., Sivasundaram, V., and Singh, S.S., “Use of High-Volume Class F Fly Ash for Structural Grade Concrete.” (1991)

Naik, T.R., Ramme, B.W., and Kraus, R.N., “Performance of High-Volume Fly Ash Concrete Pavements Constructed since 1984.” *The Indian Concrete Journal*. Vol 78, March (2004)

National Precast Concrete Association (NPCA), “Ultra High Performance Concrete (UHPC), Guide to Manufacturing Architectural Precast UHPC Elements.” (2013)

National Ready Mixed Concrete Association (NRMCA), “CIP 37 – Self Consolidating Concrete (SCC)” (2004)

National Ready Mixed Concrete Association (NRMCA), “CIP 38 – Pervious Concrete” (2004)

Natural Resources Canada, “CanmetENERGY.” Web. (n.d.)

Neville, A.M., “*Properties of Concrete, 4th Edition.*” (1995)

Olivier, J.G.J. and Muntean, M., “Trends in Global CO_2 Emissions, 2014 Report.” PBL Netherlands Environmental Assessment Agency (2014)

Paragon Ready Mix Inc. “Ready Mixed Concrete Price List.” (2016)

Perry, V.H. and Seibert, P.J., “The use of UHPFRC (Ductal®) for Bridges in North America: The Technology, Applications and Challenges Facing Commercilization.” Lafarge North America Inc. (n.d.)

Perry, V.H. and Zakariasen, D., “First Use of Ultra-High Performance Concrete for an Innovative Train Station Canopy.” *Concrete Technology Today*. Vol. 25, No. 2 (2004)

Pike, C.A., “A Preliminary Investigation of Fiber Reinforced Concrete under Quasi-Static and Dynamic Loads.” North Carolina State University (2009)

Portland Cement Association, “Ultra-High Performance Concrete.” Web. (n.d.)

Prem, P.R., Bharatkumar, B.H., and Iyer, N.R., “Mechanical Properties of Ultra High Performance Concrete.” (2012)

Probha, S.L., Dattatreya, J.K., Neelamegam, M., “Stress Strain Behaviour of Ultra High Performance Concrete Under Uniaxial Compression.” (2014)

Purnell, P., “The Carbon Footprint of Reinforced Concrete.” Advances in Cement Research. (2013)

Randl, N., Steiner, T., Baumgartner, E., and Mészöly, T., “Development of UHPC Mixtures from an Ecological Point of View.” (2014)

Ritter, R. and Curbach, M., “Material Behavior of Ultra-High Strength Concrete under Multiaxial Stress States” *ACI Materials Journal*, Sept-Oct (2015)

Rubenstein, M., “Emissions from the Cement Industry.” State of the Planet, Earth Institute | Columbia University. Web. (2012)

Russell, H.G. and Graybeal, B.A., “Ultra-High Performance Concrete: A State-of-the-Art Report for the Bridge Community.” Federal Highway Administration (2013)

Schmidt, M. and Fehling, E., “Ultra-High-Performance Concrete: Research, Development and Application in Europe.” (2004)

Shann, S.V., “Application of Ultra High Performance Concrete (UHPC) as a Thin-Bonded Overlay for Concrete Bridge Decks.” Michigan Technological University (2012)

Shaikh, F.U.A. and Supit, S.W.M., “Mechanical and Durability Properties of High Volume Fly Ash (HVFA) Concrete Containing Calcium Carbonate ($CaCO_3$) nanoparticles.” (2014)

Schmidt, M. and Fehling, E., “Ultra-High Performance Concrete: Research, Development and Application in Europe.” (2004)

Stengel, T. and Schießl, P., “Life Cycle Assessment of UHPC Bridge Constructions: Sherbrooke Footbridge, Kassel Gärtnerplatz Footbridge and Wapello Road Bridge.” Silesian University of Technology (2009)

Talebinejad, I., Iranmanesh, A., Bassam, S.A., and Shekarchizadeh, M., “Optimizing Mix Proportions of Normal Weight Reactive Powder Concrete with Strengths of 200-350 MPa.” International Symposium on Ultra High Performance Concrete. (2004)

Thomas, M., “Optimizing the Use of Fly Ash in Concrete.” Portland Cement Association (2007)

UNEP Global Environmental Alert Service, “Greening Cement Production has a Big Role to Play in Reducing Greenhouse Gas Emissions.” (2010)

United States Environmental Protection Agency (EPA), “Design for the Environmental Life-Cycle Assessments.” (n.d.)

United States Environmental Protection Agency (EPA), “Understanding Global Warming Potential.” (n.d.)

Volz, J.S., Myers, J.J., Richardson, D.N., Arezoumandi, M., Beckemeiser, K., Davis, D., Holman, K., Looney, T., and Tucker, B., “Design and Evaluation of High-Volume Fly Ash (HVFA) Concrete Mixes.” (2012)

Voort, T.V., Suleiman, M., and Sritharan, S., “Design and Performance Verification of Ultra-High Performance Concrete Piles for Deep Foundations.” Iowa State University (2008)

Wille, K., Naaman, A.E., El-Tawil, S., and Parra-Montesinos, J., “Ultra-High Performance Concrete and Fiber Reinforced Concrete; Achieving Strength and Ductility Without Heat Curing.” (2011)

Wille, K., El-Tawil, S., Naaman, A.E., “Properties of Strain Hardening Ultra High Performance Fiber Reinforced Concrete (UHP-FRC) Under Direct Tensile Loading.” (2013)

Wiss Janney Elstner Associates, “Introduction to Ultra-High Performance Concrete (UHPC).” Web. (2011)

Yoo, S.W., Ryu, G.S., and Choo, J.F., “Evaluation of the Effects of High-Volume Fly Ash on the Flexural Behavior of Reinforced Concrete Beams.” (2015)

Yu, R., Spiesz, P., and Brouwers, H.J.H., “Mix Design and Properties Assessment of Ultra-High Performance Fibre Reinforced Concrete (UHPFRC).” (2013)

Appendix A High Volume Fly Ash Concrete

A.1 DEFINITION

Concrete is currently the most used material in construction and second most consumed substance on Earth after water. Unfortunately the production of cement used in concrete accounts for 9.5% of global carbon dioxide (CO_2) emissions in 2013. (Olivier et al., 2014) Limestone (calcium carbonate) and clay are heated to 1450oC consuming large amounts of coal and gases during the process. (Rubenstein, 2012) Because cement is being consumed at an annual rate of 1.6 billion metric tons, an alternative substitution was highly sought after. Fortunately, the by-product of cement production and coal-fired power plants is called fly ash and is accepted as a substitution to portland cement. In 2003, only 38% of the 70 million tons of produced fly ash were recycled. (American Coal Ash Association, 2006) This makes fly ash a cheap and readily available product and an eco-friendly solution to rising cement production demands. According to Malhotra et al., fly ash is created based on non-combustible impurities in the form of clay, shale, quartz, feldspar, dolomite, and limestone present in pulverized coal (Malhotra et al., 2008). Any unburned residue is either carried away by flue gases and collected (fly ash) or left at the bottom of the furnace (bottom ash) and thrown away. (Thomas, 2007) Figure A.1 illustrates the fly ash production process.

There are two types of common fly ash: Class F and Class C. Table A-1 describes the ASTM definitions and its chemical requirements. Table A-2 describes the effects of Fly Ash on the Properties of Concrete with commentary and guidance of each effect.

High volume fly ash (HVFA) concrete, is defined as a concrete mix with a fly ash by mass of cementitious materials of 50% or more. The term “high volume fly ash concrete” was originally devised in the 1980’s by V. Mohan Malhotra of CANMET in Ottawa, Canada. HVFA concrete has greater workability, a low exothermic reaction during mixing and curing procedures (heat-of-hydration), early strengths that are satisfactory, low shrinkage, sustainable benefits, and comparable durability to normal strength concrete. (Malhotra et al., 2008) According to Crouch et al., the improved workability stems from the “ball bearing” action of the spherical fly ash particles. Fly ash generated from power plants have also been shown to decrease the water content by 15-20%. As a result, the HVFA concrete experiences a decrease in shrinkage creating a more crack

resistant product compared to conventional concrete. Because of the improved fine particle size distribution of the mixture, HVFA concrete has a lower water permeability making it ideal for environments with high freeze/thaw damage potential. (Crouch et al., 2007) The Leadership in Energy and Environmental Design (LEED) program also awards LEED points based on mixtures that use up to 40% substitution of fly ash for cement.

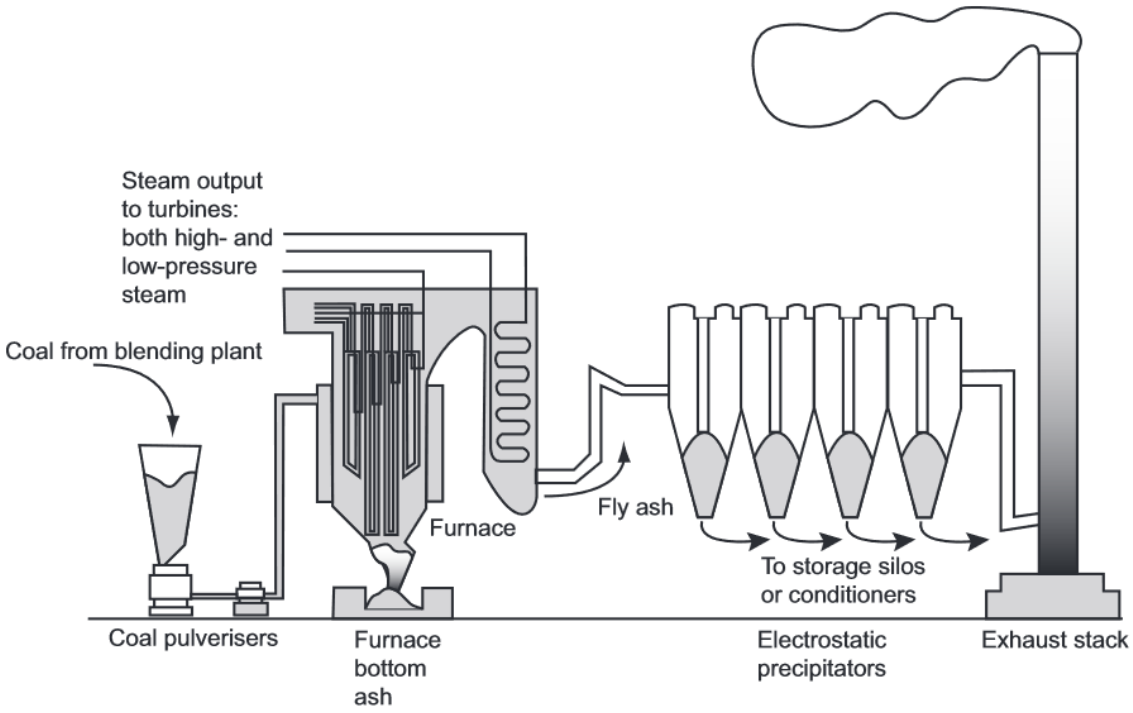

Figure A.1 Fly Ash Production Process (Thomas, 2007)

Table A-1 ASTM Specifications for Fly Ash (ASTM C 618)

Class	ASTM Description	Chemical Requirements
F	"Fly ash normally produced from burning anthracite or bituminous coal that meets the applicable requirements for this class as given herein. The class of fly ash has pozzolanic properties."	$SiO_2 + Al_2O_3 + FeO_3 \geq 70\%$
C	"Fly ash normally produced from lignite or sub-bituminous coal that meets the applicable requirements for this class as given herein. This class of fly ash, in addition to having pozzolanic properties, also has some cementitious properties. Note: Some Class C fly ashes may contain lime contents higher than 10%"	$SiO_2 + Al_2O_3 + FeO_3 \geq 70\%$

Table A-2 Effect of Fly Ash on the Properties of Concrete (Thomas, 2007)

Property	Effect of Fly Ash	Guidance
Fresh Concrete	- Workability is improved and water demand is reduced for most fly ashes. - Concrete is more cohesive and segregates less improved pumpability. - Bleeding is reduced especially at high replacement levels.	• Reduced water content by approximately 3% for each 10% fly ash compared to similar mix without fly ash. • Take precautions to protect concrete when placing conditions accelerate the rate of moisture loss (see ACI 305, Hot Weather Concreting). • Ensure bleeding has stopped before commencing final finishing operations
Set Time	- Extended – especially in cold weather. - Certain combinations of fly ash, cement, and chemical admixtures may cause rapid of severely retarded set at certain temperatures.	• Consider reducing level of fly ash during cold weather • Test fly ash-cement-admixture compatibility.
Heat of Hydration	- Reduced for Class F fly ash at normal levels of replacement. Class C fly ashes have to be…	• Use Class F fly ash if temperature control is critical. Otherwise, use high levels of Class C fly ash and/or take…
Heat of Hydration	- …used at higher levels of replacement to reduce heat (for example > 50%). - Reduction increased by using high levels of replacement, total cementitious contents, and low placing temperatures.	• … other measures to reduce temperature, such as: reduce cement content, use low-heat (Type IV or LH) or moderate heat (Type II or MH) cement, or lower concrete placing temperature (use crushed ice or liquid-nitrogen cooling).
Early-Age Strength	- Reduced - especially at 1 day. - Reduction is greater for Class F and for higher replacement levels. - Impact less for in-situ strength if there is significant autogenous temperature rise (e.g., large pours).	• Consider reducing fly ash content if early-age strength is critical. • Use accelerating admixtures, high-early strength cement (Type III or HE), or silica fume to compensate for reduced early-age strength.
Long-Term Strength	- Increased - Effect increases with the level of fly ash.	• Consider extending testing out to 56 days for mix design acceptance.
Permeability and Chloride Resistance	- Reduced significantly – especially at later ages.	• Adequate curing is essential if these benefits are to be achieved in the concrete close to the surface (cover concrete).

Expansion due to Alkali-Silica Reaction	- Reduced. - Deleterious expansion can be completely suppressed by sufficient levels of replacement. - For Class F fly ash (with up to 20% CaO) a replacement level of 20 to 30% fly ash is sufficient for most aggregates. - Higher levels of Class C fly ash are required (> 40%).	• If a reactive aggregate is being used, Class F fly ash should be used, if available. • If Class F fly ash in not available, consider using combinations of Class C fly ash with silica fume or slag. • The level of fly ash required for a particular aggregate should be determined using appropriate testing (for instance, ASTM C1293 or ASTM C1567).
Sulfate Resistance	- Increased by Class F fly ashes. - A dosage level of 20 to 30% Class F fly ash will generally provide equivalent performance to a Type II or V portland cement - (ASTM C150) cement or a Type MS or HS hydraulic cement (ASTM C1157). - Resistance to cyclic immersion in sodium sulfate solution and drying has been shown to be relatively unaffected by up to 40% fly ash.	• Do not use Class C fly ash. • Test cement—fly ash combinations using ASTM C1012. • Consider using Class F fly ash with sulfate-resisting portland cement.
Resistance to Carbonation	- Decreased for all fly ashes. - Significant decreases when high levels of fly ash are used in poorly-cured, low-strength (high w/cm) concrete.	• Provide adequate curing for concrete containing fly ash. • Ensure cover requirements are met.
Resistance to Deicer-Salt Scaling	- Decreased. - Significant scaling occurs in laboratory tests on concrete with high levels of fly ash. - Field performance with HVFA concrete is variable. - Hand-finished flatwork is most susceptible. - Class C fly ash shows slightly better resistance. - Curing membranes may increase resistance.	• Limit the level of fly ash in hand-finished flatwork (for example, sidewalks and driveways) exposed to deicing salts (ACI318 limits) - especially in late-fall placing. • Where possible, ensure adequate drying period before first application of deicing salt. • Pay special attention to the mix proportions (w/cm), air-void system, and finishing and curing practices when fly ash concrete is used in flatwork exposed to deicing salts.

High volume fly ash (HVFA) concrete, is defined as a concrete mix with a fly ash by mass of cementitious materials of 50% or more. The term “high volume fly ash concrete” was originally

devised in the 1980's by V. Mohan Malhotra of CANMET in Ottawa, Canada. HVFA concrete has greater workability, a low exothermic reaction during mixing and curing procedures (heat-of-hydration), early strengths that are satisfactory, low shrinkage, sustainable benefits, and comparable durability to normal strength concrete. (Malhotra et al., 2008) According to Crouch et al., the improved workability stems from the "ball bearing" action of the spherical fly ash particles. Fly ash generated from power plants have also been shown to decrease the water content by 15-20%. As a result, the HVFA concrete experiences a decrease in shrinkage creating a more crack resistant product compared to conventional concrete. Because of the improved fine particle size distribution of the mixture, HVFA concrete has a lower water permeability making it ideal for environments with high freeze/thaw damage potential. (Crouch et al., 2007) The Leadership in Energy and Environmental Design (LEED) program also awards LEED points based on mixtures that use up to 40% substitution of fly ash for cement.

Unfortunately, HVFA concrete is not entirely perfect. Properties of HVFA are directly affected by the type of cement and percentage of fly ash incorporated. (Bilodeau et al., 2000) The substitution of fly ash in any percentage will also increase the strength and development time of concrete at its early stages. According to Ravina et al., Class C fly ash delays strength development more than Class F fly ash due to its higher sulfate contents. Consistencies in physical and chemical characteristics can also vary within the fly ash not just between different power plants, but within the same power plant as well. (Volz, et al, 2012)

A.2 MIX DESIGN

In order to identify the most efficient and eco-friendly mix design, this literature review compiles over 30 different HVFA concrete mix designs from various sources across the world. Table A-3 shows some components of each mix design.

The variations in strength of HVFA concrete are directly related to the use of different chemical admixtures and the temperature during placement. It is known that the use of superplasticizers or other high range water reducers is imperative to the HVFA concrete's workability. Fly ash with a high carbon content will also require higher dosages of air-entraining admixtures which decrease in effectiveness as the fly ash to cementitious materials ratio increase. (Bilodeau et al., 2000) The BAPS Temple and Cultural Complexes located in Chicago, Illinois poured the same HVFA concrete foundations on two different days with varying temperatures. One placement was during

an 88°F day which resulted in a 28 day compressive strength of 5802 psi and the other on a 44.6°F day with a compressive strength of 3771 psi. (Malhotra et al., 2008)

Table A-3 HVFA Concrete Mix Designs from Various Sources

Mix No.	Cement	C Ash	F Ash	Fine Agg.	Coarse Agg.	Water	W/C	Source
1	276	277	-	1273	1910	111	0.20	Crouch et al., 2007
2	299	-	300	1224	1836	124	0.21	
3	219	511	-	1080	1754	321	0.44	Volz, 2012
4	155	360	-	1080	1754	226	0.44	
5	210	-	210	1350	1970	200	0.48	Malhotra et al., 2008
6	260	-	360	1260	2020	190	0.31	
7	300	-	370	1260	1870	190	0.28	
8	255	-	325	1126	2136	211	0.36	
9	303	-	371	1348	1854	185	0.27	
10	270	-	332	1450	1938	202	0.34	
11	329	-	329	1466	1761	212	0.32	
12	179	-	239	1591	1890	169	0.40	
13	211	362	-	1315	2031	180	0.31	
14	177	329	-	1382	2107	169	0.33	
15	379	379	-	769	2316	243	0.32	
16	379	379	-	1101	1955	243	0.32	
17	379	379	-	1568	1686	273	0.36	
18	352	-	352	956	1976	243	0.35	
19	303	-	371	738	2346	228	0.34	
20	396	-	354	922	2163	248	0.33	
21	361	-	295	1273	1906	214	0.33	Bouzoubaâ et al., 2001
22	357	-	292	1257	1884	212	0.33	
23	291	-	356	1247	1869	212	0.33	
24	293	-	358	1252	1876	212	0.33	
25	355	-	244	1499	1831	195	0.33	Naik et al., 1991
26	305	-	305	1487	1818	195	0.32	
27	244	-	366	1476	1804	195	0.32	
28	305	-	305	1501	1836	195	0.32	
29	244	-	367	1488	1870	266	0.44	
30	480	110	-	-	1930	171	0.29	Naik et al., 2004
31	224	-	450	-	1900	209	0.31	
32	305	-	351	-	1900	203	0.31	
33	457	-	244	-	1846	189	0.27	
34	460	-	248	1621	-	312	0.44	Yoo et al., 2015
35	467	-	251	1706	-	253	0.35	
36	539	-	290	1643	-	253	0.30	
37	263	-	263	1765	-	211	0.40	
38	364	-	364	1451	-	351	0.48	
39	620	-	620	1091	-	408	0.38	
40	211	-	278	1348	1972	194	0.40	Bilodeau et al., 2000
41	261	-	362	1087	2014	202	0.32	
42	303	-	371	1281	1871	185	0.28	

43	260	-	260	1300	2030	200	0.38	Mehta, 2002
44	250	-	228	1557	1886	174	0.31	Bentz et al., 2015
45	246	-	225	1537	1861	193	0.35	
46	366	154	-	1524	1844	212	0.37	
47	369	207	-	1534	1857	201	0.35	
48	246	239	-	1532	1856	198	0.35	
49	421	-	421	1086	1913	235	0.28	Li, 2003
50	405	-	270	-	2082	275	0.41	Shaikh et al., 2014
51	270	-	405	-	2082	275	0.41	

A.3 CURING METHODS

Because of the lack of cement used in a HVFA concrete mix design, the rate of pozzolanic reaction is slower than the rate of cement hydration. HVFA concrete is significantly weaker in its early ages and is usually recommended to be moisture cured for a minimum of seven days. If these minimum curing times cannot be met, it is recommended to use less fly ash in the mix design. (Malhotra, 2005) It has been shown that HVFA concrete will reach very high compressive strengths comparable to normal strength concrete at an age of 28 days.

A.4 MECHANICAL PROPERTIES

Much like UHPC, HVFA concrete is durable and more crack resistant compared to normal strength concrete. These properties are a result of reduced calcium hydroxide normally consumed during pozzolanic activities and an altered microstructure. The crack resistance is achieved through the low shrinkage properties of HVFA caused by a decreased water to cementitious materials ratio and decreased use of cement. The decreased heat-of-hydration during the mixing and curing processes considerably alleviates the potential for thermal shrinkage and cracking. (Crouch et al., 2007) Volz et al. reports that their test results were very comparable to current AASHTO LRFD Bridge Design Specifications and ACI Building Codes. Comparisons from the test results included modulus of elasticity, compressive strength, development lengths, shear strengths, creep, and shrinkage and showed that design provisions for conventional concrete is just as applicable or conservative for HVFA concrete with a 70% fly ash replacement. Yoo et al. compared the actual elastic modulus values of their HVFA test specimens with predicted normal strength concrete values and found that the data matches closely to the predicted values if the density ranges between 3700-3900 lb/yd^3. Figure A.2 shows a graph of the actual data plotted against the predicted values.

Table A-4 displays the mechanical properties of the compiled HVFA concrete mix designs from Table A-3. Because this literature review compiles various mix designs and its respective mechanical properties from different published sources, some values were unfortunately not reported or made available. Refer to Appendix A for a complete table.

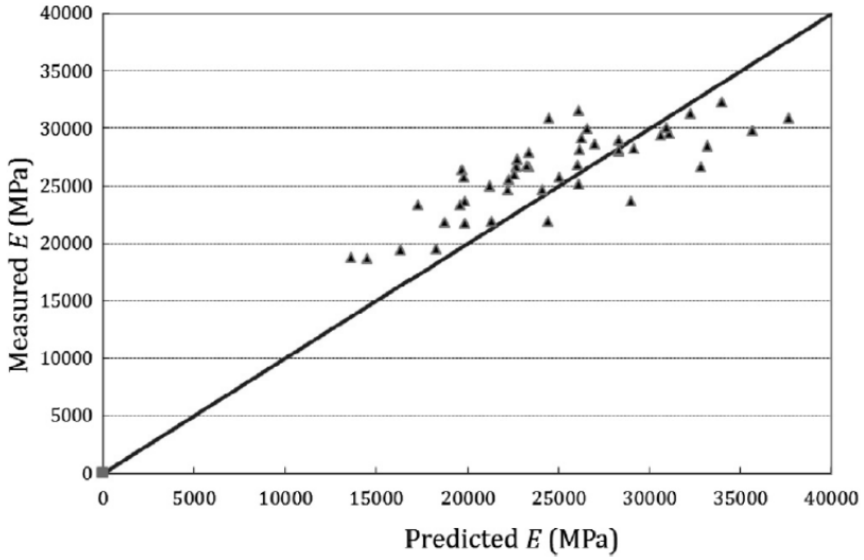

Figure A.2 Measured E vs. Predicted E for HVFA Concrete (Yoo, et al., 2015)

Table A-4 Mechanical Properties of HVFA Concrete Mix Designs from Various Sources

Mix No.	Compressive Strength [psi]	Tensile Strength [psi]	Modulus of Elasticity [psi]	Source
1	7200	-	-	Crouch et al., 2007
2	4500	-	-	
3	3540	380	-	Volz, 2012
4	4450	410	-	
5	2900	-	-	Malhotra et al., 2008
6	4350	-	-	
7	5800	-	-	
8	6686 (91 days)	-	5.62E+06	
9	4351	-	-	
10	4670	-	-	
11	5599	-	-	
12	2538	-	-	
13	6527	-	-	
14	5802	-	-	
15	6034	-	-	
16	5801	-	-	
17	5729	-	-	
18	4496	-	-	
19	4525	-	-	

20	6904	-	-	
21	6512	493	4.76E+06	Bouzoubaâ et al., 2001
22	6541	493	4.76E+06	
23	5308	435	4.50E+06	
24	5352	435	4.50E+06	
25	6343	453	4.75E+06	Naik et al., 1991
26	5140	439	4.50E+06	
27	5016	353	4.77E+06	
28	5906	393	4.33E+06	
29	4569	245	4.30E+08	
30	4467	-	-	Naik et al., 2004
31	2814	-	-	
32	3597	-	-	
33	4351	-	-	
34	4598	-	3.63E+06	Yoo et al., 2015
35	5773	-	4.11E+06	
36	6512	-	4.65E+06	
37	3713	-	3.52E+06	
38	3466	-	2.91E+06	
39	7324	-	3.86E+06	
40	2900	-	-	Bilodeau et al., 2000
41	4350	-	-	
42	5800	-	-	
43	3600	-	-	Mehta, 2002
44	5714	-	-	Bentz et al., 2015
45	4090	-	-	
46	6367	-	-	
47	5889	-	-	
48	5990	-	-	
49	7890	-	-	Li, 2003
50	5221	-	-	Shaikh et al., 2014
51	2321	-	-	

A.5 APPLICATIONS

A.5.1 Architectural Applications

Artists Live/Work Studios (Vancouver, Canada): Designed by the Canadian architect, Arthur Erickson, this reinforced concrete structure utilized HVFA concrete purely for aesthetic purposes. The HVFA concrete provided such a high quality and attractive finish that the scheduled sand blasted finish was canceled and replaced by a simple acid wash. 35300 ft^3 of concrete was placed and had a 28 compressive strength of 4351 psi. (Malhotra et al., 2008)

A.5.2 Structural Applications in Buildings

Concrete Block for Component Testing of Communication Satellites (Ottawa, Canada): Placed on March 1987, this 30 ft. x 23 ft. x 10 ft. block of concrete is the first field application of HVFA concrete. The block was cast indoors in permanent steel forms and was used for vibration testing of components for communication satellites. It was imperative that the HVFA concrete block did not develop cracks for it may affect the test results. 6357 ft^3 of HVFA concrete was placed at room temperatures of 54°F and 46°F respectively and produced a 91 day compressive strength of 6686 psi. (Malhotra et al., 2008)

Park Lane Hotel/Office Complex (Halifax, Canada): Constructed in 1988, the Park Lane Hotel/Office Complex provides 12900 yd^3 of office space divided into seven stories and a 600 car indoor parking garage. Because of the late concrete development strength requirements, HVFA concrete was ideal for this build. The lower columns, 3 ft. in diameter, required 120 day compressive strengths of 7252 psi and resulted in an actual compressive strength of 10733 psi. Using HVFA concrete was not only sustainable, but economical. The HVFA mixture saved $0.37 per cubic ft. compared to conventional portland cement concrete. (Malhotra et al., 2008)

York University Computer Science Building (Toronto, Canada): Constructed in 2001, the York University Computer Science Building utilized a 50% fly ash replacement mix design with no superplasticizer. As unusual as this was, this was most likely due to the fact that the design called for structural strength only with durability neglected. York University has since utilized HVFA concrete mix designs on various structures throughout the campus after the success of their Computer Science Building. (Malhotra et al., 2008)

University of California, Berkeley, Wurster Hall (Berkeley, California, United States): Due to monetary constraints, HVFA concrete was chosen for a seismic retrofit of reinforced concrete piers and foundations of Wurster Hall. By using a HVFA mix design, the university was able to save $13,000 over the use of conventional portland cement concrete. This HVFA concrete mix design also used no air entrainers or superplasticizers. (Malhotra et al., 2008)

Hindu Temple (Kauai Island, Hawaii, United States): In order to support a large, all-stone Hindu temple, a large foundation design was required. Because typical conventional portland cement concrete designs crack resulting in corroded steel, the owners called for a crack-resistant foundation design with no reinforcing steel. The foundation design called for two independent

HVFA concrete slabs measuring 118 ft. x 56 ft. x 2 ft. without the use of expansion or control joints. By using a HVFA concrete mix design, the thermal cracks and drying shrinkage was kept to a minimum due to the reduced use of cement in the mix design. A petrographic examination was performed and revealed that the foundation contained very minute amounts of calcium hydroxide crystals. The examination also revealed a high amount of unreacted fly ash with little to no residual cement particles. As initially desired, there was also little to no micro-cracking. (Malhotra et al., 2008)

BAPS Temple and Cultural Complexes (Chicago, Illinois, United States): Inspired by the outcome and performance of the Hindu Temple on Kauai Island, Hawaii, the BAPS Temple utilizes 250 unreinforced, cast in place HVFA concrete caissons (30 m. tall and 3m. in diameter), HVFA concrete foundations, and HVFA concrete walls. Key features of the mix design include: using Class C fly ash with a low amount of unburnt carbon, well-graded coarse aggregate with an emphasis on pea-sized gravel, effective superplasticizer, and a low cement content (65% fly ash replacement) to limit thermal cracking and drying shrinkage. The HVFA concrete mix was mixed at a local mixing plant, transferred by ready-mixed concrete trucks, and pumped into place. A very interesting note to take is the drastic strength differences when the foundation slabs were placed on different days. A slab placed on August 13, 2002, where the temperature was 88^{o}F, resulted in a compressive strength of 5802 psi. The second slab was placed October 18, 2002 where the temperature was 44.6^{o}F and the compressive strength was only 3771 psi (Malhotra et al., 2008).

Appendix B UHPC Mix Designs and Mechanical Properties

Table B-1 Compiled List of UHPC Mix Designs and Details

Mix No.	Portland Cement	White Cement	Class C Fly Ash	Granulated Blast-Furnance Slag (fine)	Fine Sand	Micro sand	Coarse Aggregate	Fine Aggregate.	Masonry Sand	River Sand	Silica Fume	Ground Quartz	Glass Powder	Quartz Sand	Limestone	High Range Water Reducer	Accelerator	Steel Fibers	Water	Source
1	1200	-	-	-	1720	-	-	-	-	-	390	355	-	-	-	51.8	50.5	263	184	Graybeal, 2007
2	924	-	-	924	-	-	-	-	523	1193	70	-	-	-	-	117	-	263	246	Khayat et al., 2014
3	1000	-	-	920	-	-	-	-	502	1187	-	-	-	-	-	91	-	263	293	
4	1118	-	619	0	-	-	-	-	529	1209	71	-	-	-	-	86	-	263	255	
5	819	-	937	0	-	-	-	-	516	1217	-	-	-	-	-	40	-	263	303	
6	-	1475	-	-	1778	369	-	-	-	-	74	-	-	-	-	77.4	-	82	341	Yu et al., 2014
7	-	1032	-	-	1778	369	-	-	-	-	74	-	-	-	443	77.4	-	82	341	
8	-	1180	-	-	1778	369	-	-	-	-	74	295	-	-	-	77.4	-	82	341	
9	1601	-	-	-	-	-	-	-	-	-	401	-	-	-	-	-	-	46	320	Yang, 2009
10	1107	-	-	705	-	-	-	-	-	-	201	-	-	-	-	-	-	44	188	Hassan, 2012
11	1107	-	-	725	-	-	-	-	-	-	201	-	-	-	-	-	-	44	166	Yang, 2010
12	1704	-	-	-	-	-	-	-	-	-	98	-	-	-	-	-	-	41	256	Toledo Filho, 2012
13	1618	-	-	-	-	-	-	-	-	-	405	-	-	-	-	-	-	57	259	Corinaldesi, 2012
14	1770	-	-	-	-	-	-	-	-	-	464	-	-	-	-	-	-	149	248	Habel 2006
15	-	1229	-	-	-	-	-	-	-	-	209	669	-	1404	-	51	-	261	337	Randl et al., 2014
16	-	676	553	-	-	-	-	-	-	-	209	669	-	1404	-	51	-	261	337	
17	-	676	-	553	-	-	-	-	-	-	209	669	-	1404	-	51	-	261	337	
18	-	676	-	553 (extra fine)	-	-	-	-	-	-	209	669	-	1404	-	51	-	261	337	
19	1878	-	-	-	-	-	-	1807	-	-	285	-	-	-	-	67	-	394	352	Hajar et al., 2004
20	2191	-	-	-	-	-	-	-	-	-	548	-	-	-	-	-	-	22	252	Talebinejad et al., 2004
21	2528	-	-	-	-	-	-	-	-	-	632	-	-	-	-	-	-	25	291	
22	2950	-	-	-	-	-	-	-	-	-	737	-	-	-	-	-	-	29	339	
23	3203	-	-	-	-	-	-	-	-	-	801	-	-	-	-	-	-	32	368	
24	3548	-	-	-	-	-	-	-	-	-	887	-	-	-	-	-	-	35	408	
25	2191	-	-	-	-	-	-	-	-	-	548	-	-	-	-	-	-	22	285	
26	2528	-	-	-	-	-	-	-	-	-	632	-	-	-	-	-	-	25	329	
27	2950	-	-	-	-	-	-	-	-	-	737	-	-	-	-	-	-	29	383	
28	3548	-	-	-	-	-	-	-	-	-	887	-	-	-	-	-	-	35	461	
29	2191	-	-	-	-	-	-	-	-	-	548	-	-	-	-	-	-	22	373	
30	2528	-	-	-	-	-	-	-	-	-	632	-	-	-	-	-	-	25	430	
31	2950	-	-	-	-	-	-	-	-	-	737	-	-	-	-	-	-	29	501	

Table B-1 Compiled List of UHPC Mix Designs and Details (Continued)

Mix No.	Portland Cement	White Cement	Class C Fly Ash	Granulated Blast-Furnance Slag (fine)	Fine Sand	Micro sand	Coarse Aggregate	Fine Aggregate.	Masonry Sand	River Sand	Silica Fume	Ground Quartz	Glass Powder	Quartz Sand	Limestone	High Range Water Reducer	Accelerator	Steel Fibers	Water	Source
32	3548	-	-	-	-	-	-	-	-	-	887	-	-	-	-	-	-	35	603	Talebinejad et al., 2004
33	3203	-	-	-	-	-	-	-	-	-	641	-	-	-	-	-	-	32	368	
34	3203	-	-	-	-	-	-	-	-	-	961	-	-	-	-	-	-	32	368	
35	3203	-	-	-	-	-	-	-	-	-	1121	-	-	-	-	-	-	32	368	
36	3203	-	-	-	-	-	-	-	-	-	641	-	-	-	-	-	-	32	384	
37	3203	-	-	-	-	-	-	-	-	-	801	-	-	-	-	-	-	32	384	
38	3203	-	-	-	-	-	-	-	-	-	961	-	-	-	-	-	-	32	384	
39	3203	-	-	-	-	-	-	-	-	-	1121	-	-	-	-	-	-	32	384	
40	3203	-	-	-	-	-	-	-	-	-	641	-	-	-	-	-	-	32	416	
41	3203	-	-	-	-	-	-	-	-	-	801	-	-	-	-	-	-	32	416	
42	3203	-	-	-	-	-	-	-	-	-	961	-	-	-	-	-	-	32	416	
43	3203	-	-	-	-	-	-	-	-	-	1121	-	-	-	-	-	-	32	416	
44	3203	-	-	-	-	-	-	-	-	-	641	-	-	-	-	-	-	32	544	
45	3203	-	-	-	-	-	-	-	-	-	801	-	-	-	-	-	-	32	544	
46	3203	-	-	-	-	-	-	-	-	-	961	-	-	-	-	-	-	32	544	
47	3203	-	-	-	-	-	-	-	-	-	1121	-	-	-	-	-	-	32	544	
48	3203	-	-	-	-	-	-	-	-	-	801	-	-	-	-	-	-	32	320	
49	3203	-	-	-	-	-	-	-	-	-	801	-	-	-	-	-	-	32	352	
50	3203	-	-	-	-	-	-	-	-	-	801	-	-	-	-	-	-	32	641	
51	3203	-	-	-	-	-	-	-	-	-	801	-	-	-	-	-	-	32	368	
52	3203	-	-	-	-	-	-	-	-	-	801	-	-	-	-	-	-	32	416	
53	3203	-	-	-	-	-	-	-	-	-	801	-	-	-	-	-	-	32	544	
54	3203	-	-	-	-	-	-	-	-	-	801	-	-	-	-	-	-	32	641	
55	3203	-	-	-	-	-	-	-	-	-	801	-	-	-	-	-	-	32	368	
56	3203	-	-	-	-	-	-	-	-	-	801	-	-	-	-	-	-	32	368	
57	3203	-	-	-	-	-	-	-	-	-	801	-	-	-	-	-	-	32	368	
58	1210	-	-	-	1734	-	-	-	-	-	394	357	-	-	-	50.6	43.8	263	189	Graybeal et al., 2008
59	1198	-	-	-	1718	-	-	-	-	-	391	354	-	-	-	50.6	43.8	261	226	
60	-	1402	-	-	-	-	-	-	-	-	228	349	-	1643	-	50	-	324	280	Ritter et al., 2015
61	-	1601	-	-	-	-	-	-	-	-	253	573	-	1129	-	51	-	51	303	Shakhmenko et al., 2012
62	-	1601	-	-	-	-	-	-	-	-	34	674	-	1129	-	42	-	34	337	Justs et al., 2012
63	-	1601	-	-	-	-	-	-	-	-	169	573	-	1129	-	42	-	34	337	
64	1053	-	-	-	-	-	1628	1332	-	-	-	-	-	-	-	26.3	-	-	275	Ha et al., 2012
65	811	-	120	-	-	-	1628	1332	-	-	-	-	-	-	-	20.3	-	-	263	
66	585	-	232	-	-	-	1628	1332	-	-	-	-	-	-	-	14.6	-	-	255	
67	696	-	118	-	-	-	1628	1332	-	-	99	-	-	-	-	17.4	-	-	258	

Table B-1 Compiled List of UHPC Mix Designs and Details (Continued)

Mix No.	Portland Cement	White Cement	Class C Fly Ash	Granulated Blast-Furnance Slag (fine)	Fine Sand	Micro sand	Coarse Aggregate	Fine Aggregate.	Masonry Sand	River Sand	Silica Fume	Ground Quartz	Glass Powder	Quartz Sand	Limestone	High Range Water Reducer	Accelerator	Steel Fibers	Water	Source
68	1257	-	-	-	1797	-	-	-	-	-	408	378	-	-	-	15	-	271	239	Ductal ®
69	1878	-	-	-	1807	-	-	-	-	-	285	-	-	-	-	67	-	394	357	BSI ®
70	1770	-	-	-	1230	-	-	-	-	-	464	-	-	-	-	59	-	792	320	CEMTEC$_{multiscale}$ ®
71	1476	-	-	-	-	-	-	-	-	-	240	-	-		-	28	-	-	315	Heinz, et al., 2012
72	375	-	-	1016	-	-	-	-	-	-	243	367	-	1660	-	22	-	-	303	
73	964	-	821	-	-	-	-	-	-	-	243	373	-	1687	-	28	-	-	315	
74	1517	-	-	-	1955	-	-	-	-	-	303	-	-	1469	-	25	-	265	303	Francisco et al., 2012
75	1328	-	-	-	-	-	-	1461	-	-	332	531	-	-	-	25	-	33	292	Prem et al., 2012
76	1328	-	-	-	-	-	-	1461	-	-	332	531	-	-	-	25	-	27	292	
77	1328	-	-	-	-	-	-	1461	-	-	332	531	-	-	-	25	-	33	292	
78	1328	-	-	-	-	-	-	1461	-	-	332	531	-	-	-	25	-	27	292	
79	1328	-	-	-	-	-	-	1461	-	-	332	531	-	-	-	25	-	-	292	
80	1*	-	-	-	-	-	-	1.1*	-	-	0.25*	0.4*	-	-	-	-	-	1%	0.17*	Prabha et al., 2014
81	1*	-	-	-	-	-	-	1.1*	-	-	0.25*	0.4*	-	-	-	2.25%	-	2%	0.17*	
82	1*	-	-	-	-	-	-	1.1*	-	-	0.25*	0.4*	-	-	-	-	-	3%	0.20*	
83	1*	-	-	-	-	-	-	1.1*	-	-	0.25*	0.4*	-	-	-	-	-	1%	0.17*	
84	1*	-	-	-	-	-	-	1.1*	-	-	0.25*	0.4*	-	-	-	-	-	2%	0.17*	
85	1*	-	-	-	-	-	-	1.1*	-	-	0.25*	0.4*	-	-	-	-	-	2%	0.17*	
86	1*	-	-	-	-	-	-	1.1*	-	-	0.25*	0.4*	-	-	-	-	-	3%	0.20*	
87	1*	-	-	-	0.28/ 0.64*	-	-	-	-	-	0.25*	-	0.25*	-	-	0.011*	-	0.27*	0.19*	Wille et al., 2013

Table B-2 Mechanical Properties of Compiled List of UHPC Mix Designs

	(Days)		(psi)			
Mix No.	**Age**	**Special Treatment**	**Compressive Strength**	**Tensile Strength**	**Modulus of Elasticity**	**Source**
20	28	Heat	37855			Talebinejad et al., 2004
21	28	Heat	39740			
22	28	Heat	44527			
23	28	Heat	47137			
24	28	Heat	34954			
25	28	Heat	33359			
26	28	Heat	36985			
27	28	Heat	42786			
28	28	Heat	30748			
29	28	Heat	23641			
30	28	Heat	27122			
31	28	Heat	33359			
32	28	Heat	22626			
33	28	Heat	41771			
34	28	Heat	44672			
35	28	Heat	42206			
36	28	Heat	39160			
37	28	Heat	44817			
38	28	Heat	42351			
39	28	Heat	40611			
40	28	Heat	36695			
41	28	Heat	41916			
42	28	Heat	38000			
43	28	Heat	34374			
44	28	Heat	26832			
45	28	Heat	33069			
46	28	Heat	30313			
47	28	Heat	28282			
48	28	Heat	32489			
49	28	Heat	39160			
50	28	Heat	25092			
51	28	Heat	35969			
52	28	Heat	35244			
53	28	Heat	29443			
54	28	Heat	23206			
55	28	Heat	36114			
56	28	Heat	33794			
57	28	None	22046			
58	28	Heat	29733			Graybeal et al., 2008
58	28	Heat	27557			
59	28	Heat	29000			
59	28	Heat	21756			
60	-	Heat	25240	1160		Ritter et al., 2015
61	7	Heat	23525			Shakhmenko et al., 2012
62	7	Heat	20755			Justs et al., 2012
63	7	Heat	21973			
64	28	Heat	16244			Ha et al., 2012
65	28	Heat	15954			
66	28	Heat	15664			
67	28	Heat	16389			
68	28	Heat	28718			Ductal ®
69	28	Heat	28863			BSI ®
70	28	Heat	24366			$CEMTEC_{multiscale}$ ®
71	28	Heat	33765			Heinz et al., 2012
72	28	Heat	23670			
73	28	Heat	28877			
74	28	Heat	27267			Francisco et al., 2012

Table B-2 Mechanical Properties of Compiled List of UHPC Mix Designs (Continued)

	(Days)		(psi)			
Mix No.	Age	Special Treatment	Compressive Strength	Tensile Strength	Modulus of Elasticity	Source
20	28	Heat	37855			Talebinejad et al., 2004
21	28	Heat	39740			
22	28	Heat	44527			
23	28	Heat	47137			
24	28	Heat	34954			
25	28	Heat	33359			
26	28	Heat	36985			
27	28	Heat	42786			
28	28	Heat	30748			
29	28	Heat	23641			
30	28	Heat	27122			
31	28	Heat	33359			
32	28	Heat	22626			
33	28	Heat	41771			
34	28	Heat	44672			
35	28	Heat	42206			
36	28	Heat	39160			
37	28	Heat	44817			
38	28	Heat	42351			
39	28	Heat	40611			
40	28	Heat	36695			
41	28	Heat	41916			
42	28	Heat	38000			
43	28	Heat	34374			
44	28	Heat	26832			
45	28	Heat	33069			
46	28	Heat	30313			
47	28	Heat	28282			
48	28	Heat	32489			
49	28	Heat	39160			
50	28	Heat	25092			
51	28	Heat	35969			
52	28	Heat	35244			
53	28	Heat	29443			
54	28	Heat	23206			
55	28	Heat	36114			
56	28	Heat	33794			
57	28	None	22046			
58	28	Heat	29733			Graybeal et al., 2008
58	28	Heat	27557			
59	28	Heat	29000			
59	28	Heat	21756			
60	-	Heat	25240	1160		Ritter et al., 2015
61	7	Heat	23525			Shakhmenko et al., 2012
62	7	Heat	20755			Justs et al., 2012
63	7	Heat	21973			
64	28	Heat	16244			Ha et al., 2012
65	28	Heat	15954			
66	28	Heat	15664			
67	28	Heat	16389			
68	28	Heat	28718			Ductal ®
69	28	Heat	28863			BSI ®
70	28	Heat	24366			CEMTEC$_{multiscale}$ ®
71	28	Heat	33765			Heinz et al., 2012
72	28	Heat	23670			
73	28	Heat	28877			
74	28	Heat	27267			Francisco et al., 2012